UNIVERSITY OF LONDON THESIS

Degree *Pho*   Year *2005*   Name of Author *DAVIES, G.M*

MAGNETISATION TRANSFER IMAGING IN THE STUDY OF EARLY RELAPSING-REMITTING MULTIPLE SCLEROSIS

Gerard Robert Davies, BSc, MBBS, MRCP

NMR Research Unit,

Dept of Neuroinflammation,

Institute of Neurology,

University College London,

Queen Square,

London, UK

A thesis submitted for the degree of

DOCTOR OF PHILOSOPHY (PhD)

UNIVERSITY OF LONDON

Date of submission: March 2005

UMI Number: U592783

UMI

Dissertation Publishing

ProQuest

ABSTRACT

Multiple sclerosis is a common cause of neurological disability in the young adult, but, at present, disease modifying medication may have little, if any, effect upon long term clinical impairment. For this reason, there is a continuing need to understand the mechanisms that lead to long term disability and – in the context of clinical trials – to develop reliable surrogate markers of disease progression. It may be especially useful to describe the *early* evolution of abnormality within normal-appearing white matter (NAWM) and grey matter; firstly because pathology in early MS may be a key determinant of later disability, and secondly because there is only a modest relationship between white matter lesion load and clinical impairment. This thesis presents a series of studies, investigating NAWM and grey matter abnormality in a cohort of patients with early relapsing-remitting MS. A key question was whether MRI measures were able to detect accumulating abnormality in NAWM and grey matter early in the clinical course. An initial investigation, using T_1 relaxation time estimation, did not detect strong evidence for a net change over time. Attention was therefore turned to the magnetisation transfer ratio (MTR) and results from a series of studies, investigating NAWM, grey matter and thalamic MTR abnormalities in early relapsing-remitting MS are presented. Of note, a clinically relevant reduction in grey matter MTR was apparent, and there was evidence for increasing MTR abnormality in the grey matter, NAWM and the thalamus over a two year follow-up period. In part three of this thesis, a model for the MT effect is used to estimate two underlying MT parameters – the semi-solid proton fraction (*f*) and the semi-solid T_2 (T_{2B}) in sixty patients with clinically-definite MS. The aim was to assess the clinical relevance of these novel parameters.

CONTENTS

PUBLICATIONS ARISING FROM THIS THESIS

Davies GR, Ramio-Torrenta L, Hadjiprocopis A, Chard DT, Griffin CM, Rashid W, Barker GJ, Kapoor R, Thompson AJ, Miller DH. Evidence for grey matter MTR abnormality in minimally disabled patients with early relapsing-remitting multiple sclerosis. J Neurol Neurosurg Psychiatry 2004;75:998-1002.

Davies GR, Ramani A, Dalton CM, Tozer DJ, Wheeler-Kingshott CA, Barker GJ, Thompson AJ, Miller DH, Tofts PS. Preliminary magnetic resonance study of the macromolecular proton fraction in white matter: a potential marker of myelin? Mult.Scler 2003;9:246-249.

Davies GR, Tozer DJ, Cercignani M, Ramani A, Dalton CM, Thompson AJ, Barker GJ, Tofts PS, Miller DH. Estimation of the macromolecular proton fraction and bound pool T2 in multiple sclerosis. Mult.Scler 2004;10:607-613.

Davies GR, Altmann DR, Hadjiprocopis A, Rashid W, Chard DT, Griffin CM, Tofts P, Barker GJ, Kapoor R, Thompson AJ, Miller DH. Increasing normal-appearing grey and white matter MTR abnormality in early relapsing-remitting MS. J Neurol 2005; in press.

Davies GR, Altmann DR, Rashid W, Chard DT, Griffin CM, Barker GJ, Kapoor R, Thompson AJ, Miller DH. Emergence of thalamic MTR abnormality in early relapsing-remitting MS. Mult.Scler 2005; in press.

LIST OF ABREVIATIONS

Δ	Off-set frequency of MT pulse
ω_{CWPE}	Effective MT pulse amplitude (continuous-wave-power-equivalent)
2D	Two-dimensional
3D	Three-dimensional
ADC	Apparent diffusion coefficient
BMS	Benign multiple sclerosis
BPF	Brain parenchymal fraction
CI	Confidence intervals
CIS	Clinically isolated syndromes suggestive of MS
COV	Coefficient of variation
CNS	Central nervous system
CSE	Conventional spin echo
CSF	Cerebrospinal fluid
CW	Continuous wave
DIS	Dissemination in space
DIT	Dissemination in time
DTI	Diffusion tensor imaging
EBV	Epstein Barr virus
EDSS	Expanded disability status scale
EPI	Echo planar imaging
ETL	Echo train length
f	The semi-solid proton fraction
FA	Fractional anisotropy
FOV	Field of view

FSE	Fast spin echo
FSPGR	Fast spoiled gradient recall
Gad/Gd	Gadolinium
Gd-DTPA	Gadolinium diethylene-triamine-pentacetic acid
GE	Gradient echo
GM	Grey matter
GMF	Grey matter fraction
HHV	Human herpes virus
HLA	Human leukocyte antigen
IFNB	Interferon Beta
IL	Interleukin
IM	Intramuscular
Ins	myo-inositol
IV	Intravenous
M_0^A, M_0^B	Native magnetisation of free water and semi-solid pools
M_Z^A, M_Z^B	Longitudinal magnetisation of free water and semi-solid pools
MAG	Myelin associated glycoprotein
MD	Mean diffusivity
MHC	Major histocompatibility complex
MRI	Magnetic resonance imaging
MS	Multiple sclerosis
MSFC	Multiple sclerosis functional composite
MT	Magnetisation transfer
MTI	Magnetisation transfer imaging
MTR	Magnetisation transfer ratio

NAA	N-acetyl-aspartate
NAWM	Normal-appearing white matter
NAGM	Normal-appearing grey matter
NEX	Number of excitations
ns	Not significant
OCB	Oligoclonal bands
PD	Proton density
PPMS	Primary progressive multiple sclerosis
pu	Percent units
R	Rate of cross-relaxation
R_A, R_B	Longitudinal relaxation rates of free and semi-solid pools
R_{RFA}, R_{RFB}	Absorption rates of free and semi-solid pools
RF	Radiofrequency
ROI	Region of interest
RRMS	Relapsing-remitting multiple sclerosis
Sc	Subcutaneous
SD	Standard deviation
SE	Spin echo
SI	Signal intensity
SPM99	Statistical Parametric Mapping 1999
SPMS	Secondary progressive multiple sclerosis
T	Tesla
T_1	Spin lattice relaxation time
T_{1Aobs}	Observed T_1 of free water
T_2	Spin-spin relaxation time

T_{2b}	T_2 of the semisolid pool (Henkelman model)
T_{2B}	T_2 of the semisolid pool (Ramani-Tozer-Tofts model)
TE	Echo time
TI	Total intracranial volume
TR	Repetition time
TNF	Tumour necrosis factor
VEP	Visual evoked potential
WM	White matter
WMF	White mater fraction

LIST OF FIGURES

LIST OF TABLES

DESCRIPTION OF THESIS

This thesis is divided into four parts.

Part 1 gives an introduction to multiple sclerosis and a number of recent pathological findings. The principles of MRI and the theory of magnetisation transfer are described. The use of MRI in MS is reviewed and an overview is given describing previous studies using magnetisation transfer imaging in MS.

Part 2 describes a series of studies investigating abnormality in the normal-appearing white matter (NAWM) and normal-appearing grey matter (NAGM) in patients with early relapsing-remitting MS. Patients and controls were imaged serially for up to three years in order to investigate the natural history and clinical relevance of early, normal-appearing brain tissue abnormality. In all subjects, the magnetisation transfer ratio (MTR) and T_1 relaxation time were determined; (T_1 is related to MTR). Baseline T_1 abnormalities were observed but there was no evidence for a definite or consistent change over time. Attention was therefore turned to the study of the early relapsing-remitting MS cohort using MTR. Baseline and longitudinal studies using NAWM and NAGM MTR histograms are presented and the results suggest that NAGM MTR abnormality is clinically relevant (it correlates with the EDSS) and that increasing MTR abnormalities are developing in the NAGM and NAWM early in the course of relapsing-remitting MS. Finally, data describing changes in thalamic MTR are presented, providing evidence for the emergence of thalamic MTR abnormality within five years of clinical onset.

In Part 3, sixty patients with clinically-definite MS were imaged using a novel MT sequence. A model for magnetisation transfer is used to estimate parameters that underlie the MT effect. These include the semi-solid (macromolecular) proton fraction (f) and the T_2 of the semi-solid pool (T_{2B}). Data on these parameters are presented and discussed.

Part 4 includes a summary of the principle findings and conclusions of the thesis.

PART 1

INTRODUCTION

CHAPTER 1

Multiple Sclerosis

1.1 Epidemiology

Multiple sclerosis (MS) is an inflammatory demyelinating disorder of the central nervous system and is an important cause of neurological disability in the young adult. In the United Kingdom, the incidence is approximately 7/100,000 (MacDonald *et al.*, 2000) while prevalence ranges from 87/100,000 in Guernsey to 287/100,000 in Orkney (Compston, 1998*a*). The age of onset peaks between the ages of 25 and 34 while onset prior to 15 or after the age of 55 is uncommon (McDonnell and Hawkins, 1998). There is also a clear gender difference and there are approximately two females with the condition for every male affected (Compston, 1998*b*).

MS is most prevalent in northern Europe, southern Australia, New Zealand, and North America but it is much less so in south-east Asia, the Arabian Peninsula and Africa. However, within regions, local gradients are also recognized. In Europe, the highest prevalence is seen in southern Scandinavia, Germany and the United Kingdom while lower rates are seen in southern Europe (Compston, 1998*a*). These regional gradients do not always conform to latitude (as was originally thought); a diagonal distribution, for instance, exists in the United States, with highest prevalence in the north-west and lowest in the south east (Bulman and Ebers, 1992).

1.2 Aetiology

Genetics

The evidence for a genetic susceptibility to multiple sclerosis comes from a number of sources. The geographical distribution of the disease, once thought to be indicative of an environmental factor, may be better explained by regional genetic differences. Genetically distinct racial groups living in the same locality often exhibit differences in risk, for instance, the lower prevalence in Wales in those with Celtic origins as opposed to those with English surnames (Swingler and Compston, 1988). Twin studies reveal that around 25% of monozygotic twins are concordant whereas concordance in dizygotic twins is similar to the sibling risk (around 3%) (Mumford *et al.*, 1994; Compston, 1998*b*; Ebers *et al.*, 1986). Furthermore, the risk of MS in a child with one affected parent is 2% while the risk with two affected parents is about 14% (Robertson *et al.*, 1997). Conversely, the risk of MS in children adopted by a parent with MS is no greater than the background risk (Ebers *et al.*, 1995; Compston, 1998*b*).

Many studies consistently point towards an association between MS and the human leukocyte antigen region (HLA) on chromosome 6 and, in particular, the major histocompatibility complex (MHC) class II phenotypes DR15 and DQ6 (Compston, 1998*b*). In one association study, the relative risk of MS in those homozygous for DR15 was found to be 48.5 (Beall *et al.*, 1995). Other genes, including regions encoding for T-cell receptors, immunoglobulins and myelin structural proteins may also be associated with susceptibility to MS (Compston, 1998*b*). ApoE, conversely, may be associated with disease severity (Kantarci *et al.*, 2004).

Systematic genome screening by groups in the UK, Canada and USA has confirmed the importance of the HLA. However, additional regions identified (such as 7p and 14q in the UK study) have little overlap with the studies from the Americas (Compston, 1998*b*). In MS, different genes may be implicated in different individuals and so genetic studies may need to delineate this, subdividing on the basis of clinical, immunological or genetic aspects (such as DR15 status) (Compston, 1998*b*). Although there is no evidence for a single, major susceptibility gene in MS, it appears likely that several genes are implicated, each exerting a moderate effect (Compston, 1998*b*).

Environmental Factors

There is no evidence to suggest that a specific infection causes MS, although, some studies have shown that the risk of a demyelinating episode is higher in the weeks following an upper respiratory tract infection (Andersen *et al.*, 1993; Panitch, 1994). Studies of childhood illness again fail to implicate a single pathogen, but viral infections in late childhood (such as measles, mumps, rubella, and particularly Epstein Barr virus (EBV)) may have an effect on those who are otherwise predisposed. Some groups have focused on viral isolates including studies of EBV (Sundstrom *et al.*, 2004), Human T-Lymphocyte virus, Human Herpes virus (HHV)-6 and HHV-8, but without, at present, firm evidence that they have a clear role in the pathogenesis. Trauma, surgery, anesthesia and emotional stress have also all been studied and, in general there is little to support the view that these have a role in MS pathogenesis (Compston, 1998*a*). A recent study, (Buljevac *et al.*, 2003), reported that the risk of a relapse doubled during the four weeks following a stressful life event but confirmation of this is now needed. Finally, the potential effect of female

sex hormones has also been studied, particularly as relapse rate is lower during pregnancy and higher in the pueperium (Confavreux *et al.*, 1998). Furthermore, it has also been suggested that oestrogens may have a disease modifying effect (Sicotte *et al.*, 2002).

Risk to migrants and MS epidemics

Some studies have shown that migrants, emigrating prior to their mid-teens, from an area with low MS risk to an area with higher risk, experience an increased incidence in comparison to that found in their country of origin. Conversely, those migrating after the mid-teens tend to retain the risk associated with the region in which they originated (Dean and Kurtzke, 1971; Compston, 1998*a*). Support for this comes from a number of sources, including a comprehensive study assessing MS risk in World War II veterans migrating within the United States as part of their military service (Kurtzke *et al.*, 1971). In contrast, an epidemiological study in Australia, (Hammond *et al.*, 2000) found that a reduction in risk also occurred in older migrants (older than their mid-teens), who emigrated from high-risk UK and Ireland to settle in lower risk Australia. These results, and the results from other studies (including those examining migration to Hawaii and Israel) support the view that the MS risk can be modified by relocation, although the protective effects of having a particular ethnicity are never entirely lost (Compston, 1998*a*).

A number of studies have described possible epidemics of MS, for instance on Orkney, the Faroes and on Iceland. However, others would argue that these are epidemics of recognition (coinciding with the appointment of new neurologists to the

islands) rather than resulting from the arrival of an exogenous aetiological factor (Compston, 1998a).

In summary, although the exact aetiology of MS remains obscure, genetic effects (with several or many genes exerting influence) clearly have a role. While no single environmental agent has been implicated, a modification of genetic risk by environmental factors seems likely.

1.3 Pathology

Historical Context

The first reports of macroscopic pathology in MS (with descriptions of multiple, plaques within the brain and spinal cord) have variously been ascribed to Jean Curveilhier (c1841), who also provided some early clinical accounts, and to Robert Carswell (1838) (Compston, 1998c). However, in 1863, Rindfleisch gave the first *histo*pathological account with his description of the loss of myelin within lesions. He also described that plaques were centred on blood vessels and that the walls of these vessels contained an increased density of small round cells. In 1868 Charcot, provided the first detailed neuropathological description of the disease and remarked upon the presence of glial scar tissue and demyelination. He even speculated on how the loss of myelin could lead to symptoms of the disease and how this could 'disturb the due execution of voluntary movements' (Charcot via Compston, 1998c). Three of the four principle pathological substrates in MS, have therefore already been alluded to (demyelination, astrogliosis and inflammatory change) and the fourth, axonal pathology, was also commented upon in the early literature (Charcot, 1877; Marburg,

1906), (Marburg described that, in acute MS, axons were relatively although *not absolutely* preserved).

The Basic Lesion

Lesions are typically sharply demarcated, and are often centred on one or several medium sized blood vessels (Lassmann, 1998a). Plaques tend to be distributed periventricularly or close to the outer surface of the brain and cord. The hallmark of the basic lesion is inflammatory demyelination and this appears to be principally T-cell mediated. Inflammatory infiltrates are typified by the presence of both $CD8^+$ and $CD4^+$ cells but lower numbers of B cells and macrophages are also consistently found (Lassmann, 1998a, 1998b). Gliosis is also a key finding (Adams, 1977) and a majority of inactive plaques in MS contain a fibrillary network of astrocytic processes.

In the rim of chronic lesions, thinly myelinated fibres, (suggestive of remyelination) are often seen (Lassmann, 1998a) while shadow plaques (discrete areas of thinly myelinated axons with astroglial proliferation) are also commonly demonstrated. It has been shown that the latter reflect remyelination (rather than incomplete demyelination) and, although remyelination can occur in early disease (Prineas *et al.*, 1993), the ability of oligodendocytes to remyelinate may diminish with time (Lassmann, 1998a).

Of note, recent studies have observed acute axonal damage within active and chronic-active lesions (Ferguson *et al.*, 1997; Trapp *et al.*, 1998). (Acute lesions have numerous T-lymphocytes and macrophages throughout, while chronic-active

lesions have few inflammatory cells at the centre but relatively more at the plaque border). Ferguson *et al.* found that the expression of amyloid precursor protein (APP) (which can be detected at sites of axonal injury) occurs most prominently in active lesions. Furthermore, axon ovoids, stained for antibodies to non-phosphorylated neurofilaments were associated with a single axon connection, indicative of axonal transection (Trapp *et al.*, 1998). The number of axons transected appears to be highest in active lesions, less in the demyelinating border of chronic-active lesions and least in their inactive centres. It is noteworthy that axonal transection within MS lesions occurs at an early stage in MS, and has been observed within a year of clinical onset (Kuhlmann *et al.*, 2002).

Lesions appear to be heterogeneous between patients but *active lesions* from the same patient may be homogenous (Lucchinetti *et al.*, 2000). Four lesion types have been identified. In patterns 1 & 2, a T-cell mediated attack on the myelin sheath is the hallmark; this occurs either via macrophage released toxins (such as TNF-alpha) (pattern 1) or via B-cell mediated antibody release and complement attack (pattern 2). In patterns 3 and 4, oligodendrocyte cell body degeneration and an absence of remyelination are characteristic. In pattern 3, lesions have ill defined borders and are not centred on veins; Myelin associated glycoprotein (MAG) is lost and oligodendrocyte apoptosis is observed. Interestingly, patients with Balo's rings typically have type 3 lesions. In type 4 lesions, perivascular inflammation is associated with oligodendrocyte loss and apoptotic figures are *not* seen. Lucchinetti *et al.* (2000) did not show a clear association between these lesion patterns and the four MS clinical phenotypes. However, there was some evidence that patients with established relapsing-remitting or secondary progressive disease exhibited pattern 2

24

while those with acute MS had either patterns 1, 2 or 3. Patients with primary progressive MS had patterns 2 or 4. Barnett and Prineas, (2004) have recently reported on the pathology of acute symptomatic lesions (where patients died shortly following the onset of a relapse). In many of these lesions there were very few lymphocytes and myelin phagocytes but extensive oligodendrocyte apoptosis and microglial activity. It remains unclear whether the differences seen in lesion pathology truly reflect pathological disparity between MS clinical subgroups. It is possible, for instance, that different lesion pathologies arise at different stages of the disease.

Grey matter and the macroscopically normal white matter

While there has been considerable focus on the pathological mechanisms seen within white matter lesions, cortical lesions have also been observed. These appear to be a consistent feature of the disease (Lumsden *et al.*, 1970; Brownell and Hughes, 1962; Kidd *et al.*, 1999; Peterson *et al.*, 2001; Bø *et al.*, 2003*a*, *b*) and although grey matter lesions are less inflammatory than those in white matter (Peterson *et al.*, 2001; Bø *et al.*, 2003*a*), and are less visible on MRI (Kidd *et al.*, 1999), they are associated with axonal and dendritic transection, neuronal apoptosis and demyelination (Peterson *et al.*, 2001). Recently it has been suggested that grey matter demyelination could be extensive in some patients and a proportion of those examined at post-mortem were found to have a generalised subpial loss of myelin (Bø *et al.*, 2003*b*).

Neuropathological examination of the macroscopically normal white matter has also revealed clear abnormalities. These include astrogliosis, microglial activation, patchy demyelination and perivascular inflammation (Allen and McKeown, 1979; Allen *et*

al., 2001). However, there is also evidence for axonal loss (Evangelou *et al.,* 2000*a*,

b) and it has been shown that the degree of axonal loss within the corpus callosum is

related to the regional lesion load (Evangelou *et al.*, 2000*b*). A further study

suggested that small caliber fibres were more susceptible to damage than those of

larger diameter (Evangelou *et al.*, 2001). Furthermore, there is now evidence (from a

post-mortem study investigating the cord) that axonal loss within normal-appearing

tissue may be a factor underlying permanent disability (Bjartmar *et al.*, 2000).

Although axonal injury within lesions, occurring acutely (Trapp *et al.*, 1998), or in

chronically demyelinated lesions (Kornek and Lassmann, 2003), may lead to axonal

degeneration in normal-appearing tissue, other processes may also play a role

(Bjartmar *et al.*, 2003). It has been suggested that, later in the disease course, axonal

and neuronal degeneration could promote the loss of surviving neurons via the

withdrawal of pre and post synaptic trophic signals (Bjartmar *et al.*, 2003; Compston

and Coles, 2002); and that this, in turn, could lead to a vicious cycle of neuronal

injury. It is noteworthy that, in the natural history study of Confavreux *et al.*, (2003)

the time course between EDSS 4 and 6 was similar among patients. In contrast there

was much more variability in the time taken to reach EDSS 4. It is possible that, at

EDSS 4, there is sufficient neuronal injury to allow the vicious cycle to propagate,

whereas it is the frequency of inflammatory activity (which varies from patient to

patient) that determines the time taken to reach EDSS 4.

At present, this hypothesis of Bjartmar and others remains unproven but if such a

process exists, it would imply that the prevention of *early* axonal injury would be key

in the treatment of MS. Questions arising might ask: (1) whether white matter lesions

are the main cause of axonal injury in early MS, or whether other processes are also important (such as grey matter demyelination); (2) whether is it possible to monitor early axonal damage (in the normal appearing white matter and grey matter) such that the effect of therapies can be assessed?

1.4 Immunology.

The immunological mechanisms that are associated with MS pathology are complex and are briefly summarized here. Initially, (and for unknown reasons) there may be a failure in the regulation of auto reactive anti-myelin T-cells. This results in T-cell clonal expansion and entry of the primed T-cells into the circulation (Compston and Coles, 2002). Changes in the cerebral endothelia allow the primed lymphocytes to migrate into the CNS, particularly via the expression of lymphocyte adhesion molecules (and reciprocal changes within the endothelia). The migrating lymphocytes activate microglia which, in turn, re-present auto-antigen (bound to MHC II molecules) leading to a loop of pro-inflammatory stimulus. Toxic mediators are released including nitric oxide (which induces physiological conduction block), together with a range of pro inflammatory cytokines (IL2, tumour necrosis factor (TNF)-alpha, gamma interferon (IFN) are pro-inflammatory while IL4, IL6 and IL10 down regulate the immune response). The inflammatory reaction leads to further breakdown of the blood brain barrier and a secondary influx of immune cells. Damage to the oligodendrocyte via toxic mediators, free radicals, complement attack, and myelin phagocytosis, may all lead to myelin loss. Similar processes may also be responsible for axonal injury. In particular, nitric oxide has been shown to produce axonal damage when conjoined with a high axonal firing frequency; however

oedema, cytotoxic $CD8^+$ T lymphocytes and glutamate excitotoxicity may also play a role (Bjartmar *et al.*, 2003).

1.5 Pathophysiology

There is a complex relationship between the pathology of MS and how this leads to the symptoms of the disease. Conduction block arises as a result of demyelination and inflammation (the inflammatory mediator, nitric oxide, has been shown to block saltatory conduction). Conduction block will give rise to the 'negative' symptoms associated with MS relapses, including upper motor neuron weakness and sensory deficits. Conversely, positive symptoms, for instance paraesthesia, are thought to occur as a result of the hyperexcitability of previously demyelinated axons. Recovery from a relapse will depend on a number of processes including the reduction of inflammation and nitric oxide levels, remyelination, the redistribution of sodium channels along the axonal membrane, and cortical plasticity.

However, conduction velocity is often not fully restored following a relapse and this accounts for the visual-evoked-potential (VEP) delay observed in patients following an episode of optic neuritis (Halliday *et al.*, 1972). A block in conduction velocity may also account for the transient symptoms experienced when a patient's body temperature is raised. At higher temperatures, nerve conduction across a demyelinated segment will falter and symptoms (such as the visual blurring of Uhthoff's phenomenon) will be unmasked.

Although there are a number of mechanisms underlying recovery, the process of remyelination may fail for a number of reasons. Astrogliosis may create a physical

barrier to remyelination (Compston and Coles, 2002), and axonal loss will naturally limit myelin repair. It was also once thought that oligodendrocyte precursors were depleted in chronic MS, but recent work suggests that such precursors are more abundant than once supposed (Reynolds *et al.*, 2002).

Acute axonal transection within lesions may further contribute to any irreversible deficit arising from a relapse. Although these axons may undergo Wallerian degeneration in early MS (Simon *et al.*, 2000) this does not appear to produce short term clinical progression. Such a process, however, may have a *delayed* clinical impact and progressive axonal and neuronal degeneration in late disease are likely to be of importance in the development of progressive, irreversible disability.

1.6 Clinical Manifestations & Natural History

The majority of individuals affected by MS (over 80%) initially experience an acute attack of neurological dysfunction (most typically affecting the optic nerve, brain stem or spinal cord) followed by a period of recovery and remission (Matthews, 1998). The first attack of demyelination – (or clinically isolated syndrome suggestive of MS) is followed, in many but not all, by further attacks – indicative of new inflammatory demyelinating events. In one series (a 40 year optic neuritis follow-up study) the rate of conversion to clinically definite MS was 60% (Rodriguez *et al.*, 1995).

Relapses can take many forms. A cord episode can result in pyramidal limb weakness, sensory loss and dysaethesia, while a brain stem episode can lead to eye

movement abnormalities, vertigo and ataxia. Optic neuritis typically results in painful unilateral visual loss with a central scotoma (Matthews, 1998).

In relapsing-remitting MS, relapses typically evolve over hours or days and resolve over weeks to months. Symptoms resolving within 24 hours are not considered to be due to a relapse. The relapse frequency varies from patient to patient but initially may be about 1.3/year (IFNB MS Study Group, 1993) and this falls with time. The degree of recovery from each relapse is also variable but many patients may make good recoveries. Despite this, the natural history, in a proportion, is of increasing disability, either as a result of incomplete recovery from relapses, or from secondary progression. Approximately two-thirds of those with relapsing-remitting MS eventually enter the secondary progressive phase, the point of transition usually corresponding to EDSS 4.0 (Runmarker and Andersen, 1993). In those with secondary progressive MS, relapses are less frequent, and are largely replaced by a slow and gradual deterioration in neurological function. This most typically takes the form of a progressive spastic paraparesis worsening over many years, although other forms (such as a progressively worsening ataxia) are also commonly encountered.

The prognosis of MS has been well described. In natural history studies the median time from onset to the use of a unilateral walking aid is ~15 years (Weinshenker et al., 1989), while the median time to the use of a wheelchair is ~25-30 years (Confavreux et al., 2003). Life expectancy, however, is only marginally reduced: A recent study of Danish patients, diagnosed between 1949 and 1996, revealed that survival was approximately 10 years less in comparison to an age matched healthy population. However, the probability for survival improved during the study period,

with a near halving of this 10 year excess mortality (Brønnum-Hansen *et al.*, 2004). MS may also follow a benign course and, in a recent series (Pittock *et al.*, 2004), 17% of patients had an EDSS of 2.0 or less after more than 20 years of follow-up. However, approximately 10-15% of MS patients have a progressive course from onset (Thompson *et al.*, 1997). Although in primary progressive MS, the time to reach EDSS 6.0 is short in comparison to those with relapsing remitting MS (a median of 6 years in the study of Runmarker and Andersen, 1993), the *rate* of progression is similar to those who have just entered the secondary progressive phase (Thompson *et al.*, 1997; Kremenchutzky *et al.*, 1999).

Confavreux *et al.*, (2003) used natural history data to show that MS patients vary widely in the time taken to reach Expanded Disability Status Scale (EDSS) 4.0 (irreversible limitation of ambulation). A number of factors appeared to influence the time taken, one being the nature of the presenting symptoms: those who presented with isolated optic neuritis took a median of 14 years to reach EDSS 4.0, while those who initially presented with brain stem or long tract signs took between 6 and 10 years. Other influencing factors were: age of onset (those presenting later reached EDSS 4.0 more rapidly); the degree of recovery from relapses; time to second neurological episode; and the number of relapses in the first 5 years. Conversely, the time taken to *progress* from EDSS 4.0 to EDSS 6.0 (use of a walking aide) was more constant (taking a median of 6 years) and this was not influenced substantially by any of the above factors. It has been argued that the initial, unpredictable events, (relapses which result from the development of new and multifocal inflammatory lesions), are replaced by a more gradual and progressive pathological process later in the disease course. The Lyons natural history data may indicate that a critical amount

of CNS damage (corresponding to EDSS 4.0) is necessary to initiate this self propagating, progressive process. The frequency and severity of the early relapses do not affect the rate of later progression, although they do effect the time taken to reach the critical threshold.

1.7 Diagnosis

In MS, lesions develop at different times and at different sites throughout the CNS and, characteristically, the development of new lesions will be disseminated in space and time. While this concept is central in the diagnosis of MS, it is of equal importance that clinical evidence used in the diagnosis is characteristic of the disease and that alternative diagnoses have been excluded. The differential for MS is wide and includes a number of other conditions where CNS lesions are disseminated in space and time (see Table 1.1a).

Table 1.1a. The Differential Diagnosis of MS.

Differential Diagnosis of Multiple Sclerosis (or Clinically Isolated Syndromes Suggestive of MS)
➢ Inflammatory Causes:
• Acute Disseminated Encephalomyelitis
• Devic's Neuromyelitis Optica
• Systemic Lupus Erythematosus
• Systemic Sclerosis
• Primary Sjögren's Syndrome
• Behçet's Disease
• Sarcoidosis
• CNS Vasculitis
• Susac's Syndrome
➢ Infectious Causes:
• Lyme Borreliosis
• Meningovascular Syphilis
• HIV
• HTLV-1 Myelopathy
➢ Cerebrovascular Disease
➢ Paraneoplastic Syndromes
➢ Hereditary Ataxias and Paraplegia's
➢ Leucodystrophies :
• Krabbe's (adult onset myeloneuronopathy)
• Adrenoleucodystrophy
• Alexander' s Disease (adult onset)
• Metachromatic Leucodystrophy
➢ Motor Neuron Disease (Primary Lateral Sclerosis)
➢ Intermittent symptoms secondary to tumours or vascular malformations.
➢ Subacute combined degeneration of the cord
➢ Progressive symptoms due to spinal cord compression, a syrinx or a Chiari malformation.

Table 1.1b. The Differential Diagnosis of Optic Neuritis.

Differential Diagnosis of Optic Neuritis
o Anterior ischaemic optic neuropathy
o Compressive causes of optic neuropathy
o Inflammatory causes (eg sarcoid and CRION)
o Infective causes eg syphilis,
o Leber's optic neuropathy,
o Central serous choroidoretinopathy
o Neuroretinitis

Based on these concepts, the diagnostic criteria of Schumacher *et al.*, (1965), Poser *et al.*, (1983) and McDonald *et al.*, (2001) have been proposed. Schumacher's criteria relied on the collection of clinical evidence (from history taking and clinical examination), providing proof of dissemination in space and time. Provided that other aspects of the presentation were consistent with MS and alternative diagnoses had been excluded, it was possible to reach a diagnosis of definite MS. In 1983, Poser and colleagues published a set of revised criteria whereby information from CSF examination and paraclinical investigations (evoked potentials, urological assessments and imaging studies) could be substituted for clinical information where the clinical information alone did not provide proof of dissemination in space and time (see Table 1.2). To establish a diagnosis of *clinically definite* MS, the criteria required that there had been at least two attacks and clinical evidence of at least two lesions; (or clinical evidence of one lesion and paraclinical evidence for the other).

Table 1.2: Poser's Diagnostic Criteria for Multiple Sclerosis

Diagnosis	No. of Attacks	No. of lesions (clinical evidence)		Paraclinical evidence of a lesion	CSF
Clinically Definite MS					
	2	2			
	2	1	And	1	
Laboratory-supported Definite MS					
	2	1	Or	1	+
	1	2			+
	1	1	And	1	+
Clinically Probable MS					
	2	1			
	1	2			
	1	1	And	1	
Laboratory-supported probable MS					
	2				+

Positive CSF: Intrathecal synthesis of oligoclonal bands or increased IgG index

Reproduced from Poser et al., (1983)

More recently, new diagnostic criteria (McDonald *et al.*, 2001) have integrated the evidence provided by MRI with clinical and paraclinical evidence (VEPs and CSF examination). In particular, MRI can be used to demonstrate dissemination in space (by the distribution of lesions on T_2 weighted images) and dissemination in time (by the presence of enhancing lesions or of new T_2 lesions). The new criteria allow for the diagnosis of MS to be made earlier and, in some instances, after the first clinical attack. Furthermore, the McDonald criteria can be applied more readily to those with primary progressive MS. (See Table 1.3). The provision of an earlier diagnosis may be useful, particularly if it is shown that early treatment prevents later disability (although that data is currently lacking). At present, the provision of an earlier diagnosis needs to be balanced on a patient by patient basis (particularly as in the UK disease modifying treatment is not available for those with clinically isolated syndromes). Some patients may seek an early and full explanation for their symptoms, while others may not.

Table 1.3. McDonald's Diagnostic Criteria for Multiple Sclerosis.

Clinical Presentation	Additional Data Needed for MS Diagnosis
2 or more attacks, objective evidence of 2 or more lesions	None
2 or more attacks, objective evidence of 1 lesion	DIS (or >2 MRI lesions consistent with MS and unmatched CSF OCB), or wait further attack implicating new site
1 attack; objective evidence of 2 or more lesions	DIT or 2nd attack
1 attack; objective clinical evidence of 1 lesion	(i)DIS (or >2 MRI lesions consistent with MS and unmatched CSF OCB) and DIT, or (ii) 2nd attack
Insidious neurological progression suggestive of MS	unmatched CSF OCB and: (i){DIS: [(1) >9 cerebral T_2 lesions or (2) >2 cord lesions or (3) 4-8 brain plus 1 cord lesion or (4) abnormal VEP with 4-8 brain lesions or (5) abnormal VEP <4 brain plus 1 cord lesion]. AND DIT} or (ii) continued progression for 1 year

DIS: Dissemination in space: Need 3 of the following: (1) 1 Gad lesion or 9 T_2 lesions. (2) >1 infratentorial lesion, (3) > 1 juxtacortical lesion, (4) >3 periventricular lesions; one cord lesion can be substituted for one brain lesion.

DIT: Dissemination in time: enhancing lesion on a scan done >3 months after a clinical event. If no gad lesion, repeat imaging must show a new T_2 lesion or gad lesion. If the initial scan is done within 3 months of the clinical event, a scan must be repeated >3months later. A new T_2 lesion or Gad lesion on this scan will prove DIT.

OCB: Intrathecal oligoclonal bands (or raised IgG index)

VEP: Visual evoked potentials.

Reproduced from McDonald et al., (2001)

37

1.8 Treatment and management

Disease modifying medication – treatment of acute attacks

High dose, pulsed methylprednisolone is used for disabling relapses. Intravenous steroids hasten the recovery from a relapse (Milligan *et al.*, 1987; Beck *et al.*, 1993) but they do not improve the long term outcome (Beck *et al.*, 1993). While a comparison between oral conventional-dose and intravenous high-dose methylprednisolone did not show a clear difference in MS patients (Barnes *et al.*, 1985), data from the optic neuritis treatment trial (Beck *et al.*, 1993) suggested that high dose intravenous steroids followed by an oral taper was more efficacious in comparison to conventional doses of oral prednisone alone. However, high dose oral methylprednisolone has recently been shown to be effective in comparison to placebo (Sellebjerg *et al.*, 1998).

Symptomatic treatments

A number of treatments are used to ameliorate the symptoms of MS (Compston, 1998*d*). Spasticity is common and symptoms may be improved with baclofen, tizanidine, dantrolene or gabapentin. Side effects are frequent and sedation or an increase in muscle weakness often limits the use of such medication. Recently, cannabinoids have been tested in patients with lower limb spasticity and this, when assessed subjectively by the patients themselves, was reduced in the treatment arm; however no treatment benefit was observed on an objectively measured spasticity scale (Zajicek *et al.*, 2003). For more marked spasticity, local botulinum toxin injection, intrathecal phenol or the insertion of an intrathecal baclofen pump may be of benefit. The urinary symptoms resulting from detrussor hyperexcitability can often

be improved with an anticholinergic while intranasal vasopressin (DDAVP) may also be of help. Intermittent self catheterization is helpful when there is incomplete bladder emptying; while, if there is intractable incontinence, use of an indwelling catheter can improve the quality of life. Neurological pain, such as trigeminal neuralgia or myelopathic pain may respond to carbamazepine, gabapentin or amitriptyline, while, for cerebellar tremor, propanolol, clonazaepam or isoniazid may be of benefit. Clinical trials have shown that MS fatigue can be improved by amantidine (The Canadian MS research group, 1987) or modafinil (Rammohan *et al.*, 2002).

Neurorehabilitation

A number of studies have investigated the effect of neurorehabilitation in MS (Petajan *et al.*, 1996; Kidd and Thompson, 1997; Freeman *et al.*, 1997). Aerobic exercise improved mood, fatigue levels and levels of domestic activity (Petajan *et al.*, 1996), while a 25 day intensive inpatient therapy regime reduced the level of disability (but not clinical impairment) in chronic progressive patients in comparison to controls on the waiting list (Freeman *et al.*, 1997). Such an improvement may be sustained for up to three months following discharge (Kidd and Thompson, 1997).

Disease modifying medication – relapse reduction and prevention of progression

A range of potential MS disease modifying therapies have been assessed in the context of double blind randomized placebo controlled trials (Table 1.4).

Table 1.4. Treatments assessed for potential disease modifying effect

MS treatments assessed in double blind randomized placebo controlled trials	
Beta interferon 1a and 1b	Plasma exchange
Glatiramer acetate	Intravenous immunoglobulin
Mitoxantrone	Cyclophosphamide
Azathioprine	Cyclosporine
Methotrexate	Linomide
Cladribine	Natalizumab

Currently, beta-interferon (IFNB) and glatiramer acetate are the only disease modifying agents licensed for use in the UK. Beta-interferons were first used in MS for their possible antiviral properties, but in 1993, a definitive clinical trial revealed that IFNB1b produced a significant 31% reduction in relapse rate (IFNB MSSG, 1993). An improvement in MRI outcomes was also reported (Paty *et al.*, 1993). In 1996, a comparable reduction in relapse rate was seen with intramuscularly injected (IM) IFNB1a (Jacobs *et al.*, 1996) while, two years later, similar findings were obtained with subcutaneous (sc) IFNB1a (PRISMS, 1998). By 1998, a large trial also reported that IFNB was of clinical benefit in secondary progressive MS patients (European Study Group on Interferon B1b in Secondary Progressive MS, 1998). A clear improvement was also seen using MRI end points (Miller *et al.*, 1999), however, there was no evidence that IFNB1b slowed the rate of brain atrophy in this secondary progressive cohort (Molyneux *et al.*, 2000). Subsequent trials in secondary progressive MS have not observed a slowing of disability progression (as measured

by the EDSS) in patients treated with IFNB (SPECTRIMS, 2001; Cohen *et al.*, 2002); (although the later observed borderline evidence for a slowing of disability progression as measured by the MSFC). Interestingly, recent data from the ETOMS (early treatment of MS) study, (assessing the role of IFNB1a in clinically isolated syndromes suggestive of MS), revealed that treatment at this stage may have an ameliorating effect on brain atrophy (Filippi *et al.*, 2004).

Glatiramer acetate has also been assessed in the context of a phase III clinical trial of relapsing-remitting MS and was found to have similar clinical efficacy to IFNB in reducing relapse rate by 29% (Johnson *et al.*, 1995). In addition, glatiramer acetate produced an improvement with MRI endpoints (Comi *et al.*, 2001). However, it was not effective in a large trial in primary progressive MS (Wolinsky, 2004).

Mitoxantrone is occasionally used in the UK, albeit off-license. A phase III clinical trial revealed that mitoxantrone therapy reduced clinical progression and exacerbation rates in patients with worsening relapsing-remitting and secondary progressive MS (Hartung *et al.*, 2002). However, mitoxantrone may be cardiotoxic at high cumulative doses and it appears to be associated with a 1 in 500 risk of acute leukaemia. Therefore it tends to be reserved for patients with rapidly worsening relapsing MS.

Emerging therapies

Newer therapies are currently being investigated and may emerge in the coming years. These include Natazulimab (Tubridy *et al.*, 1999; Miller *et al.*, 2003) and Campath-IH (Coles *et al.*, 1999). Natazulimab is a humanized monoclonal antibody raised against α4 integrin and blocks the migration of lymphocytes into the CNS. As a mediator of immune cell migration, α4 integrin (which is expressed on the surface of T lymphocytes) binds to vascular cell adhesion molecule-1 (VCAM-1), and mediates the capture and subsequent transfer of T-cells across the vascular endothelia (Tubridy *et al.*, 1999). Conversely, Campath 1H is a humanized antibody which is raised against the lymphocyte antigen, CD52, and thereby results in lymphocyte depletion and immunosupression (Coles *et al.*, 1999).

In a six-month phase II controlled trial of relapsing-remitting and secondary progressive MS patients (Miller *et al* , 2003), patients treated with Natazulimab had a 90% reduction in new lesion formation and a 50-70% reduced relapse rate in comparison to those treated with placebo. The 90% reduction in lesion formation is similar to that seen with Campath-1H (Coles *et al.*, 1999) but superior to the 50-75% seen with IFNB (Miller *et al.*, 1999; Paty *et al.*, 1993; Simon *et al.*, 1998). Interestingly, despite the marked suppression of inflammatory activity seen with Campath-1H, brain atrophy continued in treated patients, while clinical progression also continued in those who had high baseline lesions volumes (Coles *et al.*, 1999).

1.9 Summary

This chapter has given an overview of multiple sclerosis and focused on a number of interesting recent advances. Studies have revealed that axons are transected in inflammatory lesions; that axonal density is reduced in normal-appearing brain tissue; and that grey matter demyelination is a consistent feature of the disease. Some studies also suggest that the Wallerian degeneration of axons, transected in lesions, may result in the loss of axons in the normal-appearing white matter. Axonal degeneration may initially be clinically silent, but in late disease, could underlie much of the permanent disability encountered in MS. Once a critical threshold of tissue damage has been reached, (corresponding to EDSS 4.0), brain injury may self-propagate, possibly because of a loss of trans-synaptic trophic support. In all, early changes in MS may have a delayed rather than an immediate clinical effect. Questions arising include 1) what are the principle causes of axonal degeneration in early disease – does grey matter demyelination have a role? 2) Can early, clinically silent tissue degeneration be monitored, allowing for treatments to be more effectively assessed? The next chapter will focus on how MRI techniques might investigate these questions.

The following (Figure 1.1) is a *hypothetical* scheme that suggests that the monitoring

of normal-appearing tissue abnormality may provide a more complete assessment of

factors that lead to later disability:
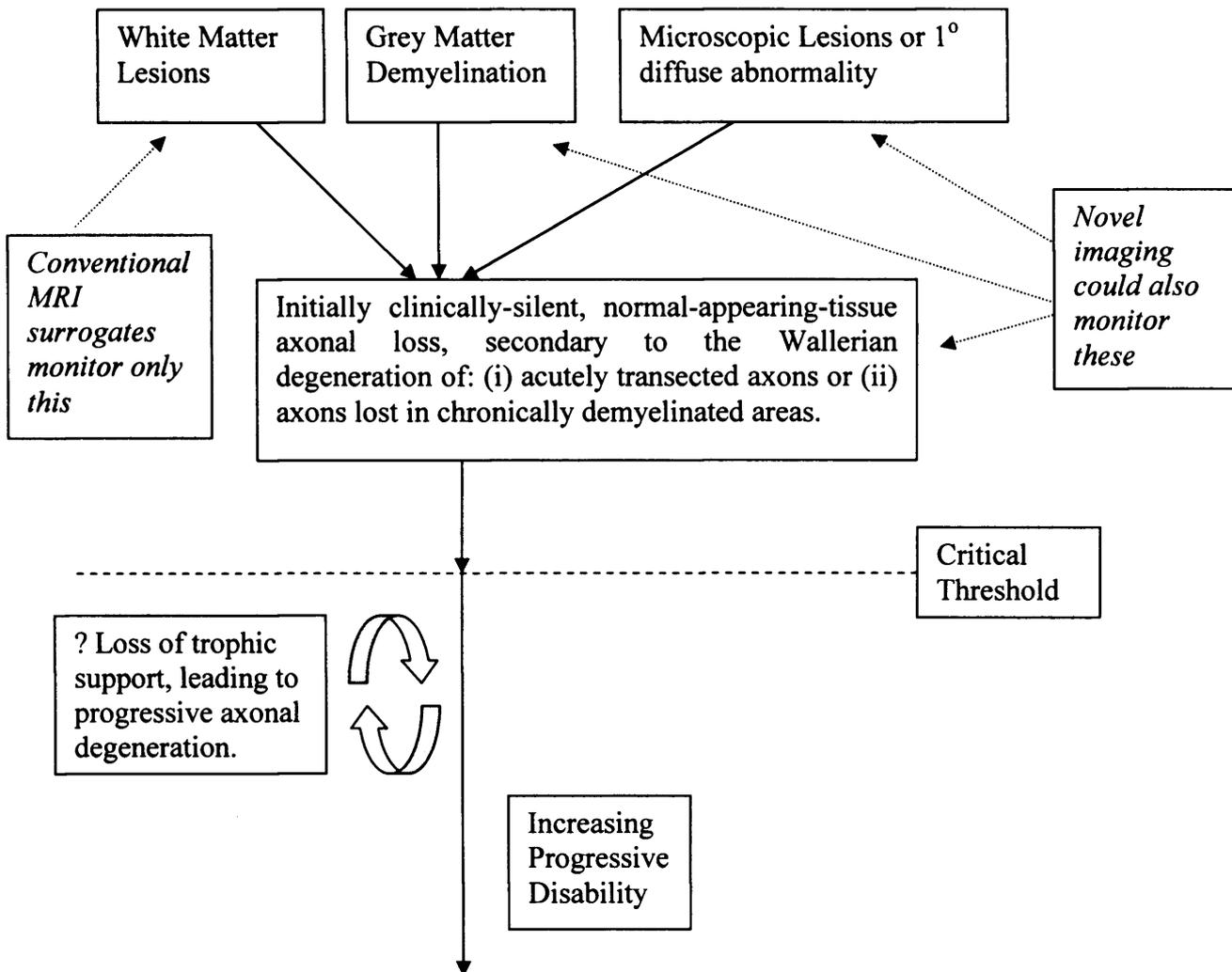
Figure 1.1. Hypothetical scheme for MS pathogenesis

CHAPTER 2

Magnetic Resonance Imaging

2.1 Basic Principles

The physics of nuclear magnetic resonance was first described by Rabi, Purcell and Bloch (Bloch, 1946), but it would take 30 years before Lauterbur and Mansfield would develop the technique for medical imaging (Lauterbur, 1974; Mansfield, 1976). Magnetic resonance imaging (MRI) is feasible because atomic nuclei develop a nuclear paramagnetic polarization in a constant magnetic field (Bloch, 1946) and, in biological tissue, this process includes the protons within water, an effect that has particular relevance in medical imaging (Hashemi and Bradley, 1997). In a clinical scanner, the static field, (typically 1.5-3.0 Tesla), is produced by the main coil, and this is applied parallel to the long axis of the subject (by convention the z-axis). While protons align with the static field (B_0), they will also precess (or rotate) about B_0 at an angular frequency (ω), the frequency of the precession depending upon the field strength, and the gyromagnetic ratio for the hydrogen proton, (γ). This relationship is given by the Larmor equation [1].

$$\omega_0 = \gamma B_0 \qquad\qquad [1]$$

To produce an MR signal, a radio-frequency pulse (B_1), is applied in the transverse (x-y) plane, at a frequency that matches ω. The resulting resonance produces two effects: 1) the protons now precess *in phase* about B_0 and 2) they slowly precess about B_1 (while continuing to rotate much more rapidly about the B_0 axis). This additional rotation tips the protons into the transverse plane (x-y) (Figure 2.1).
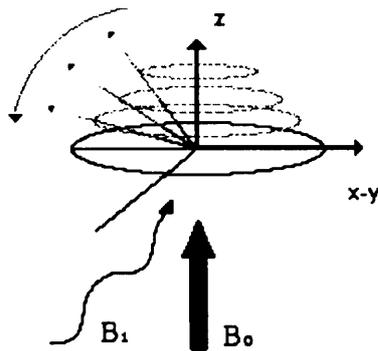
Figure 2.1. Protons precess about the B_0 field applied in the longitudinal (z) axis. The RF pulse (B_1) is applied in the transverse (x-y) plane, producing a rotation of the protons into this plane.

The MR signal is produced by the synchronous rotation of protons in the x-y plane and can be detected by the transmit-receive coil. Following the radio-frequency (RF) pulse the precessing protons rapidly dephase, resulting in a decay of the signal (this is known as T_2 decay). Simultaneously, the spins return to the longitudinal axis, and this recovery of longitudinal magnetisation is known as T_1 relaxation (see Figure 2.2). T_1 and T_2 relaxation times vary between tissues and this forms the basis for much of the tissue contrast observed in conventional MRI.

T_1 and T_2 contrast

The scanner settings can be varied to produce a difference in tissue contrast. In spin-echo imaging, the echo time (TE) is defined as the time between the 90° RF pulse and the echo centre, while the repetition time (TR) is the time between one 90° pulse and the corresponding 90° pulse repeated in the next sequence. A short TR will provide insufficient time for the longitudinal magnetisation to recover, thus providing less magnetisation for the next sequence. A difference in tissue T_1 relaxation times will result in differences in signal intensity, and a T_1 weighted image will be produced. A long TE will accentuate any difference resulting from T_2 effects, thus producing T_2 weighting. A short TE and long TR will minimize both T_1 and T_2

46

effects and tissue contrast will mainly result from the proton density of the tissue

(proton density (PD) weighting).

Figure 2.2. T_1 and T_2 relaxation.
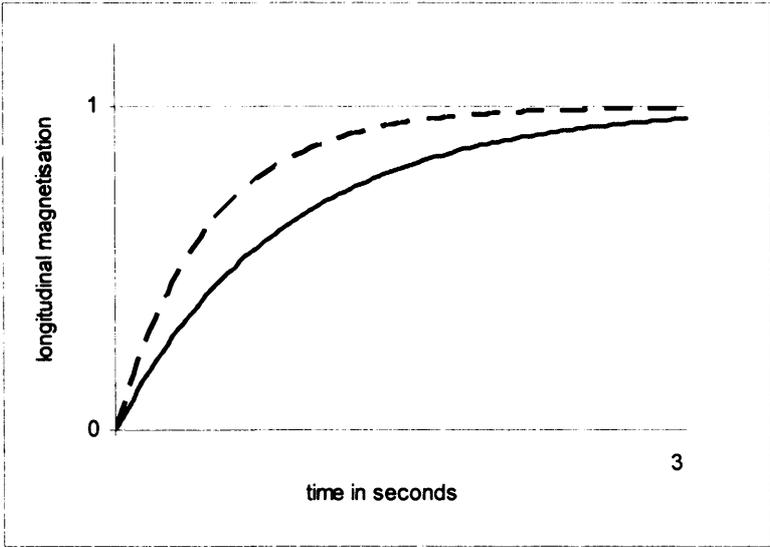
T_1 recovery of longitudinal magnetisation (after it has been completely destroyed), from tissues with T_1 relaxation times of (a) 500ms (upper) and (b) 900ms (lower)
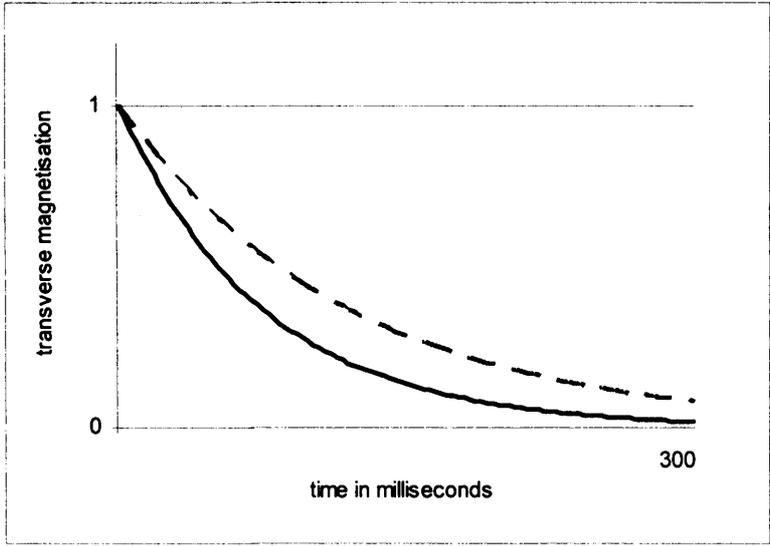
T_2 decay of transverse magnetisation from tissues with T_2 relaxation times of (a) 120ms (upper) and (b) 75ms (lower)

Gradients and k-space

The gradients used in MRI allow for an image to be reconstructed. (Gradients are magnetic fields that change from point to point, usually in a linear manner). In 2D imaging, a slice select gradient (directed along the z-axis, for axial imaging) is applied at the time of the excitation pulse. Now, only protons within the slice of interest will precess at the Larmor frequency and thus be excited by the RF pulse. Next, a phase encoding gradient is directed along the y-axis, shifting the phase of the spins depending on their y-axis position. Finally, and at the time of sampling, the frequency encoding gradient is applied along the x-axis, altering the frequency of spins (and thereby the frequency of the signal they produce) in a manner dependent on their x-axis position.

The data are collected in a data format known as k-space (the data in k-space have been algebraically manipulated so that they are in the spatial frequency domain). To successfully reconstruct the image, the phase encoding gradient alters every TR and a slightly different signal fills each line of k-space. To acquire an image with a 256x256 matrix, it is necessary to fill 256 lines of k-space (provided that the number of excitations (NEX) = 1), and this requires 256 TRs. Each line of k-space contains information from the *whole slice* and to decode this, using the spatial information provided by the phase and frequency encoding gradients, a 2D Fourier transform is performed. Essentially, the Fourier transform extracts information from complex wave forms, providing information about the amplitude and frequency of the signal. The signal intensity in each voxel can then be determined using the spatial information provided by the gradients.

The conventional spin echo (CSE) sequence uses many of the components mentioned above (see Figure 2.3). The sequence includes a slice-select, a phase-encoding and a frequency-encoding gradient together with a 90° excitation pulse. In addition, a 180° refocusing pulse is applied, inverting the direction of spin and refocusing the signal at TE. The effect of the 180° pulse is to minimize T_2^* decay effects resulting from B_0 inhomogeneity, leaving only the effect of spin-spin interaction.

Figure 2.3. Conventional spin echo pulse sequence
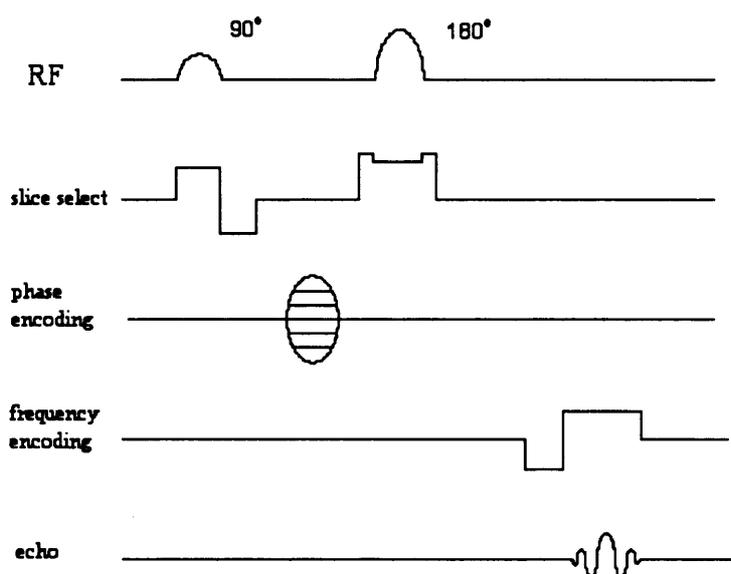
Imaging time can be reduced with the use of fast spin echo (FSE). With FSE, multiple 180° refocusing pulses are applied during every TR, (together with multiple phase encoding gradients prior to each 180° pulse). In this way, several lines of k-space can be filled during one TR, and imaging time can be reduced by a factor equal to the echo train length (the number of echoes per TR).

Gradient echo (GE) sequences also allow for fast imaging. In GE imaging, the 90°

pulse is replaced by a pulse that produces a smaller flip angle, reducing the time

needed for recovery of the longitudinal magnetisation. This allows TRs to be shorter

and for imaging time to be reduced. However, GE sequences do not include a 180°

refocusing pulse and, therefore, GE images are prone to susceptibility artifact.

The decreased imaging time afforded by GE is also useful in 3D imaging. Here the

slice select-gradient is replaced by an additional phase-encoding gradient which is

employed along the z-axis. Lines in k-space contain data from the whole three

dimensional matrix and are then reconstructed using a 3D Fourier transform.

Finally echo planar imaging also allows for images to be acquired rapidly. To

acquire an echo planar image, the frequency encoding gradient is rapidly cycled back

and forth while the phase encoding gradient is applied as a series of blips. This traces

out a trajectory in k-space and, by acquiring multiple echoes during this time, k-

space can be filled in a single TR. This allows images to be acquired very rapidly,

although image quality is significantly reduced in comparison to spin-echo or

gradient-echo imaging.

2.2 The theory of magnetisation transfer imaging

The magnetization transfer (MT) effect was first described by Wolff and Balaban (Wolff and Balaban, 1989). MT provides a novel form of tissue contrast and provides an indirect assessment of the semi-solid content of tissue. Macromolecular protons and protons within phospholipid bilayers are both semisolid, and thus are motionally restricted in comparison to water. Such protons will have a rapid T_2 decay (approximately 10^{-5} s) and the rapid loss of signal makes it impossible to directly detect them with MRI. However, motionally restricted protons have broad absorption line shapes (Figure 2.4) and will absorb energy at frequencies not included within the narrow line shape of water. In conventional MRI, the frequency of the RF pulse must match the resonant frequency of free water; (an off-resonance pulse will fail to excite the free water pool and an MR signal will not be obtained). With MTI, an additional pulse is included (with a frequency off-set from water resonance), and this semi-selectively excites the semi-solid pool while having little direct effect on free water (see Figure 2.4).

Figure 2.4. Water and semi-solid absorption rates for a range of RF frequencies.

51
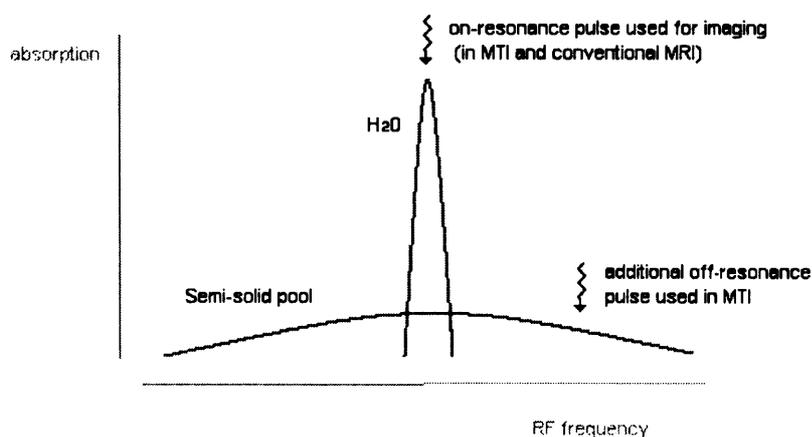
Following the off-resonance pulse, magnetisation is exchanged between the pools, resulting in a reduction of the free-water longitudinal magnetisation. This produces a saturation effect upon the image and a reduction in the signal intensity for any given voxel. The greater the semi solid content of the tissue, the greater the saturation effect, and this can be quantified using the MT ratio (MTR):

$$MTR = [M_0 - M_s]/M_0 \times 100 \text{ percent units (pu)} \quad [2]$$

M_0 : Signal intensity without MT presaturation.

M_s : Signal intensity with MT presaturation.

The absolute MTR values obtained will depend upon the amplitude and off-set frequency of the off-water-resonance pulse (as well as upon other scanner settings) (Berry *et al.*, 1999). A comparative multi-centre study, investigating healthy control subjects on six different scanners, found that cerebral white matter MTR values varied between 10 and 50 pu (Berry *et al.*, 1999). Results, however, are much more consistent if the imaging is performed using the same sequence and the same imager. In a normative study of 41 healthy subjects, (Silver *et al.*, 1997*a*), data was obtained using an interleaved spin-echo MT sequence, (Barker *et al.*, 1996), and white matter MTR values ranged between 37.6 pu and 40.6 pu. An earlier normative study, (Mehta *et al.*, 1995), investigated 68 healthy volunteers (using a different MT sequence), and found that white matter and grey matter MTR values were 36 pu and 28 pu respectively.

In the CNS, phospholipid bilayers are likely to make up a significant component of the semi-solid pool and reductions in myelin and axonal density will therefore result in a reduced MTR. Support for this comes from a number of sources:

- In MS brain at post mortem, MTR correlates with myelin and axonal density in lesions and in the normal-appearing white matter (Schmierer *et al.*, 2004*a*; van Waesberghe *et al.*, 1999). The correlation, however, between axonal density and MTR may be *secondary* to the strong underlying association between myelin and MTR (and between myelin density and axonal density) (Schmierer *et al.*, 2004*a*). MTR also correlates with myelin and axonal density in the cord (Mottershead *et al.*, 2003).

- Although a number of studies involving animal models have shown that inflammation alone can result in small MTR reductions (Dousset *et al.*, 1992; Gareau *et al.*, 2000; Stanisz *et al.*, 2004*a*), it appears that the most marked reductions are seen with demyelination and axonal loss (Dousset *et al.*, 1992, 1995, 1997; Lexa *et al.*, 1994; Kimura *et al.*, 1996; Silver *et al.*, 1996). These studies are summarized in Table 2.1 over. The *in-vivo* studies in MS patients will be covered later.

Study	Subject Group or Model	Findings
Dousset *et al.*, 1992	Experimental allergic encephalomyelitis	Small MTR decreases with oedema
Lexa *et al.*, 1994	Feline model for Wallerian degeneration	MTR reductions corresponded to areas of myelin degradation
Dousset *et al.*, 1995	Lysolecithin induced demyelination in primates	Marked MTR reductions found in areas of myelin and axonal loss
Kimura *et al.*, 1996	Porcine model of brain trauma	MTR reduced in areas of pathologically proven axonal damage
Silver *et al.*, 1996	A patient with central pontine myelinolysis	MTR reduced in the demyelinated pontine lesion.
Dousset *et al.*, 1997	HIV positive patients with radiological evidence for progressive multifocal leukencephalopathy (PML)	Markedly reduced MTR in the demyelinating lesions of PML
Gareau *et al.*, 2000	Experimental allergic encephalomyelitis	Reductions of MTR were reversed with suppression of inflammation
Stanisz *et al.*, 2004*a*	Rat sciatic nerve model of inflammation without demyelination	MTR reduced by inflammation

2.3 Quantitative models for MT

While MTR may be a useful measure, sensitive to a number of pathological changes that occur in MS, and appears to show a semi-specific link to myelin, it is not completely specific for any single pathological change. MTR, however, is a composite measure, which depends upon a number of more fundamental parameters (including the relative size and T_2 values of the semi-solid and free-water pools, and the rate of cross-relaxation between them); and the estimation of such parameters may yield additional pathological insight. *Hypothetically*, a particular pathology may exhibit a characteristic pattern of parameter abnormality, allowing the nature of pathological change to be determined. Furthermore, as these parameters are absolute measures, they also have the potential to be less dependent on scanner and acquisition parameters, making comparisons between studies more straightforward.

To estimate fundamental MT parameters it is necessary to derive a model for the MT effect, and a number have been proposed. The original models, (Henkelman *et al.*, 1993; Morrison and Henkelman, 1995), described systems where continuous saturation powers were applied. More recently, models have been developed that describe the situation on a clinical imager, where off-resonance irradiation must be applied as a series of MT pulses (Sled and Pike, 2000, 2001, Yarnykh, 2002; Yarnykh and Yuan, 2004; Ramani *et al.*, 2002; Tozer *et al.*, 2003; Tofts *et al.*, 2005). The model used in the present work (Ramani *et al.*, 2002; Tozer *et al.*, 2003; Tofts *et al.*, 2005), is based on that of Henkelman *et al.*, (1993) and Henkelman's model will therefore be discussed in detail here.

Henkelman based his model on two proton pools: the free water and semi-solid pool, (see Figure 2.5) and mathematically described the magnetisation of the two pools with sets of coupled Bloch equations (see below).
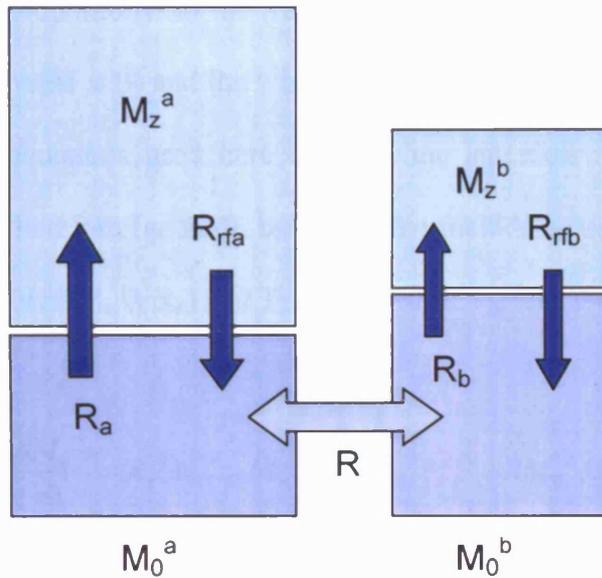
Figure 2.5: Binary spin bath model

M_0^a and M_0^b :the size of the free and semi-solid pools
M_z^a and M_z^b :remaining longitudinal magnetisation for the free and semi-solid pools
R_a and R_b : free and semi-solid longitudinal relaxation rate constants
R: rate of cross relaxation,
R_{rfa} and R_{rfb}: absorption rate constants of the free and semi-solid pool

The model includes a cross-relaxation rate (R) and the following terms for both pools: longitudinal relaxation rates (R_a and R_b), absorption rates (R_{rfa} and R_{rfb}), native magnetisations (M_0^a and M_0^b) and longitudinal magnetisations (M_z^a and M_z^b). Factors that contribute to the absorption rates (R_{rfa} and R_{rfb}) include the amplitude (ω) and off-set frequency (Δ) of the continuous MT power (ie of the off-resonance B_1 field), and the T_2 of the free and semi-solid pools respectively (T_{2a} and T_{2b}). Henkelman normalized his experiment by setting $M_0^a = 1$. The system can be

described with six coupled Bloch equations, giving the time derivatives for the magnetisation in the x, y and z planes, for both the free and semi-solid pools. If applied at *off-resonance*, B_1 exerts its effect at an angle off-set to the x-y plane (Bloch, 1946) and the magnitude of the x-y component of the B_1 vector will be proportional to ω_1/γ (since $B_1 = \omega_1/\gamma$) while the z component of the B_1 vector will be proportional to the RF offset: $2\pi\Delta/\gamma$. Bloch equations take the general form: $dM/dt = \gamma(M \times B)$ and the γ in the B_1 terms will therefore cancel (leaving ω_1 and $2\pi\Delta$). The equations used here describe the situation in the rotating frame, (B_0 effects are therefore ignored), but they also include cross relaxation terms (with R), T_1 effects (with R_a or R_b) and T_2 effects (with T_{2a} and T_{2b}).

$$\frac{dM_z^a}{dt} = R_a\left(M_0^a - M_z^a\right) - RM_0^b M_z^a + RM_0^a M_z^b + \omega_1 M_y^a \qquad [3]$$

$$\frac{dM_z^b}{dt} = R_b\left(M_0^b - M_z^b\right) - RM_0^a M_z^b + RM_0^b M_z^a + \omega_1 M_y^b \qquad [4]$$

$$\frac{dM_x^a}{dt} = -\frac{M_x^a}{T_{2a}} - 2\pi\Delta M_y^a \qquad [5]$$

$$\frac{dM_x^b}{dt} = -\frac{M_x^b}{T_{2b}} - 2\pi\Delta M_y^b \qquad [6]$$

$$\frac{dM_y^a}{dt} = -\frac{M_y^a}{T_{2a}} + 2\pi\Delta M_x^a - \omega_1 M_z^a \qquad [7]$$

$$\frac{dM_y^b}{dt} = -\frac{M_y^b}{T_{2b}} + 2\pi\Delta M_x^b - \omega_1 M_z^b \qquad [8]$$

Assuming that the system reaches steady state, the six time derivatives will equal zero. Equations [5-8] can then be re-arranged to eliminate M_y and M_x, and [3,4] can be solved for M_z^a, (recalling that $M_0^a = 1$):

$$M_z^{\ a} = \frac{R_b R M_0^{\ b} + R_{rfb} R_a + R_b R_a + R_a R}{\left(R_a + R_{rfa} + R M_0^{\ b}\right)\left(R_b + R_{rfb} + R\right) - R^2 M_0^{\ b}}$$ [9]

where:

$$R_{rfa} = \frac{\omega_1^{\ 2} T_{2a}}{1 + \left(2\pi\Delta T_{2a}\right)^2} \qquad R_{rfb} = \frac{\omega_1^{\ 2} T_{2b}}{1 + \left(2\pi\Delta T_{2b}\right)^2}$$ [10,11]

R_{rfa} and R_{rfb} describe Lorentzian line-shapes for the free and semi-solid pools, (a line-shape in this instance is the rate that the pools absorb RF irradiation for any given off-set). Henkelman, however, found that the accuracy of his model could be improved by using a Gaussian line shape for the semi-solid pool while retaining the Lorentzian line shape for free water. Although Henkelman substituted a Gaussian line shape for R_{rfb}, other line-shapes including the superLorentzian (Morrison and Henkelman, 1995) may be more appropriate for biological tissue (See part 3 for more details).

Equation [9] can be simplified by noting that $(2\pi\Delta T_{2a})^2 \gg 1$, re-substituting the Lorentzian term for R_{rfa} and dividing by R_a:

$$M_z^{\ a} = \frac{R_b\left[\dfrac{RM_0^{\ b}}{R_a}\right] + R_{rfb} + R_b + R}{\left[\dfrac{RM_0^{\ b}}{R_a}\right]\left(R_b + R_{rfb}\right) + \left(1 + \left(\dfrac{\omega_1}{2\pi\Delta}\right)^2\left[\dfrac{1}{R_a T_{2a}}\right]\right)\left(R_b + R_{rfb} + R\right)} \qquad [12]$$

This MT model is now close to the actual model used in the present work (as can be seen by comparing equation [12] with the model used in Chapter 7 of this thesis). The modifications made by Ramani *et al.*, (2002), Tozer *et al.*, (2003) and Tofts *et al.*, (2005) allow the model to be applied to a *pulsed* MT sequence, and these modifications are expanded on in Part 3.

Henkelman normalized his experiment by setting $M_0^{\ a} = 1$. In these circumstances, $M_z^{\ a}$ will equal 1-MTR and, if 1-MTR is plotted against off-set-frequency, a set of 'Z-spectra' are obtained; (each Z-spectrum corresponds to a separate MT-power amplitude) (Figure 2.6). The shape of the Z-spectra, derived from a particular tissue will depend upon the fundamental properties of the tissue, including the relative size of the semi-solid pool ($M_0^{\ b}$), the rate of cross relaxation between the two pools (R), and the motional restriction of the semi-solid protons (T_{2b} - obtained via R_{rfb}). Differing pathologies may have different patterns of parameter abnormality, hypothetically allowing pathological processes to be distinguished.

In vivo parameter estimation can then be achieved by acquiring a number of data points, each acquired using a unique MT-power offset-frequency - amplitude combination. For each data point, the MTR is measured within a region of interest and a least-squares fitting technique is used to fit the model to the data. Estimates of the fundamental parameters can then be derived.

Figure 2.6. Z spectra obtained for three MT pulse amplitudes. As the offset of the MT pulse increases, saturation diminishes (and 1-MTR approaches 1). The steep portion of the curve relates to direct water saturation, whereas the shoulder relates to the indirect saturation of water via the semi-solid pool (ie the MT effect).
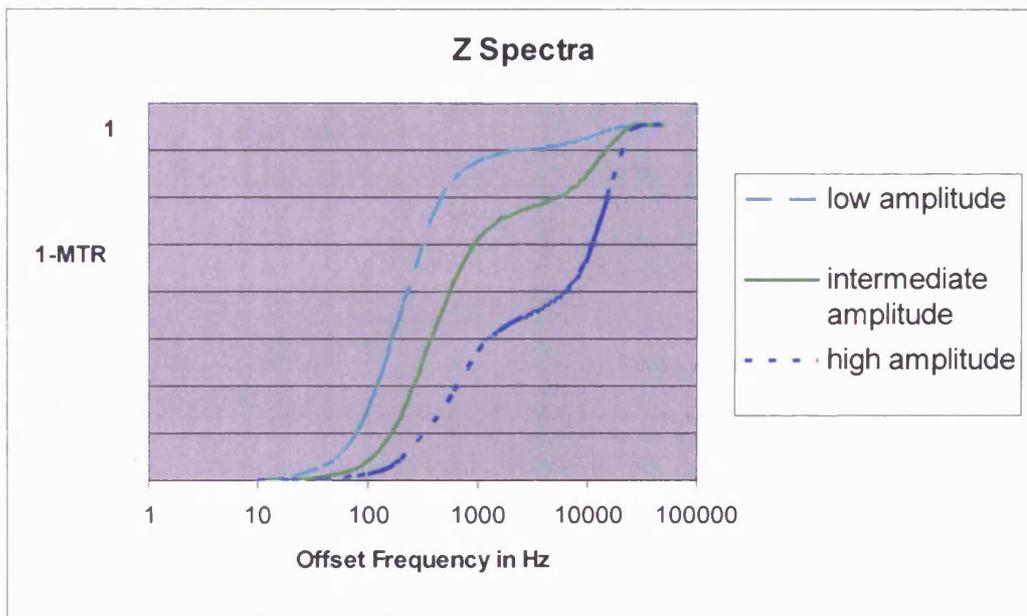
Figures 2.7a (above) and 2.7b (below). Fitting the model to data obtained from an MS white matter region of interest (reproduced from Davies *et al.*, 2003) (see text below for explanation). A Gaussian line shape has been assumed for the absorption line shape of the semi-solid pool.
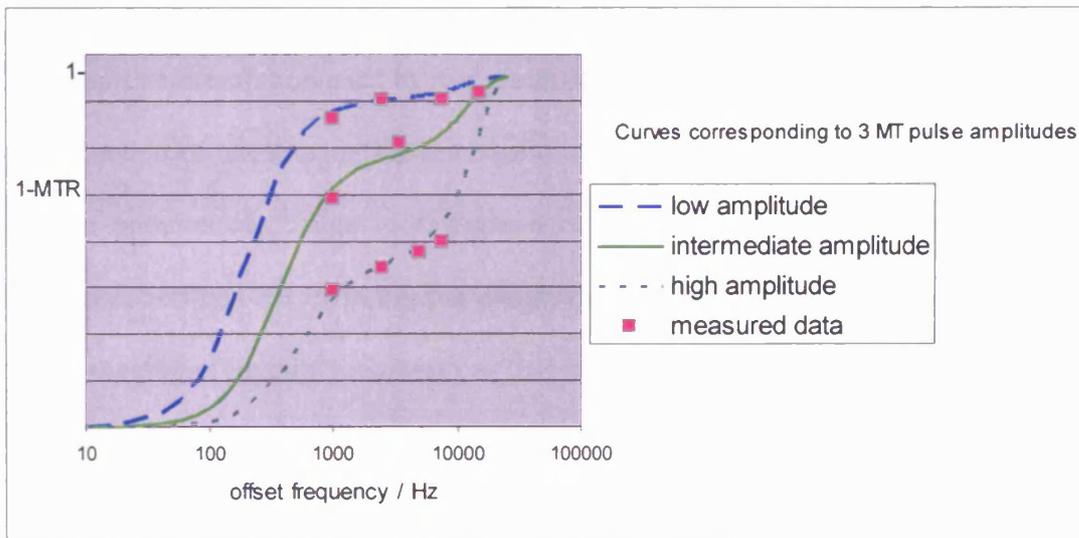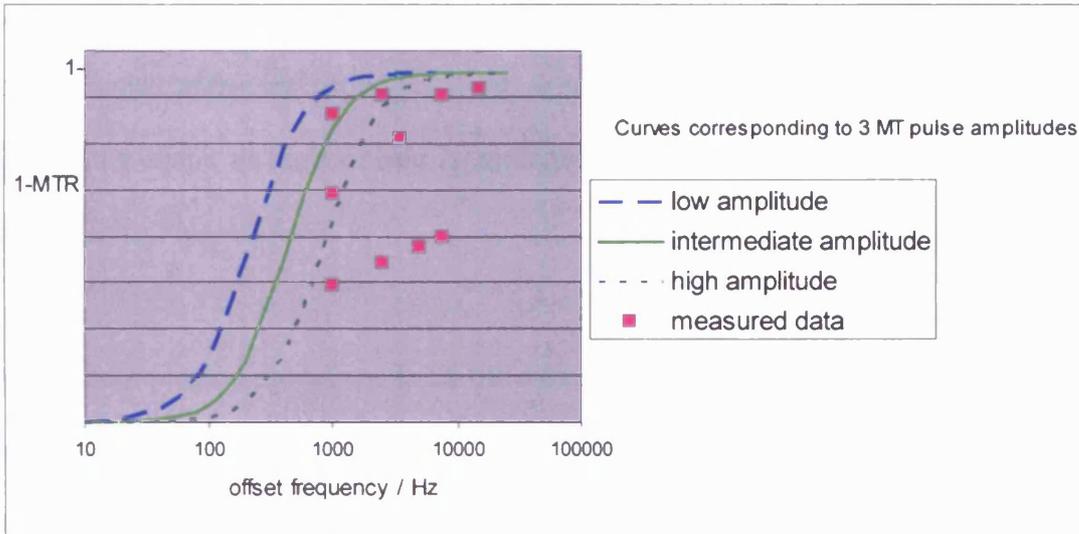
Figure 2.7 provides an example of curve fitting. To illustrate this, M_0^b (the size of the semi-solid pool) is increased while other parameters are kept constant. The upper Z spectra (Figure 2.7a) reflect a scenario where the semi-solid content of tissue is zero ($M_0^b = 0$). In this case, the only effect that the MT power can have is to *directly*

61

saturate the free water, a phenomenon that only occurs if the MT RF is close to water resonance. The Z-spectra are therefore steep and the saturation effect rapidly diminishes with increasing RF off-set. Furthermore, when $M_0^b = 0$, the Z spectra describe the Lorentzian line-shape of free water and are analogous to the water line-shape illustrated in Figure 2.4. As the semi-solid concentration increases (Figure 2.7b), the curve develops a shoulder at high off-sets an effect resulting from the magnetisation of the semi-solid pool, and an *indirect* effect on water. The broadening of the line shape at high offsets is analogous to the broad semi-solid line shape illustrated in Figure 2.4.

In this example, the model has been fitted simply by altering M_0^b, but, in reality, all parameters within the model (including T_{2b} and R) will also have an effect on the spectral shape and are estimated during the least squares fitting.

One simple reformulation used by our group is the derivation of the parameter f. This is the fraction of tissue which is semi-solid and is defined as $f = M_0^b/(M_0^a + M_0^b)$. Whether patterns of change in f, T_{2b} and other underlying MT parameters could distinguish between the differing pathological processes in MS, or be more specific for the imaging of myelin, are questions that are asked in part three of this thesis.

2.4 The use of MRI in the study of multiple sclerosis

2.4.1 Conventional MRI

The first MRI studies of multiple sclerosis (Young *et al.*, 1981; Bailes *et al.*, 1982) revealed that the technique was particularly sensitive for the detection of MS lesions. Lesions are visible on T_2 weighted imaging (Bailes *et al.*, 1982) and these correspond to MS plaques at post mortem (Stewart *et al.* 1984; Ormerod *et al.* 1987). MRI allows for disease activity to be assessed: acute inflammatory lesions will enhance with gadolinium (whereas chronic lesions typically do not) (Grossman *et al.*, 1986; Katz *et al.*, 1993), and an indication of the extent of the disease can be obtained by measuring the total volume of lesions on T_2 weighted images (IFNB MSSG, 1995). MRI has therefore been used to monitor the effect of treatment (Miller, 2002) and to study the natural history of the disease.

Diagnosis of MS

MRI is invaluable in the diagnosis of MS and a number of diagnostic criteria, integrating the information provided by MRI, have been devised (Paty *et al.*, 1988; Fazekas *et al.*, 1988; Barkhof *et al.*, 1997; McDonald *et al.*, 2001). The current guidelines of McDonald *et al.*, (2001) (See Chapter 1 for details) may be particularly sensitive and specific for the diagnosis of MS (Dalton *et al.*, 2002).

T_2 lesions and the prognosis following a clinically isolated syndrome

Studies have also shown that prognostic information can be provided by MRI. The presence of brain lesions at the time of a clinically isolated syndrome (CIS) suggestive of MS indicates that there is an increased risk for the subsequent

development of clinically definite MS. One study (O'Riordan *et al.* 1998) showed that the risk of MS, ten years following a CIS, was 83% in those with an abnormal brain MRI at baseline but only 11% in those with normal brain imaging.

Early changes in T_2 lesion load and disability

Conventional MRI has also provided an invaluable insight into the pathological mechanisms that occur in MS. The accrual of lesions (on T_2 weighted imaging), early in the disease course, has a greater impact on long term disability than the accumulation of lesions later. A study investigating a cohort of CIS patients (Sailer *et al.*, 1999) showed that increases in lesion volume during the first five years, correlated well with changes in disability during that period. However, increases in lesion volume, in the subsequent five year period, correlated relatively poorly with changes in disability over that time. At 14 years, the change in lesion load over the first five years was the best predictor of long term disability (r = 0.61) (Brex *et al.*, 2002).

Gadolinium enhanced imaging

Gadolinium (Gd), chelated to diethylene-triamine-pentacetic acid (Gd-DTPA) is used as a contrast agent in MRI. Gadolinium shortens the T_1 relaxation time of surrounding water protons and the presence of Gd will manifest as a bright hyperintensity on T_1 weighed images. Gadolinium is intravenously injected and therefore the breakdown of the blood-brain-barrier, (a process known to occur in acute MS lesions), will result in Gd enhancement (Bruck *et al.*, 1997). Most new lesions enhance, (Lai *et al.*, 1996), including newly symptomatic lesions (Miller *et al.*, 1988). However, enhancing lesions occur within the brain five to ten times more

frequently than clinical relapses (Miller *et al.*, 1988). Although the predictive value

for disability is poor (Kappos *et al.*, 1999), Gd enhancement is a useful measure of

disease activity and has been used widely in MS clinical trials (Miller, 2002).

T_1 hypointense lesions

A proportion of lesions remain hypointense on T_1 weighted images following

cessation of Gd enhancement (Bagnato *et al.*, 2003). Lesions which are persistently

hypointense, (as opposed to lesions with less marked T_1 abnormality), are associated

with a reduced N-acetyl-aspartate concentration (Brex *et al.*, 2000*a*; van Walderveen

et al., 1999) and reduced axonal density (Bruck *et al.*, 1997; van Waesberghe *et al.*,

1999). Some studies have shown that there is a stronger correlation between T_1

lesion load and the EDSS than between T_2 lesion load and the EDSS (van

Walderveen *et al.*, 1995; Truyen *et al.*, 1996).

Conventional MRI of the spinal cord

Imaging of the spinal cord in MS may also be important, particularly as the cord may

be the only region of the CNS were lesions are detected (Thorpe *et al.*, 1996*a*). Cord

lesions are more commonly found in the cervical as opposed to the thoracic cord

(Kidd *et al.*, 1993) and new cord lesions, (as opposed to new brain lesions), are more

likely to cause a relapse (Thorpe *et al.*, 1996*b*). Furthermore, diffuse signal change

within the cord is associated with disability (Nijeholt *et al.*, 1997).

2.4.2 Novel Imaging Measures in MS

While conventional MRI has been of considerable use in the study of MS, it should be noted that brain lesion load (as calculated using T_2 weighted imaging) appears to account for – at most - a third of the variability in clinical status (Brex *et al.*, 2002; Molyneux *et al.*, 2001). The modest correlation between disability and lesion load may partly be explained by the pathological heterogeneity of lesions (Barnes *et al.*, 1991; Brex *et al.*, 2000; van Walderveen *et al.*, 1999) and by their varying anatomical distribution (Hickman *et al.*, 2001). However, abnormality within normal-appearing tissue may also contribute to disability. Focus has therefore turned to the investigation of lesions and normal appearing tissue using a number of quantitative MR parameters. Novel MRI techniques include: the measurement of brain and cord atrophy, MR spectroscopy (MRS), diffusion tensor imaging (DTI), T_1 relaxation time measurement, and magnetisation transfer imaging.

Atrophy

In relapsing-remitting MS, brain atrophy occurs at a rate greater than that seen in the normal healthy population (Losseff *et al.*, 1996a; Rudick *et al.*, 1999; Simon *et al.*, 1999; Fox *et al.*, 2000; Ge *et al.*, 2000; Chard *et al.*, 2004). Loss of brain volume affects both grey matter and white matter, and grey matter atrophy is already present at a very early stage of the disease (Chard *et al.*, 2002a; De Stefano *et al.*, 2003; Dalton *et al.*, 2004). Of note, measures of brain atrophy may make a reliable surrogate for axonal/neuronal loss, particularly as 46% of white matter volume consists of axons whereas only 24% consists of myelin (Miller *et al.*, 2002). Furthermore, atrophy measures are associated with disability (Kalkers *et al.*, 2001).

Early changes in lesion load have been associated with subsequent brain volume loss (Chard *et al.*, 2003), but the modest correlation suggests that lesions are not the only factor resulting in global volume changes (Kalkers *et al.*, 2002).

A number of studies have also demonstrated the presence of cord atrophy in MS patients and an association between cervical cord volume and disability has been observed (Hickman and Miller, 2000). A semi-automated technique, measuring cervical cord volume from fast-spoiled gradient echo images, has proven particularly reproducible (Losseff *et al.*, 1996). Studies using the technique found a good correlation between cord cross-sectional area and disability (Losseff *et al.*, 1996) and that cord atrophy progressed over time (Stevenson *et al.*, 1998).

T_1 relaxation time

T_1 relaxation is abnormally prolonged in MS normal appearing white matter (Miller *et al.*, 1989; Kesselring *et al.*, 1989; Barbosa *et al.*, 1994; Haughton *et al.*, 1992; Larsson *et al.*, 1998), although the abnormality may partly be due to the contribution from microscopic lesions (Barbosa *et al.*, 1994). Measuring T_1 globally (with relaxation times from numerous voxels represented as a histogram) could provide a better assessment of disease burden (Vaithianathar *et al.*, 2002; Griffin *et al.*, 2002*a*., Parry *et al.*, 2002). T_1 histogram metrics derived from normal appearing brain tissue (Griffin *et al.*, 2002*a*) and white matter (Parry *et al.*, 2002) have been correlated with disability, while T_1 metrics from normal appearing white matter correlate with both T_2 lesion load and atrophy (Vaithianathar *et al.*, 2002). Of note, normal appearing brain tissue T_1 abnormality was apparent in clinically early relapsing-remitting MS, within three years of symptom onset (Griffin *et al.*, 2002*a*). Furthermore, a recent

67

study (Parry *et al.*, 2003) reported that T_1 relaxation time in the neocortical grey matter and the normal appearing white matter progressively increased in clinically definite MS patients followed-up for ~20 months.

MR Spectroscopy

MR spectroscopy (MRS) is a technique that allows for the quantification of metabolites in human brain tissue. Each metabolite precesses with a distinct Larmor frequency and, by performing a Fourier transform on the free induction decay, a spectrum of metabolites can be produced. A number of additional steps are needed including suppression of the dominant water peak but, once achieved, the amplitude of each peak in the spectrum provides an estimate of metabolite concentration. Prominent metabolite peaks from brain tissue include: N-acetyl-aspartate (NAA) (a metabolite found exclusively in neurons), myo-inositol, choline, creatine and glutamate. Studies of MS using MRS have reported reductions in NAA concentration in lesions and NAWM (Davie *et al.*, 1997; Fu *et al.*, 1998; van Walderveen *et al.*, 1999); with the latter occurring within three years of clinical onset (Chard *et al.*, 2002*b*). Myo-inositol, a potential marker for glia is elevated in the NAWM in CIS suggestive of MS and in early relapsing-remitting MS (Fernando *et al.*, 2004; Chard *et al.*, 2002*b*), suggesting that glial proliferation within NAWM is also an early event. In cortical grey matter, NAA and glutamate concentrations are also reduced, again at an early stage of the disease (Chard *et al.*, 2002*b*).

Diffusion Tensor Imaging

Diffusion tensor imaging (DTI) allows for the characterization of fibre tract integrity and anatomy. A diffusion gradient is applied, followed by a 180^0 refocusing pulse and then by a further diffusion gradient. The phase shift produced by the first gradient is inverted by the 180^0 pulse and then refocused by the second gradient. Molecules that have diffused during this time will be subjected to a different field with the second gradient and, as a result, will not fully refocus. The amount of resulting signal loss relates to the distance that molecules have diffused and this can be quantified with the apparent diffusion coefficient (ADC). Diffusion imaging can also provide information about the preferential direction of diffusion (anisotropy) and since diffusion along a nerve fibre tract should be greater than diffusion across fibre tracts, fibre tract orientation can be determined. The extent that diffusion is anisotropic can be quantified by analyzing the diffusion tensor (a matrix describing the diffusion coefficient in three dimensions); and the two most commonly used parameters resulting from this analysis are the mean diffusivity (MD) and fractional anisotropy (FA). The ADC, MD and FA are sensitive to pathological change in MS and the following salient findings have been reported: (1) DTI parameters are abnormal in lesions, NAWM and deep grey matter (Cercignani *et al.*, 2000; Ciccarelli *et al.*, 2001) and (2) that DTI measures from NAWM correlate with disability (Ciccarelli *et al.*, 2001). ADC increases have also been observed in NAWM that later develops into a lesion (Werring *et al.*, 2000). However, the changes in diffusion characteristics observable within normal-appearing tissues in early disease are subtle and difficult to detect (Rashid *et al.*, 2004).

Magnetisation Transfer Imaging In MS

(i) Early Studies

In the first magnetisation transfer imaging study of MS patients, MTR was found to be reduced in MS lesions (Dousset *et al.*, 1992); (the MTR was reduced by ~26%, substantially more than the 5-8% seen in the purely oedematous lesions of guinea pig experimental-allergic-encephalomyelitis). Significant reductions were also seen in the normal appearing white matter (NAWM). The presence of MTR abnormality in MS NAWM was later confirmed using a region of interest approach (Filippi *et al.*, 1995; Loevner *et al.*, 1995). Another, early study reported that mean lesion MTR correlated with measures of disability (Gass *et al.*, 1994).

(ii) MS clinical subgroup studies using whole brain MTR histograms

Histogram analysis, (whereby MTR values from the whole brain are represented in a histogram), allows for a global assessment of disease burden. Histogram metrics are likely to show increased sensitivity in comparison to measures derived from small regions of interest, particularly as histograms may be more effective at detecting the subtle abnormalities found within normal-appearing brain tissue (van Buchem *et al.*, 1996). A number of studies have reported differences between MS clinical subgroups using whole brain MTR histograms (Filippi *et al.*, 1999; Tortorella *et al.*, 2000; Dehmeshki *et al.*, 2001, Traboulsee *et al.*, 2003). These studies have shown the following: (1) patients with benign MS had similar histogram metrics to those with clinically isolated syndromes suggestive of MS; and both showed only subtle abnormality in comparison to healthy controls; (2) patients with relapsing-remitting MS had more marked abnormality than either benign MS or CIS patients; and (3)

those with secondary progressive and primary progressive MS had more severely affected histogram metrics in comparison to those with relapsing-remitting MS. Furthermore, a study comparing secondary progressive and primary progressive MS patients (Rovaris *et al.*, 2001) found that there was no difference between these groups in terms of their MTR histogram metrics, despite the fact that the secondary progressive cohort had a higher lesion volume.

(iii) Whole brain MTR histograms are sensitive to change over time

Measures derived from whole brain MTR histograms are able to detect a progressive decline in MTR over time, in patients with secondary progressive MS, relapsing-remitting MS or both (Rocca *et al.*, 1999; Patel *et al.*, 1999; van Buchem *et al.*, 1998). A year-long follow-up study, investigating patients from all MS clinical subgroups, revealed that whole brain MTR decreased over time in all types of MS and in those with a CIS suggestive of MS (Filippi *et al.*, 2000*a*). A further serial study of CIS patients, (Iannucci *et al.*, 2000), reported the presence of MTR abnormality in the normal appearing brain tissue of CIS patients, and that lower MTR values were obtained from those who eventually developed clinically definite MS. In contrast, similar MTR abnormalities were observed when comparing the normal appearing brain tissue of patients who had experienced a recent CIS (~4 months previously) in comparison to those who had presented with a CIS 14 years previously (but who had not subsequently developed clinically definite MS) (Traboulsee *et al.*, 2002).

(iv) MTR histogram metrics correlate with disability in MS

Measures derived from whole brain MTR histograms are associated with disability. Studies have shown a relationship with physical disability (van Waesberghe *et al.*, 1998*a*; Iannucci *et al.*, 1999; Traboulsee *et al.*, 2003), and with cognitive impairment (Rovaris et al., 1998; Comi *et al.*, 1999; Rovaris *et al.*, 2000; Zivadinov *et al.*, 2001). The use of principle component analysis (which maximizes the variability between histograms), appears to improve the correlation between whole brain MTR and disability measures (Dehmeshki *et al.*, 2001).

(v) MTR measures from pre-lesional MS NAWM

A number of serial MTI studies have investigated regions of NAWM which later developed into a lesion. Some have shown that the MTR falls in the months prior to lesion enhancement (Filippi *et al.*, 1998; Goodkin *et al.*, 1998; Laule *et al*, 2003); while others have not (Silver *et al.*, 1998; Dousset *et al.*, 1998). MTR has also been reported to fall prior to the development of a new T_2 lesion (Pike *et al.*, 2000). These findings suggest that microscopic changes occur within the NAWM prior to the marked blood-brain barrier breakdown detected by Gd enhancement. Following lesion enhancement, the MTR may either recover (Lai *et al.*, 1997), remain depressed, or continue to progressively decline, presumably reflecting heterogeneity in lesion pathology and repair (van Waesberghe *et al.*, 1998*b*; Dousset *et al.*, 1998; Laule *et al.*, 2003).

(vi) MTR measures of MS normal-appearing grey and white matter

Recent advances in image analysis software have enabled images to be segmented into grey matter and white matter and, therefore, for the investigation of both tissues separately. Studies have reported that grey matter MTR is reduced in clinically definite MS (Cercignani *et al.*, 2001), and that grey matter MTR abnormality in relapsing-remitting MS is related to the EDSS (Ge *et al.*, 2001). Furthermore, grey matter MTR abnormality is more marked in those with secondary progressive MS than in those with relapsing-remitting MS (Ge *et al.*, 2002). Grey matter MTR abnormality has also been observed in patients with clinically isolated syndromes suggestive of MS (Traboulsee *et al.*, 2002), and MTR abnormality is also apparent within the *deep* grey matter of such patients (Audoin *et al.*, 2004).

Furthermore, studies (using measures derived from small regions of interest) have revealed the presence of NAWM MTR abnormality (although not grey matter abnormality) in minimally disabled patients with early relapsing remitting MS (Griffin *et al.*, 2002*b*; De Stefano *et al.*, 2002).

(vi) Predictive value of normal-appearing brain tissue MTR

Recent evidence suggests that normal-appearing brain tissue MTR abnormality might predict future disability. In a longitudinal study, (Santos *et al.*, 2002), NAWM MTR values at baseline were related to the change in clinical disability over the subsequent five years (r = -0.76). Furthermore, a study of 73 MS patients followed up for a mean of 4.5 years (Rovaris *et al.*, 2003) found that the change in whole brain MTR over the first year and the baseline T_2 lesion load were predictive of medium term disability (r^2 = 0.23).

(vii) *MTI of the optic nerves and spinal cord*

A number of studies have observed a decline in optic nerve MTR following an episode of optic neuritis (Hickman *et al.*, 2004; Inglese *et al.*, 2002; Thorpe *et al.*, 1995). Following optic neuritis, MTR continues to decline on average for approximately 8 months before showing some recovery (Hickman *et al.*, 2004). Of note, lower MTR values were observed in those who had a poor visual recovery in comparison to those who recovered well (Inglese *et al.*, 2002).

MTR has also been measured in the cervical cord of patients with MS (Silver *et al.*, 1997*b*). Lower MTR values were observed in those with locomotor disability (Bozzali *et al.*, 1999) and those with progressive forms of MS (Filippi *et al.*, 2000*b*). The EDSS was also seen to correlate weakly with upper cord MTR (Nijeholt *et al.*, 2000).

(viii) *The use of MTI in therapeutic trials*

Several studies have assessed the effect of MS therapy on MTR. The rate of MTR recovery in acute lesions, (following the onset of enhancement), was more rapid when patients were treated with steroids (Richert *et al.*, 2001) or IFNB (Richert *et al.*, 2001; Kita *et al.*, 2000). However, IFNB had no effect on whole brain MTR, either in a IFNB1b crossover trial investigating patients with relapsing-remitting MS (Richert *et al.*, 1998); or in a multi-centre, double-blind, placebo-controlled trial of IFNB1b in secondary progressive MS (Inglese *et al.*, 2003).

2.4.3 Surrogate Outcome Measures in MS

There are a number of difficulties in conducting clinical trials in MS using clinical endpoints alone. Disability in MS develops slowly, typically over decades, and placebo controlled clinical trials need to run for 2-3 years and recruit several hundred patients if therapies are to be adequately assessed (Miller, 2002). To assess the effect of therapy on *long* term disability further follow-up may be required, (possibly as part of an open-label study since it may not be feasible to run a placebo controlled study for more than 3 years). However, even a long term open label study would be a major undertaking and it might be useful to assess whether a therapy has *potential* to prevent long term disability, prior to embarking on such a study. Surrogate outcome measures may be helpful in this regard, particularly if they are sufficiently sensitive to detect treatment effects in small numbers of patients followed up for short periods. It is essential however, that such measures are predictive of future disability and that they are accurate, objective and reproducible (Miller, 2002).

A consensus has recently been reached concerning the key requirements needed for any MS surrogate (McFarland *et al.*, 2002): Importantly, a surrogate should predict a clinically meaningful outcome and it should be sensitive and specific for pathological change that leads to later disability.

Ideally, a surrogate would also be sensitive to change over time in *early* MS, at a stage prior to the onset of major disability. (A measure that only detected abnormality following the onset of permanent disability would be of little use in assessing the effect of therapy on *preventing* disability).

In some regards, the measurement of T_2 lesion load fulfills the requirements for a surrogate: (1) T_2 lesion load increases over time in CIS suggestive of MS (Sailer *et al.*, 1999), allowing the effects of treatment to be detected (IFNB MSSG, 1995); and (2) early changes in T_2 lesion load are, to a limited extent, predictive of permanent disability (Brex *et al.*, 2002). However, in one particularly long follow-up study (14 years, Brex *et al.*, 2002), changes in T_2 lesion load only explained a proportion (~30-40%) of the variance in long term disability, raising the possibility that, even with a marked suppression of T_2 lesion accrual, long term disability could still occur (possibly via changes not detected by T_2 weighted imaging). Furthermore, there is evidence that IFNBs almost completely stabilize T_2 lesion volume in secondary-progressive MS, but that they don't prevent an increase in disability (Miller *et al.*, 1999; SPECTRIMS, 2001).

In Chapter 1, evidence was presented on the existence of pathological abnormality within the NAWM and grey matter. By quantifying such changes, and combining these with lesion load measures, it may be possible to obtain a more complete assessment of the disease. *Hypothetically*, this may improve the predictive power of MRI for future disability allowing therapies to be more effectively assessed. In this way, it may be possible to gain some insight into which therapies might *potentially* prevent long term disability (and which therapies should be assessed further using clinical endpoints).

However, it should also be noted that there are a number of additional reasons for the modest correlation between T_2 lesion load and disability (beyond the fact that grey matter and NAWM abnormality may contribute to disability). These include (1) the pathological heterogeneity of lesions; (2) the varying distribution of lesions; (3) measurement error; (4) the fact that lesions may have different effects on disability accumulation at different stages of MS: more so in early relapsing-remitting disease and less so during the progressive stages.

Long term natural history studies are therefore needed to ascertain whether grey matter and NAWM abnormality contribute to future disability. The early relapsing-remitting MS patients studied in this thesis have currently been followed up for ~3 years and the long term data needed to answer this last question is not yet available. However, it has been possible to address an equally important question: whether MTR and T_1 relaxation time can detect change over time in early MS.

2.5 Summary

In this chapter, conventional and novel MRI techniques have been reviewed. A number of novel MRI techniques (including T_1 relaxation time measurement and MTR) appear to be sensitive to MS pathology in NAWM and grey matter, even at the earliest stages of the disease.

By studying a cohort of patients with early relapsing-remitting MS and minimal disability it may now be possible to describe the evolution of the NAWM and grey matter change in early MS. It would also be useful to investigate whether such changes are clinically relevant. Furthermore, it would be interesting to investigate the clinical relevance of parameters (such as f and T_{2b}) that underlie the MT effect.

With relevance to Chapters 3-8, questions that, at the time of the study, were unanswered included:

- Can histogram analysis detect grey matter MTR abnormality in early MS?

- Is grey matter and/or NAWM MTR abnormality in early MS clinically relevant?

- Can T_1 or MTR histograms detect changes over time in early MS?

- Can MTR abnormality be detected in the deep grey matter?

- Are the underlying MT parameters (f and T_{2b}) of clinical relevance in MS?

PART 2

THE INVESTIGATION OF EARLY RELAPSING-REMITTING

MULTIPLE SCLEROSIS

CHAPTER 3

Normal appearing grey and white matter T_1 abnormality in early relapsing remitting multiple sclerosis: a longitudinal study.

In the last chapter, evidence was presented suggesting that the brain T_2 lesion load in MS might account for a modest proportion - possibly up to a third - of the variability in clinical status (Molyneux et al., 2001; Brex et al., 2002). As mentioned, the modest correlation may partly arise because lesions are pathologically heterogeneous (Barnes et al., 1991; Brex et al., 2000; van Walderveen et al., 1999) and because they vary in their anatomical distribution (Hickman et al., 2001). However, widespread abnormality - outside of macroscopic lesions - within the brain and cord could also contribute to clinical impairment, and measures that quantify this change might explain a greater proportion of the variance in disability. Indeed, such measures could be of potential use in the assessment of disease modifying therapy, (for instance, if they are used as secondary surrogate endpoints in clinical trials).

As mentioned, the T_1 relaxation time is a quantitative MR measure that is abnormally prolonged in MS normal appearing white matter (NAWM) (Miller et al., 1989; Kesselring et al., 1989; Barbosa et al., 1994; Haughton et al., 1992; Larsson et al., 1998). Furthermore, a number of recent studies have suggested that the global measurement of T_1 (with relaxation times from numerous brain tissue voxels represented as a histogram) could provide a good assessment of disease burden (Vaithianathar et al., 2002; Griffin et al., 2002a; Parry et al., 2002). Recently, Parry et al., (2003) reported that grey matter and NAWM T_1 abnormality increased over

time in a cohort of secondary progressive and relapsing remitting MS patients followed-up for ~20 months.

It should also be noted that whole brain T_1 histograms are sufficiently sensitive to detect the subtle abnormalities occurring within the normal appearing brain tissue in minimally disabled patients with early relapsing-remitting MS (Griffin *et al.*, 2002*a*). A region of interest analysis of the same cohort revealed that T_1 was not only prolonged in NAWM but was also abnormal in NAGM (Griffin *et al*, 2002*b*).

Early change in GM and NAWM may play a role in the development of disability (Rovaris *et al.*, 2003; Chard *et al.*, 2002*b*) and MR techniques that can detect this change could potentially be of use as secondary endpoints in clinical trials. In the previous chapter, it was noted that, to act as a surrogate endpoint, measures must be predictive of a clinically relevant outcome (McFarland *et al.*, 2002) and, ideally, they should be sensitive to change over time prior to the onset of permanent disability. Therefore, the aim of this study was to assess whether the present technique was able to detect increasing NAWM and NAGM T_1 abnormality in a cohort of minimally disabled patients with early relapsing-remitting MS.

3.1 Methods.

Subjects

Twenty three patients with early clinically-definite relapsing-remitting MS (Poser *et al.*, 1983; Lublin and Reingold, 1996) (Six male and 17 female; mean age 36 years, range 24-55 years; mean disease duration at baseline (time from first symptoms): 2.0 years, range 1.2 to 3.7 years; median expanded disability status scale (EDSS) (Kurtzke, 1983) score 1.0, range 0-2.5) were imaged six monthly. At baseline, no subjects with MS were taking disease-modifying medication. Fourteen healthy controls (seven male and seven female, mean age 35 years, range 27-52 years) were also studied. Mean follow up was 26 months for MS subjects (range 6-38 months) and 24 months for controls (range 6-36 months).

The study was approved by the ethics committee for the National Hospital for Neurology and Neurosurgery, Queen Square, UK. Written informed consent was obtained from all subjects.

Magnetic Resonance Imaging

Three sequences were obtained in all subjects: Firstly, a dual-echo fast spin-echo (FSE) sequence was acquired for lesion identification (repetition time (TR) 2000ms, echo time (TE) 19/95ms, 28 contiguous 5mm axial slices covering the whole brain). In addition, proton-density and T_1 weighted gradient-echo data sets were acquired for

T_1 estimation. The TR/TE/flip angle/no. of averages for the PD and T_1 weighted images were 1500ms/11ms/45°/8 and 50ms/11ms/45°/2 respectively.

T_1 was estimated while accounting for B_1 inhomogeneity and an imperfect slice profile (Parker *et al.*, 2001). In brief, flip angles vary throughout the thickness of a slice, and differ from the nominal flip angle prescribed. Although the prescan sequence will adjust the pulse profile, (setting the central portion of the slice to the nominal value), flip angles will nonetheless vary with distance perpendicular to the slice plane. To obtain a more accurate assessment of the signal contribution from the whole slice, Parker *et al.* (2001) used Bloch simulations to estimate the resultant response of the magnetization vector across the 5mm slice thickness (for a range of nominal flip angles). Signal contributions could then be integrated across the slice profile, providing an estimate of the true total signal (Parker *et al.*, 2001). The coil B_1 distribution was also determined with the use of a phantom (with uniform proton density, T_1 and T_2), and this data was used to describe how B_1 varies relative to the centre of the head coil (Parker *et al.*, 2001). With this information, T_1 can be estimated with the use of a look-up table relating the signal intensity (SI) ratio (obtained from the T_1 and PD weighted GE data sets) to the T_1 relaxation time at any given distance from the coil centre. The look-up table's ratios (namely, the ratio of T_1-weighted SI to PD-weighted SI) are calculated, accounting for the slice profile as above. (A *ratio* is used to avoid dependence on scanner gain settings and T_2 weighting). A T_1 map can then be produced, using the *measured* T_1-weighted signal intensity and the *measured* PD-weighted signal intensity, together with knowledge of the slice position.

Image post processing

Following registration of FSE data to the T_1 weighted image (using the AIR package) (Woods *et al.*, 1993), lesions were contoured on the short echo FSE image using a previously described method (Sailer *et al.*, 1999). Segmentation of the T_1 weighted images into grey matter, white matter and CSF segments was achieved using SPM99 (Statistical Parametric Mapping, Wellcome Department of Cognitive Neurology, Institute of Neurology, Queen Square, London) (Ashburner and Friston, 1997, 2000). A whole brain mask (that excludes CSF and other non-brain parenchyma) was generated in SPM99 and then applied to the T_1 map. An algorithm, utilizing the GM, WM and CSF probability outputs from SPM99, was then used to segment the T_1 whole brain map into WM and GM matter segments: Voxels were classified as GM, WM or CSF depending upon which probability map demonstrated the greatest probability at that location. Lesions were excluded from the analysis by setting their pixel value to zero, leaving only NAWM and NAGM. Partial volume voxels were minimized with a 1000ms threshold for NAWM and a 1700ms threshold for NAGM while two successive erosions of WM and a single erosion of GM were performed (two erosions of GM resulted in only a few GM voxels remaining). (See the Appendix for figures illustrating the segmentation algorithm). Normalized NAWM and NAGM histograms were generated with a bin width of 1ms and a smoothing window of +/- 5ms. The histogram mean, peak location and peak height were then determined.

Statistical Analysis

Changes in T_1 over time were modelled using hierarchical regression (Goldstein, 1995) with random subject-specific intercepts and a common slope on time. In a random intercept - common slope model, a subject-specific intercept is determined for each individual while a common gradient is found that best describes the change over time in the group of subjects.

For the ith subject at time j, the T_1 value (y_{ij}) is given by the following equation:

$$y_{ij} = \left(\beta_{mean} + \beta_i \right) + \mu x_j + \varepsilon_{ij}$$

where the subject-specfic intercept (β_i), and the common gradient (μ) are numerically determined using a least squares technique (which iteratively minimizes the model residuals – ε_{ij}). Essentially, each data point can be described with the equation and the sum of ε_{ij} minimized to find the best estimate for μ and the best estimates for β_i. The mean regression line is given by the mean intercept (β_{mean}) and the common slope (μ). Models can be adapted to include, for instance, a patient-indicator term (to allow patients to be compared with controls) and terms for age and gender.

In the present study, the model used a random subject-specific intercept and common slope on time with a time scale with an origin at study baseline. Patient indicator and patient x time interaction terms were used to assess patient vs. control differences. Terms for age and gender were retained in the final model if they contributed at the $p<0.1$ level. Gender was therefore included in models for NAWM mean-T_1, NAWM peak-height and NAWM peak-location, but age was omitted. Both age and gender

85

were omitted from the model for NAGM mean-T_1. Age (but not gender) was included in the model for NAGM peak-location, while gender (but not age) was included in the model for NAGM peak-height. Baseline comparisons between patients and controls were estimated using the longitudinal models. The coefficient of variation (COV) was used as a measure of repeatability (the COV is calculated by averaging the intra-subject variance, calculating the standard deviation from this and dividing by the mean T_1). A Wilcoxon signed rank test was used to assess serial change in the EDSS.

3.2 Results.

Reproducibility

Coefficients of variation (COVs) were calculated using data obtained from the first six months of the study (13 controls and 20 patients were included in this analysis as other subjects were not imaged at six months). The COVs for NAWM and NAGM are given in Table 3.1 below.

Table 3.1 Coefficients of variation in patients and controls

Tissue	Parameter	COV in 13 controls (%)	COV in 20 patients (%)
NAWM	Mean T_1	2.7	2.2
	Peak Location	3.1	2.5
	Peak Height	2.3	5.6
NAGM	Mean T_1	2.8	2.1
	Peak Location	4.2	2.5
	Peak Height	3.1	6.1

Baseline MRI findings

Mean baseline T_2 lesion load was 7.3 ml (median: 4.6 ml, range 0.9 to 26.6 ml). The mean-T_1, peak-location and peak-height values are given in Table 3.2 below.

Table 3.2 Baseline T_1 values

		Patients n = 23	Controls n = 14	p*
NAWM	Mean T_1	669 ms (29 ms)	630 ms (23 ms)	<0.001
	Peak Location	644 ms (28 ms)	610 ms (27 ms)	0.002
	Peak Height	0.0082 (0.0009)	0.0088 (0.0008)	0.001
NAGM	Mean T_1	1138 ms (40 ms)	1099 ms (24 ms)	0.01
	Peak Location	1116 ms (39 ms)	1085 ms (46 ms)	0.2
	Peak Height	0.0024 (0.0001)	0.0025 (0.0001)	0.3

*Note that the patient vs. control comparisons are made using the adjusted baseline patient-control differences, estimated using the longitudinal models. The model baseline differences (see text below) will therefore differ slightly from the crude baseline cross-sectional differences.

Compared to controls, the patients' mean T_1 was significantly higher in NAWM (mean gender adjusted difference: 29ms; 95% confidence interval (CI) 14ms, 45ms; $p < 0.001$). In NAWM, males had a slightly higher T_1 value in comparison to females (mean difference: 15ms; 95%CI 1ms, 30ms, $p = 0.04$), but when gender was excluded from the NAWM model, there was little effect on the patient-control difference (mean difference (non-gender adjusted): 33ms; $p < 0.001$). Peak height and peak location from the NAWM T_1 histogram were also significantly different between patients and controls (gender adjusted patient-control differences: -0.0008;

95% CI -0.001, -0.0003, p = 0.001 and 25ms; 95% CI 9ms, 41ms p = 0.002 respectively).

In NAGM, mean T_1 was also significantly higher in patients than in controls. The mean patient-control difference was 26ms; 95% CI 6ms, 47ms; p = 0.01. There was no evidence that NAGM peak height and peak location differed between patients and controls.

Longitudinal changes

Clinical follow up

Median EDSS increased from 1.0 (range 0-2.5), at study entry, to 1.5 (range 0-6) at the last imaging time point; p = 0.02.

Regression analysis of serial NAWM and NAGM T_1 data

In NAWM and in NAGM, for both the mean T_1 and the peak location, there was no evidence of a serial change over time in patients or controls (See Tables 3.3a and 3.3b over). (There was also no evidence for a difference in the rates of change between patients and controls for either of these parameters). There was weak evidence that the NAWM peak height was declining in patients (-0.001/year, p = 0.02); and while there was no significant decline in controls (p = 0.4), the patient-control rate of change was not significant (p = 0.5). However there was also weak evidence that the NAGM peak height was declining in *controls* (-0.00004 / year, p = 0.03); the patient-control rate of change was significant (0.00005 / year, p = 0.03); but there was no significant decline in patients (p = 0.5).

Time point		Baseline	6 months	12 months	18 months	24 months	30 months	36 months	P
N patients		23	20	17	18	14	10	7	
NAWM	T_1 mean mean and (SD)	669ms (29ms)	675ms (19ms)	672ms (33ms)	673ms (24ms)	672ms (34ms)	677ms (30ms)	681ms (28ms)	0.5
	Peak location mean and (SD)	644ms (28ms)	651ms (18ms)	650ms (32ms)	650ms (23ms)	647ms (28ms)	648ms (29ms)	656ms (32ms)	0.5
	Peak Height mean and (SD)	0.0082 (0.0009)	0.0082 (0.0010)	0.0082 (0.0012)	0.0081 (0.0011)	0.0080 (0.0012)	0.0075 (0.0013)	0.0075 (0.0007)	**0.02**
N controls		14	13	11	9	9	8	1	
NAWM	T_1 mean mean and (SD)	630ms (23ms)	644ms (24ms)	636ms (23ms)	641ms (24ms)	631ms (25ms)	631ms (34ms)	608ms (0ms)	0.5
	Peak location mean and (SD)	610ms (27ms)	625ms (29ms)	613ms (28ms)	619ms (25ms)	610ms (27ms)	611ms (32ms)	584ms (0ms)	0.4
	Peak Height mean and (SD)	0.0088 (0.0008)	0.0091 (0.0007)	0.0089 (0.0009)	0.0087 (0.0006)	0.0087 (0.0006)	0.0080 (0.0007)	0.0084 (0.0000)	0.4

Tissue		Baseline	6 months	12 months	18 months	24 months	30 months	36 months	P
N patients		23	20	17	18	14	10	7	
NAGM	T_1 mean mean and (SD)	1138ms (40ms)	1137ms (30ms)	1143ms (48ms)	1137ms (29ms)	1134ms (46ms)	1135ms (46ms)	1147ms (30ms)	0.9
	Peak location mean and (SD)	1116ms (39ms)	1119ms (30ms)	1129ms (44ms)	1124ms (33ms)	1113ms (51ms)	1108ms (41ms)	1135ms (7ms)	0.7
	Peak Height mean and (SD)	0.0024 (0.0001)	0.0026 (0.0002)	0.0025 (0.0001)	0.0025 (0.0002)	0.0025 (0.0001)	0.0025 (0.0002)	0.0025 (0.0002)	0.5
N controls		14	13	11	9	9	8	1	
NAGM	T_1 mean mean and (SD)	1099ms (24ms)	1126ms (32ms)	1106ms (23ms)	1118ms (14ms)	1103ms (36ms)	1101ms (48ms)	1096ms (0ms)	0.4
	Peak location mean and (SD)	1085ms (46ms)	1124ms (26ms)	1105ms (47ms)	1114ms (34ms)	1081ms (56ms)	1072ms (52ms)	1118ms (0ms)	0.3
	Peak Height mean and (SD)	0.0025 (0.0001)	0.0025 (0.0001)	0.0025 (0.0002)	0.0025 (0.0001)	0.0023 (0.0001)	0.0024 (0.0001)	0.0024 (0.0000)	**0.03**
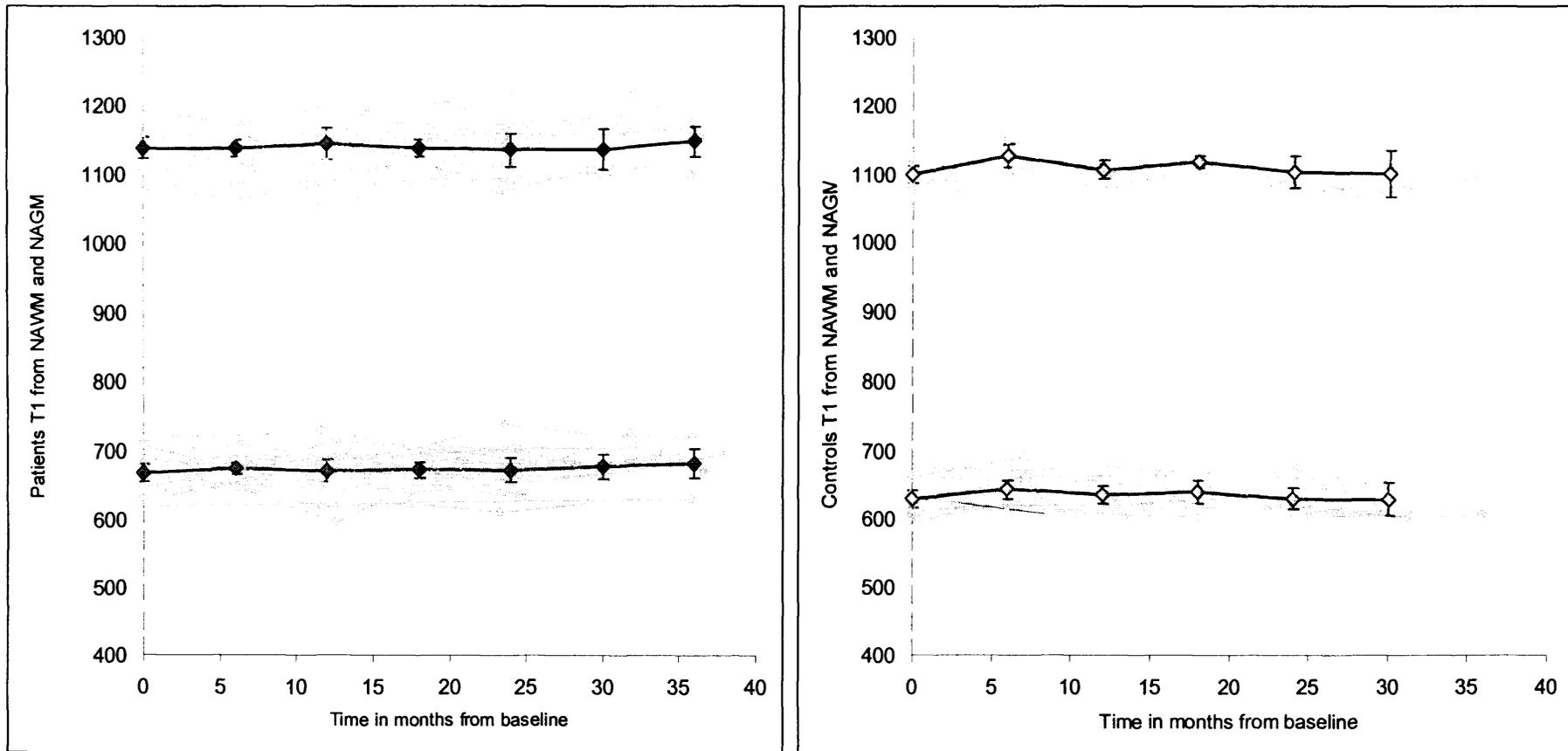
Figure 3.1. Individual and group mean T_1 values (with 95 % CI) for MS patients (left) and healthy control subjects (right), from NAGM (upper) and NAWM (lower).

3.3 Discussion

This longitudinal study of clinically early relapsing-remitting MS patients has revealed the presence of T_1 relaxation time abnormality in both NAWM and NAGM. This supports the earlier cross-sectional study of Griffin *et al.* (2002*a*) in which T_1 abnormality was observed in the NABT of MS patients within three years of clinical onset. Of note, in the present work, there was no detectable net change in mean T_1 during the period of study.

There was weak evidence for a decline in NAWM peak height in MS patients, (albeit without evidence for a significant patient-control difference). However, there was also evidence for a decline in the NAGM peak height in *controls*, without evidence for a change in patients. When considered in conjunction with the COV data, (in which the peak-height-COV in patients was found to be high in comparison to other parameters), it seems likely that these conflicting peak-height findings may relate to the limited reproducibility of the peak height measure. In all, although there was a decline in patient NAWM peak height, when this result is considered together with the mean and peak location data, there is little overall evidence for a serial change in T_1.

In MRI, protons excited with a radio-frequency (RF) pulse, rotate from the plane of the static magnetic field to later re-align with this plane following cessation of the RF power. The T_1 relaxation time describes the rate at which protons make this re-alignment and it is an inherent property of protons and their local environment. Various pathological processes are known to affect T_1 relaxation time in brain

parenchyma. Naruse *et al.* (1982) investigated experimental oedema and found that changes in tissue T_1 were closely mirrored by changes in tissue hydration, while a further study (Barnes *et al.*, 1988) demonstrated that experimentally induced gliosis increased T_1. Others have shown that T_1 can be affected specifically by myelin content (Fischer *et al.*, 1989, 1990) while, in lesions, the concentration of N-acetyl aspartate (a neuronal marker) has been shown to correlate with T_1, thus implying that axonal density also has influence on T_1 (Brex *et al.*, 2000; van Walderveen *et al.*, 1999). T_1 relaxation time measurement therefore appears to be a sensitive but non-specific technique that can detect a number of pathological processes known to occur in MS.

In this study, a degree of intra-subject variability was observed (for all measures, the COV was >2.0% and, for patient peak height, the COV was ~6%). This variation could, in part, be due to biological processes (for instance, due to fluctuation in tissue hydration), and in part be methodological in origin. However, the fact that the peak-height COV was higher in patients than controls might suggest that the parameter was detecting a disease-associated fluctuation in T_1, (possibly secondary to inflammatory change). Nonetheless, it should also be noted that a technique which relies on a two-point calculation, using two data sets acquired sequentially and not simultaneously (as in interleaved sequences), may be prone to short term fluctuations in scanner gain (Jackson *et al.*, 2004). With this in mind, future work may need to further investigate the stability of quantitative MRI.

Even with a degree of intra-subject variability, clear differences between patients and controls were apparent and abnormality was observed in both NAWM and NAGM. However, there was no strong evidence for a serial change and this could reflect one of two possibilities (or a combination of both). Firstly, if abnormality in MS NABT were due to an irreversible pathology (such as axonal loss) which evolved very gradually at an early stage of the disease, a technique with limited reproducibility may fail to detect a gradual serial change. (This would be particularly true if a serial change was small in comparison to the COV). Secondly, changes in T_1, in early MS, may reflect a reversible or fluctuating pathological process, such as inflammation; if these changes fluctuated rather than progressively deteriorated, there may be little or no net change over time. [Of note, previous studies have revealed evidence for inflammatory change within the NAWM in patients with early relapsing-remitting MS: Myo-inositol is elevated in white matter (Chard *et al.*, 2002*b*), and there is an association between Gd enhancement and changes in white matter volume (Tiberio *et al.*, 2005)]. A combination of both possibilities, however, may be the most likely: While T_1 measurement could, in part, be detecting early non-reversible abnormalities (such as axonal loss), variability in the measurement (due to measurement error and/or the detection of inflammatory change), might prevent the detection of any progressive abnormality.

This study has confirmed that T_1 abnormality in NAWM and NAGM is an early event in relapsing-remitting MS but there was no conclusive evidence for a net change over time. Possible reasons for the latter include 1) that T_1 is a non-specific measure of MS pathology and 2) that a non-interleaved two point method is insufficiently reproducible to detect a subtle underlying change. Further studies of

CIS or early relapsing-remitting MS patients using alternative T_1 calculation techniques (for instance those that acquire three or more points, or interleave the data sets) may be warranted. However, the potentially non-specific nature of T_1 abnormality may still limit its' usefulness as a surrogate endpoint.

Although the measurement of T_1 relaxation time failed to detect a definite and or consistent change over time, it remains possible – for reasons given above – that increasing pathological abnormalities are genuinely occurring; this possibility is also reinforced by studies that have detected progressive grey matter atrophy in the same cohort (Chard *et al.*, 2004, Tiberio *et al.*, 2005). As discussed in Chapter 2, MTR has been particularly useful in the study of MS and attention was therefore turned to the study of the early relapsing-remitting MS cohort using MTR. At the time of performing the studies in this thesis it was not known whether grey matter MTR was abnormal in early relapsing-remitting MS and whether NAWM and NAGM MTR progressively decreased in early disease. These questions are addressed in Chapters 4 and 5.

CHAPTER 4

Evidence for grey matter MTR abnormality in minimally disabled early relapsing-remitting multiple sclerosis patients

While MTR abnormality has been observed in the normal-appearing white matter (NAWM) in clinically isolated syndromes suggestive of MS (Iannucci et al., 2000), and in patients with early relapsing-remitting MS, (within three years of symptom onset) (Griffin et al., 2002b); comparatively little is known about grey matter MTR abnormality at such an early stage of the disease.

Normal-appearing grey matter (NAGM) MTR abnormality has been observed in relapsing-remitting MS, in patients with disease durations up to 15 years (Ge et al., 2001), but, in contrast, a study using small regions of interest (ROIs) placed within the grey matter of patients with early relapsing-remitting MS (within three years of symptom onset) did not detect evidence for grey matter MTR abnormality (Griffin et al., 2002b). It is possible, however, that by measuring MTR globally throughout grey matter (via histogram analysis), subtle abnormalities may be detected. Of note, two recent studies have shown that grey matter and thalamic MTR are abnormal in patients with clinically isolated syndromes suggestive of MS, implying that grey matter MTR is likely also to be abnormal in early relapsing-remitting MS (Traboulsee et al., 2002; Audoin et al., 2004).

This study builds on the earlier work of Griffin *et al.* (2002*b*) by imaging a larger cohort of non-disabled early relapsing-remitting MS patients and, rather than analysing small ROIs, MTR measurements have been achieved using a tissue segmentation technique that allows for a global, but tissue specific (i.e. of grey and white matter separately) assessment of MTR change in early MS. The aims of the study were 1) to establish whether MTR histograms are sensitive to normal appearing grey matter change in early relapsing-remitting MS in the absence of significant disability and (2) to assess whether grey matter or white matter MTR measures were associated with clinical measures of impairment in early relapsing-remitting MS.

4.1 Methods

Subjects – MTR and lesion load measures

Thirty eight patients with clinically definite early relapsing-remitting MS (Poser et al., 1983; Lublin and Reingold, 1996) (28 female and 10 male; mean age 36.3 years, range 24-56 years; disease duration at baseline (time from first symptoms): 1.9 years, range 0.5-3.7 years; median expanded disability status (EDSS) (Kurtzke, 1983) score 1.5, range 0-3) and 35 healthy controls (19 female and 16 male; mean age 38.5 years. Range 23-59 years) were studied. Patients were not on disease modifying medication when imaged. EDSS scores (Kurtzke, 1983) and MS functional composite (MSFC) scores (Fischer *et al.*, 1999) were determined in all patients. The MSFC is a composite measure of clinical impairment, encompassing a test of cognition [the Paced Auditory Serial Addition Test (PASAT)], a test of upper limb function [the

Nine Hole Peg Test] and a test of lower limb function [a 25 foot timed walk]. The patients were not significantly disabled (by definition EDSS equal or less than 3) but they did have a range of milder clinical impairments that were quantified using the EDSS and MSFC.

Subjects – Atrophy measures

A subset of those imaged with the MT sequence also underwent 3D imaging of the brain permitting brain volume determination. Thirty seven of the MS patients (28 female and 9 male, mean age 36.1 years, range 24-56 years; disease duration1.8 years, range 0.5-3.7 years; median EDSS score 1.5, range 0-3) and 17 of the healthy controls (10 female and seven male; mean age 35.9 years. Range 30-54 years) were studied with this additional sequence.

The study was approved by the joint ethics committee of the Institute of Neurology and the National Hospital for Neurology and Neurosurgery, Queen Square, UK. Written informed consent was obtained from all subjects.

MRI acquisition

Imaging was performed on a 1.5 Tesla Signa scanner (General Electric, Milwaukee).The 2D dual echo interleaved spin echo (SE) MTI sequence has been described previously (Barker *et al.*, 1996) and was acquired in all controls and MS subjects. Repetition time (TR) was 1500ms with echo times (TE) of 19/90 ms. Images were acquired with a 128x256 matrix over a 24cm field of view (FOV) and reconstructed as a 256x256 matrix. Twenty eight contiguous 5mm axial slices covering the whole brain were acquired both with and without presaturation. The saturating MT pulse was 64ms in duration and 2kHz off water resonance. The power of the MT pulse was 14.6µT with a flip angle of 1430^0 .Saturated and unsaturated

images were interleaved resulting in inherently registered, saturated and unsaturated data sets. MTR was calculated from the short echo images on a pixel by pixel basis according to $\{[M_o-M_s]/[M_o]\} \times 100$ percent units (pu) where M_s and M_o represent the signal intensities with and without the saturation pulse respectively. In a subset of subjects, a 3D inversion-prepared fast spoiled gradient recall (3D FSPGR) sequence [TR 16ms, TE 4.2ms, inversion time 450ms, matrix 256x160, FOV 300x225mm (interpolated during reconstruction to a final in-plane resolution of 1.2x1.2mm), NEX 1, with 124x1.5mm slices covering the whole brain] was also acquired during the same scanning session. The acquisition time was 30 minutes.

Image post processing: MTR and lesion load analysis

Lesions were contoured using Dispimage (Plummer, Dept of Medical Physics and Bioengineering, UCL, UK) on the unsaturated proton density weighted images according to previously defined criteria (Sailer et al., 1999). Segmentation of the T_2 weighted images into grey matter, white matter and CSF segments was achieved using SPM99 (Statistical Parametric Mapping, Wellcome Department of Cognitive Neurology, Institute of Neurology, Queen Square, London). (Figures illustrating the segmentation methodology can be seen in the Appendix and in Figure 4.2 at the end of the results). A whole brain mask (excluding CSF and other non brain parenchyma) was generated in SPM99 and then applied to the (inherently registered) MTR map. An algorithm, utilizing the grey and white matter probability outputs from SPM99 was then used to segment the MTR whole brain map into white matter and grey matter segments: (Voxels were determined as grey matter or white matter depending upon which probability map demonstrated the greatest probability at that location). Lesions were excluded from the analysis by setting their pixel value to zero, leaving

only (NAWM) and (NAGM). Partial volume voxels were minimized with a 10 pu threshold and two successive erosions of white matter and a single erosion of the grey matter (two erosions of grey matter resulted in only a few GM voxels remaining). Normalized NAWM and NAGM histograms were generated with a bin width of 0.1pu and a smoothing window of +/- 0.3pu. The mean MTR for NAWM and NAGM were calculated from these histograms.

Image post processing: Atrophy measures

Brain volume measurements were determined using the 3D FSPGR data which was processed in SPM99 to generate probability maps as described above. Brain stem and spinal cord were excluded from the analysis by visually determining the slice immediately caudal to the cerebellum. Volumes were then estimated using in-house software as previously described by Chard *et al.*, (2002*a*). Lesion masks were derived (using lesion segmentations performed manually) and voxels lying within these masks were defined as lesional tissue. All other voxels were then defined as grey matter (GM), white matter (WM), CSF or other brain parenchyma (eg skull of scalp) depending upon which probability map demonstrated the greatest probability at that location. The total intracranial volume (TI) was then estimated by adding the GM, WM, CSF volumes and lesion volumes. Brain parenchymal fraction (BPF) was then calculated as (GM + WM + lesion volume)/ TI. The grey matter fraction (GMF) and white matter fraction (WMF) were also estimated by calculating GM/TI and (WM + lesion volume)/TI respectively.

Validation of segmentation technique in the presence of focal white matter lesions

As the presence of lesions may have an effect on SPM99 tissue segmentation, and thus differentially affect MS and control subject results, an assessment of the degree of lesion associated bias was made. (Further details can be seen in the Appendix). In all controls, 60 artificial lesions (uniform cylindrical volumes, each 0.25 ml) were placed within white matter, providing a simulated lesion volume of 15ml per subject. This corresponded to the average lesion volume observed in the MS subjects. The signal intensity of artificial lesions was set at a value that appears to have the most marked effect upon SPM99 segmentation (mid way between grey matter and CSF signal intensity). The average change in mean white matter MTR and mean grey matter MTR was +0.03 pu and -0.09pu respectively. This small effect was insufficient to account for any differences subsequently seen between MS patients and control subjects (see Appendix for more details).

Statistical Analysis

MTR and atrophy were compared between MS subjects and controls using linear modelling (SPSS 11.0). Gender and diagnosis (MS or control) were included as fixed factors, with age as a continuous covariate. This approach was prospectively defined on the basis of the age and gender imbalances between patients and controls. Associations between clinical parameters and MTR were estimated using Spearman's Rank Correlation test.

4.2 Results

Imaging

Average T_2 lesion load in the MS subjects was 14.9ml (mean), 12.4 ml (median), range 2.1ml to 47.7ml.

Mean NAWM MTR in MS subjects was 37.9 pu, standard deviation (SD) 0.5 pu while in controls, NAWM MTR was 38.3 pu, SD 0.4 pu. Linear modelling revealed a significant disease effect on NAWM MTR ($p = 0.001$) but no significant effect for either age or gender (Table 4.1). Mean NAGM MTR in MS subjects was 31.9 pu, SD 0.6 pu while in controls NAGM MTR was 32.3 pu, SD 0.5 pu. Linear modelling revealed a significant disease effect on NAGM MTR ($p < 0.001$) and also a significant effect of gender ($p < 0.001$), with female subjects having higher grey matter MTR than males. No effect of age on NAGM MTR was observed (Table 4.1). It should be noted that when artificial lesions were added to the control images and comparisons made between patients and controls (using the same linear model) the linear model disease effect remained significant for NAGM ($p = 0.004$) and NAWM ($p < 0.001$) (see Appendix for more details).

Table 4.1. mean NAWM and NAGM MTR values (and Standard Deviations) in patients and controls.

	MS Subjects n = 38	Controls n = 35	p value[a]
NAWM MTR	37.9 pu	38.3 pu	p = 0.001
	(0.5 pu)	(0.4 pu)	
NAGM MTR	31.9 pu	32.3 pu	p < 0.001
	(0.6 pu)	(0.5 pu)	

[a] significance of disease effect factor (MS or control) in linear model

T_2 lesion load was inversely correlated with NAGM (Spearman's correlation coefficient (r) = -0.56 p < 0.001) and NAWM MTR (r = -0.53, p = 0.001). In subjects with MS, NAGM MTR correlated with NAWM MTR (r = 0.43, p = 0.008). In controls, only a trend for an association between NAGM MTR and NAWM MTR was seen (r = 0.33, p = 0.06).

Volume measures derived from the 124 slice 3D data set (a sub set of the cohort) revealed evidence for increased whole brain and WM atrophy in MS subjects. BPF was 0.810 (SD 0.026) in MS subjects versus 0.835 (SD 0.28) in controls, linear model disease effect: p < 0.001. WMF was 0.263 (SD 0.017) in MS subjects versus 0.282 (SD 0.012) in controls, linear model disease effect term: p < 0.001. GMF was 0.547 (SD 0.023) in MS subjects versus 0.552 (SD 0.023) in controls, linear model disease effect term: non significant (p = 0.18). BPF correlated with NAGM MTR (r = 0.69, p < 0.001) but not with NAWM MTR (r = 0.21, p = 0.21). The effect of

atrophy on NAGM MTR was therefore assessed by including BPF as a covariate in the linear model (with gender as a fixed factor). This revealed that the disease effect on NAGM MTR remained significant (p = 0.009).

Clinical Status

Median EDSS in MS subjects was 1.5 (range 0-3). EDSS was inversely correlated with NAGM MTR (r = -0.45 p = 0.005) (see Figure 4.1) but not with NAWM MTR (r = -0.2, p = 0.9). BPF was inversely related to EDSS (r = -0.39, p = 0.02). Borderline significance was seen for an association between T_2 lesion load and EDSS (r = 0.31, p = 0.06). The MSFC score and the three Z scores from which the MSFC is derived (Z-arm, Z-cognition and Z-leg) were also determined in this cohort[16]. Borderline evidence for an association was seen between Z-arm and NAGM MTR (r = 0.31, p = 0.06) but no other association was seen between the MSFC or Z scores and MTR measures. T_2 lesion load was inversely correlated with the MSFC (r = -0.36, p = 0.03) and also correlated with the Z-leg score (r = 0.44, p = 0.005). (More positive values correspond to greater disability with the Z-leg score yet the converse is true with the MSFC). Borderline evidence was seen for an inverse association between disease duration and NAWM MTR (r = -0.29, p = 0.08) but not with NAGM MTR.
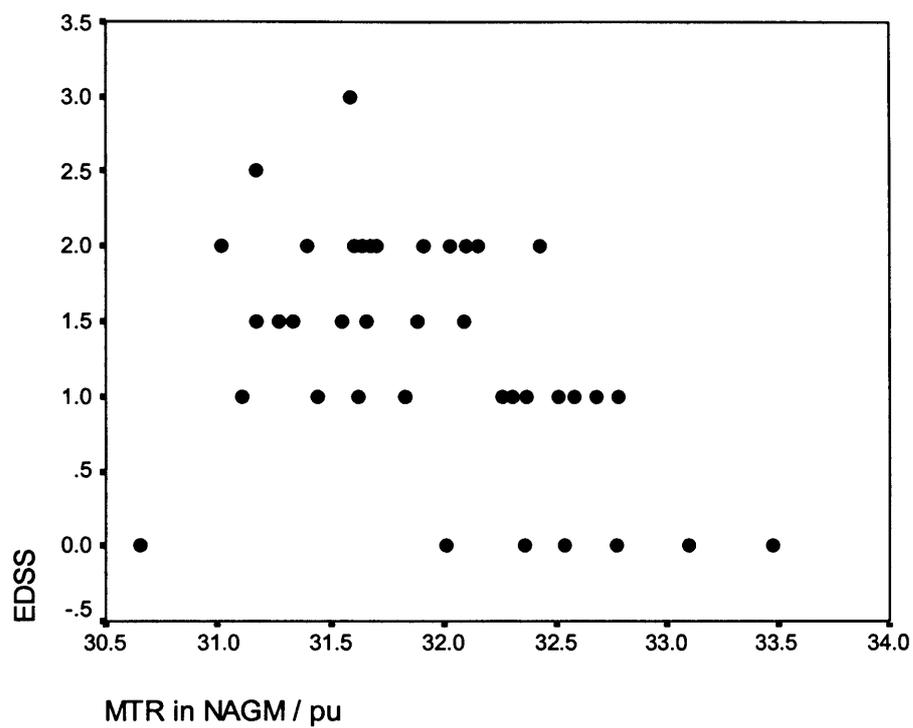
Figure 4.1. Correlation between EDSS and NAGM MTR, r = -0.45, p = 0.005.
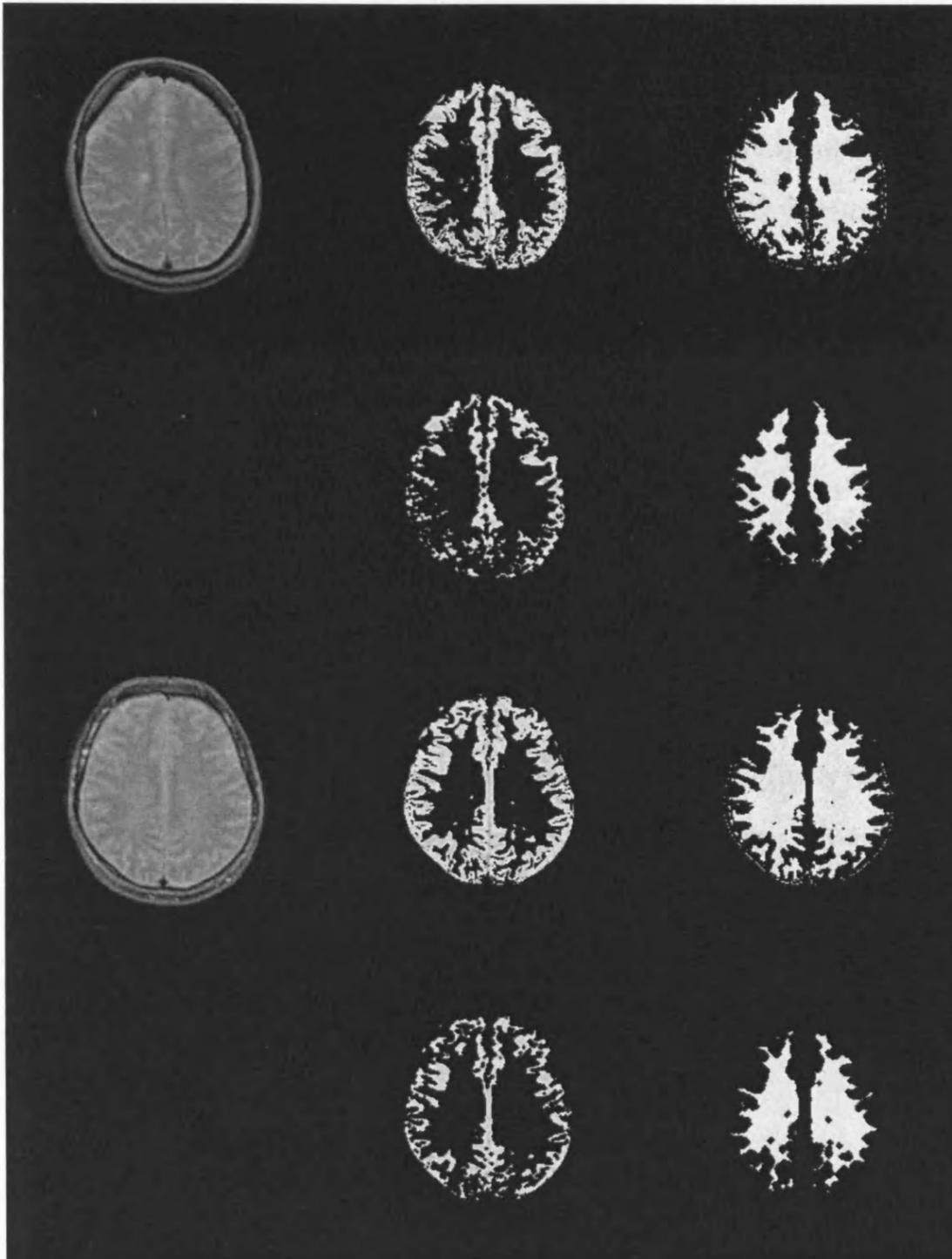
Figure 4.2. Images from a patient with MS (top two rows) and healthy control (lower two rows). Left column: T_2 weighted images. Central column: grey matter segments of the MTR map (above) subjected to a 10pu threshold and one erosion (below). Right column: white matter segments of the MTR map (above) subjected to a 10pu threshold and two erosions (below).

4.3 Discussion

This study detected NAGM and NAWM MTR abnormalities in relapsing-remitting MS, in a cohort who have early disease (mean disease duration 1.9 years) and mild clinical impairments. Furthermore, clinical impairments in this early relapsing-remitting MS cohort were associated with NAGM abnormality but not with changes in NAWM.

The ability to detect grey matter abnormality with MTR has previously been demonstrated in a cohort with established relapsing-remitting MS (mean disease duration 5 years, range 1-15 years, EDSS range 1-6) (Ge *et al.*, 2002) but it has not been shown in relapsing-remitting MS patients with minimal disability and early disease. Grey matter involvement however appears to be a feature of early relapsing-remitting MS and this has been shown in studies using several other MR measures, including T_1 relaxation, spectroscopic metabolites, and atrophy (Griffin *et al.*, 2002; Chard *et al.*, 2002*a*, 2002*b*). Also in a recent study of patients with clinically isolated syndromes suggestive of MS, a reduction of 0.3 pu NAGM MTR was observed (Traboulsee *et al.*, 2002).

Changes within normal-appearing brain tissue in MS have potential to play an important role in the development of disability particularly as changes in lesion load correlate only modestly with clinical status (Molyneux *et al.*, 2001; Paolillo *et al.*, 2002). MR methods of assessing change within normal-appearing tissue may therefore be of use in clinical trials. This would particularly be true if such measures are shown to be good predictors of future impairment or disability, since a key

requirement of a validated surrogate outcome measure is that it should be associated with a clinically relevant outcome (McFarland *et al.*, 2002). An additional valuable feature would be that such measures be sensitive to normal appearing tissue abnormality early in the course of the disease, prior to the onset of significant disability.

Whilst NAGM MTR was associated with clinical impairment using the EDSS, T_2 lesion load was associated with clinical impairment using the MSFC. Potentially both lesions and NAGM abnormalities contribute to clinical dysfunction, and although they were partly correlated with each other, their effects on clinical function may be different. However, before concluding that such outcome measures have complementary roles in studies of natural history and treatment monitoring, it would be important to study larger cohorts and serial data.

The present study relied upon accurate tissue segmentation and, in particular, that the presence of MS lesions did not significantly effect voxel classification. In order to quantify this, lesion simulation was performed in controls. The effect noted, however, was small and insufficient to account for the MTR changes observed. In addition, the segmentations were independently verified by a rater (Waqar Rashid), blinded to the clinical details of the subjects, and the segmentations appeared to be anatomically valid.

The effect of partial volume voxels at the CSF – grey matter interface proportionally have a greater effect on the mean grey matter MTR as atrophy occurs. In this cohort, atrophy has been shown to occur (albeit principally within white matter) and

therefore it is possible that some of the MTR decrease is partial volume related. As a result, every possible attempt has been made to reduce partial volume voxels via the use of a CSF-reducing-threshold and erosion of outer voxels. One erosion was used in grey matter as further erosions resulted in only very limited amounts of grey matter remaining. With these steps, it seems more likely that the NAGM MTR abnormality reflects true intrinsic abnormality rather than partial volume effects of atrophy. Partial volume voxels at the GM-WM interface and the WM-CSF interface may also have an effect on MTR but as erosions where performed at the inner surface (as well as the outer) these partial volume voxels will also have been minimized.

In further support of NAGM MTR abnormality being secondary to intrinsic tissue pathology rather than atrophy per se, BPF was included as a covariate in the statistical analysis. Such an analysis is conservative as it is liable not only to eliminate MTR differences secondary to partial volume artifact but also to eliminate intrinsic MTR differences which are associated with atrophy. Nonetheless, when this analysis was performed differences were still observed between patient and control NAGM MTR.

The atrophy noted in this cohort appears to be principally secondary to white matter volume change although GM volume in the patients was lower (albeit non-significantly) than the controls. A previous study (Chard et al., 2002a) did show a small but significant degree of GM atrophy in early RRMS and the inability to detect it here might result from the fact that the present study had fewer controls.

A further concern is that juxta cortical lesions and peri-lesional tissue may have been erroneously classified as grey matter. However, overt lesions are removed by lesion masking and subtle areas of abnormality, (not detected on PD weighted imaging) would have MTR values mid-way between grey matter and white matter. Such areas therefore would not decrease NAGM MTR.

The statistical analysis used was prospectively designed and used linear modelling to account for age and gender imbalances seen between MS and control subjects. Where positive disease effects were found, differences between patients and controls were verified with the Mann-Whitney U test (which proved to be significant, p < 0.01) for all such results. Corrections for multiple comparisons have not been performed (principally as the number of comparisons was not large) and so some of the weaker correlations should be viewed with caution.

What is the pathological basis for the observed normal-appearing brain tissue MTR abnormality in early MS? It is known that MTR correlates with axonal and myelin density (van Waesberghe *et al.*, 1999), but also, to a certain extent, with inflammatory change (Gareau *et al.*, 2000). In NAWM, histopathological findings include gliosis, inflammatory infiltrates and axonal loss (Allen and McKeown, 1979; Evangelou *et al.*, 2000) with the latter occurring possibly as a result of Wallerian degeneration of axons transected in lesions. It is notable that acute axonal transection occurs in inflammatory lesions (Trapp *et al.*, 1998), more so at an early stage of the disease (Kuhlmann *et al.*, 2002). In grey matter, neuronal and myelin loss has been reported in grey matter lesions, which are less inflammatory (Peterson *et al.*, 2001)

and less MR visible than lesions in white matter (Kidd *et al.*, 1999). Such changes might account for the MTR abnormalities seen in this study.

In conclusion, this study demonstrates that MTR is sensitive to NAGM (and NAWM) abnormalities in relapsing-remitting MS in a cohort who have early disease (mean disease duration 1.9 years) and only mild clinical impairments. The correlation of EDSS and grey matter MTR suggests that NAGM MTR abnormality is clinically relevant in early relapsing-remitting MS and therefore may have potential as a surrogate marker in clinical trials. However, these modest correlations are preliminary and so should be confirmed in a larger cohort. In addition, in order to act as a surrogate marker, it is necessary to demonstrate that MTR in early MS is sensitive to change over time (this is addressed in Chapter 5) and that MTR changes correlate with future disability. If such associations are shown, it would imply that MTR measures could be a clinically relevant outcome for therapeutic interventions.

CHAPTER 5

Increasing normal-appearing grey and white matter MTR abnormality in early relapsing-remitting MS

Chapter 4 focussed on the baseline MTR characteristics of this early relapsing-remitting MS cohort. In this chapter, serial NAWM and NAGM MTR changes are investigated in a subset of patients followed up for two years with yearly scans. The study addressed the following questions: (i) Are longitudinal changes occurring in NAWM, NAGM or in both regions? (ii) Using back projection methods, when did the changes probably start?

5.1 Methods

Subjects

Twenty three patients with clinically-definite early relapsing-remitting MS (Poser *et al.*, 1983; Lublin and Reingold, 1996) were studied. [Note that the 23 patients studied here were not identical to those studied in Chapter 3 (although there is a large overlap) – the patients include here had MTR data sets available for at least two of the three yearly time points]. The demographics of the patients were as follows: (19 female and four male; mean age: 37 years, range: 27-55 years; disease duration at baseline (time from first clinical event): 1.9 years, range: 0.5-3.7 years; Median EDSS score: 1.0, range: 0-3.0). Nineteen healthy controls were also imaged: (10 female and nine male; mean age: 34 years, range: 27-52 years). All subjects were imaged at baseline with 22 MS patients and 18 controls imaged one year later (range:

11-15 months) and 21 MS patients and 10 controls imaged two years later (range: 23-28 months). Patients were not on disease modifying medication at baseline; however, seven of the 23 MS patients commenced treatment with Beta-interferon (IFNB) during the study period; all of whom completed the two year follow up. The patients had not been administered steroids within a month prior to imaging. EDSS scores and MS function composite (MSFC) scores (Fischer *et al.*, 1999) were determined at each visit. The study was approved by the joint ethics committee for the Institute of Neurology and the National Hospital for Neurology and Neurosurgery, Queen Square, London, UK. Written informed consent was obtained from all subjects.

Magnetic Resonance Imaging

Imaging was performed on a 1.5 Tesla Signa (General Electric, Milwaukee, USA). The 2D interleaved dual spin echo magnetisation transfer imaging sequence has been described previously (Barker *et al.*, 1996) and was acquired in controls and MS patients at all time points. The imaging parameters have been given previously (Chapter 4). As mentioned, saturated and unsaturated images were interleaved resulting in inherently registered saturated and unsaturated data sets. MTR, in percent units (pu) was calculated from the short echo images on a pixel by pixel basis according to $\{[M_o-M_s]/[M_o]\} \times 100$ where M_s and M_o represent the signal intensities with and without the saturation pulse respectively. The acquisition time was 20 minutes.

Image Post Processing.

Lesions were outlined on the unsaturated short echo images according to previously defined criteria (Sailer *et al.*, 1999), using a semi-automated contouring method implemented within the Dispimage program (Plummer, 1992). Segmentation of the MTR map into NAWM and NAGM segments was achieved using an identical technique to that described in Chapter 4.

Volume measures were also determined using the SPM99 probability outputs (from the MTR data sets). These volume measures were obtained in order that a measure of atrophy could be included as a covariate in the statistical analysis. Brain stem and spinal cord were excluded from the analysis by visually determining the slice immediately caudal to the cerebellum and volumes were then determined using in-house software as described in Chapter 4.

Statistical Analysis

Changes in MTR over time were modelled using hierarchical regression (Goldstein, 1995) with random subject-specific intercept and common slope on time, using a time scale with origin at study baseline; patient indicator and patient x time interaction terms were used to assess patient vs. control differences. The same model was used to investigate changes in atrophy measures over time. There was no evidence that a random slopes model gave a better fit. Potential confounding by age, gender and BPF was examined by adding these terms and interactions into the regression. For NAWM MTR, BPF and its interaction with patient indicator contributed to the model, but terms in age and gender were omitted from the model as there was no evidence of confounding by these. For NAGM, BPF and its

interaction with patient indicator, gender, gender x BPF interaction were included, and age omitted as there was no evidence that it confounded. Non-parametric bias-corrected bootstrap estimates (Carpenter and Bithall, 2000) were derived (1000 replicates) to confirm parametric results where normality could not confidently be assumed; where bootstrap and parametric results differed materially the former are reported in the text.

Reported baseline patient vs. control differences in MTR are the covariate adjusted estimates given by these longitudinal models, and therefore differ slightly from the crude cross-sectional difference. The former estimates are preferred not only because of adjustment for confounding, but because all the data points are used, thus reducing the error of estimates from just one time point.

The statistical comparison between the rates of change in NAWM MTR and NAGM MTR was carried out in *patients only* by testing for a difference in the coefficients on time from baseline in two models: for NAWM MTR, only time was entered as predictor (other terms did not contribute and were omitted). For NAGM MTR, gender, BPF and their interaction were also entered. Quadratic terms in time were used to test for non-linearity, on both baseline and onset origin time scales.

To estimate by back extrapolation when patient MTR diverged from normal control values, the latter were estimated as the mean across the time points in controls, reflecting an *a priori* assumption of no change in controls, and the regression, in patients only, used the onset origin time scale. No covariates were entered for NAWM or NAGM MTR; BPF was omitted in order to estimate the rate of change

due to the whole disease process, rather than the MTR component only, which is estimated in the BPF adjusted models. Gender was omitted to simplify the comparison and presentation in Figures 5.1 and 5.2. To check consequences of this simplification, the GM back projection was also calculated with gender and gender x time interaction, using females as comparator to give a time to normality in females only. Non-parametric bias-corrected bootstrap (1000 replicates) was used to derive confidence intervals for the time at which abnormality begins.

Associations between atrophy and MTR variables were examined with random intercept regression models using MTR outcome and atrophy and time predictors. Longitudinal changes in EDSS and lesion load were examined with Wilcoxon signed rank tests, and in the MSFC with a paired t-test. Cross-sectional associations between MR parameters, and between these and clinical variables, were assessed using Spearman rank correlation.

5.2 Results

Baseline MRI Findings

Mean baseline T_2 lesion load was 16.6ml (median: 13.3ml, range: 2.1-47.7ml). The mean MTR values from NAWM and NAGM are given in Table 5.1. Compared to controls, the patients' mean MTR was significantly lower in both NAWM (mean difference -0.6pu; 95% confidence interval (CI) -0.3pu, -0.9pu; $p < 0.001$) and NAGM (mean difference -0.5pu; 95% CI -0.1pu, -0.8pu; $p = 0.004$).

Table 5.1: Baseline values for patient and control NAWM and NAGM MTR.

	Patients n = 23		Controls n = 19		p value*
	Mean (SD)	Range	Mean (SD)	Range	
NAWM MTR	37.8pu (0.5pu)	36.3-38.7pu	38.3pu (0.4pu)	37.4-39.1pu	< 0.001
NAGM MTR	32.0pu (0.7pu)	30.7-33.5pu	32.4pu (0.5pu)	31.1-33.0pu	0.004

p values derived from covariate adjusted estimates of baseline patient-control

difference in longitudinal model. SD = standard deviation, pu = percent units.

Longitudinal Changes

Clinical follow up at two years

Clinical comparisons between baseline and the two year time point revealed no

significant change in MSFC scores (p = 0.76). Median EDSS increased from 1.0

(range 0 to 3.0) to 1.5 (range 0 to 4.0) (p = 0.02). All but one patient had an EDSS of

less than 4.0 at two years. Mean annual relapse rates prior to, and following study

entry were 1.5 and 0.7 respectively. The mean time between the first and second

attack (prior to study entry) was 9 months; (median 8 months).

Serial T_2 lesion load measurement at baseline and at two years

Significant changes in T_2 lesion load were not seen during follow up. In the 21 patients followed up for two years, the mean T_2 lesion load at baseline was 14.6ml compared to 15.0ml at two years (p = 0.82). Over the two years, T_2 lesion load increased in 11 patients and decreased in 10. Seven of the 21 MS subjects followed up at two years were taking IFNB (having started since baseline scan) and five of these had reductions in T_2 lesion load. However, when those on IFNB were excluded, there was still no significant increase in T_2 lesion load over time.

Regression analysis of serial NAWM MTR data (Figure 5.1)

In patient NAWM, MTR was progressively declining at an estimated annual rate of -0.10pu (p = 0.001; 95% CI: -0.04, -0.15). In controls, the annual rate of WM MTR change was not statistically significant: +0.04pu (p = 0.20; 95% CI: -0.02, +0.10). The patient-minus-control difference in the annual rate of MTR change was also statistically significant: -0.14pu (p = 0.001; 95% CI: -0.05, -0.22).

Regression analysis of serial NAGM MTR data (Figure 5.2)

In patient NAGM, MTR was progressively declining at an annual rate of -0.18pu (p < 0.001; 95% CI: -0.11, -0.24). In controls, the annual rate of GM MTR change was not statistically significant: +0.01pu (p = 0.74; 95% CI: -0.06, +0.09). There was a statistically significant patient-minus-control difference in the annual rate of MTR change: -0.19pu (p < 0.001; 95% CI: -0.09, -0.28).

Comparison of NAWM and NAGM rates of change in MS patients

The rate of change in NAGM was significantly greater than the rate of change in NAWM (p = 0.004). No significant correlations were found between relapse rate and MTR change in NAGM or NAWM; nor between changes in MTR and changes in EDSS or MSFC. Furthermore, no significant correlations were seen between the cognitive component of the MSFC (the Z-*cog* score) and MTR change. There was also no correlation found between changes in NAGM or NAWM MTR and either baseline T_2 lesion volume or change in T_2 lesion volume. Finally there was no significant difference between the rates of NAWM and NAGM MTR change in those who started IFNB and those who did not.

Backwards extrapolation of rates of change

There was no evidence of non-linearity in NAWM or NAGM MTR change over the time range of the data, either on the baseline or onset origin time scales. Assuming that the gradient of change in controls was zero, and in patients was linear at all times, NAWM MTR abnormality began 2.9 years before clinical onset (95% CI: 0.7 to 11.1 years before, p = 0.015) (see Figure 5.1), and NAGM MTR abnormality began 0.4 years after clinical onset (95% CI: 1.0 year before to 1.2 years after, p = 0.6) (See Figure 5.2). [Inclusion of gender in the NAGM model revealed that NAGM MTR abnormality began 0.1 years after clinical onset (95% CI: to 1.4 years before to 1.4 years after, p = 0.8)]. The *difference* between the extrapolated times of onset for the two tissues was statistically significant: NAWM abnormality preceded NAGM abnormality by 3.3 years (95% CI: 1.5 to 11.3 years, p < 0.001).

Tissue volume measures (Table 5.2)

Tissue volume measures were calculated in order that BPF could be included as a potential confounder in the longitudinal analysis. NAGM MTR in patients was positively correlated (independently of time) with BPF ($p < 0.001$) but not GMF ($p = 0.1$ bootstrap) or WMF ($p = 0.89$). NAWM MTR did not correlate (independently of time) with BPF ($p = 0.45$), GMF ($p = 0.98$) or WMF ($p = 0.40$). WMF was lower at baseline in patients than controls ($p = 0.01$), but there was no evidence of decline in either patients or controls. There was weak evidence that GMF at baseline was higher in patients than controls ($p = 0.04$, bootstrap), and there was some evidence of decline in GMF in both patients ($p = 0.01$, bootstrap) and controls ($p = 0.02$ bootstrap), but not a statistically significant difference in rate ($p = 0.7$, bootstrap). BPF showed a significant decline in patients ($p < 0.001$) (with no statistical evidence of non-linearity), but not in controls ($p = 0.24$), though there was no statistically significant difference between patients and controls at baseline or in rate of decline.

Table 5.2: Tissue volumes: mean BPF, GMF and WMF (and standard deviations) in patients and controls.

		Baseline Patients n = 23 Controls n =19	12 months Patients n = 22 Controls n =18	24 months Patients n = 21 Controls n =10
Patients	BPF	.848 (.022)	.841 (.022)	.840 (.021)
	GMF	.495 (.026)	.488 (.022)	.487 (.024)
	WMF	.353 (.015)	.353 (.014)	.353 (.017)
Controls	BPF	.849 (.016)	.850 (.020)	.849 (.017)
	GMF	.483 (.031)	.476 (.017)	.475 (.012)
	WMF	.366 (.025)	.374 (.014)	.374 (.013)

BPF = brain parenchymal fraction, GMF = grey matter fraction, WMF = white matter fraction
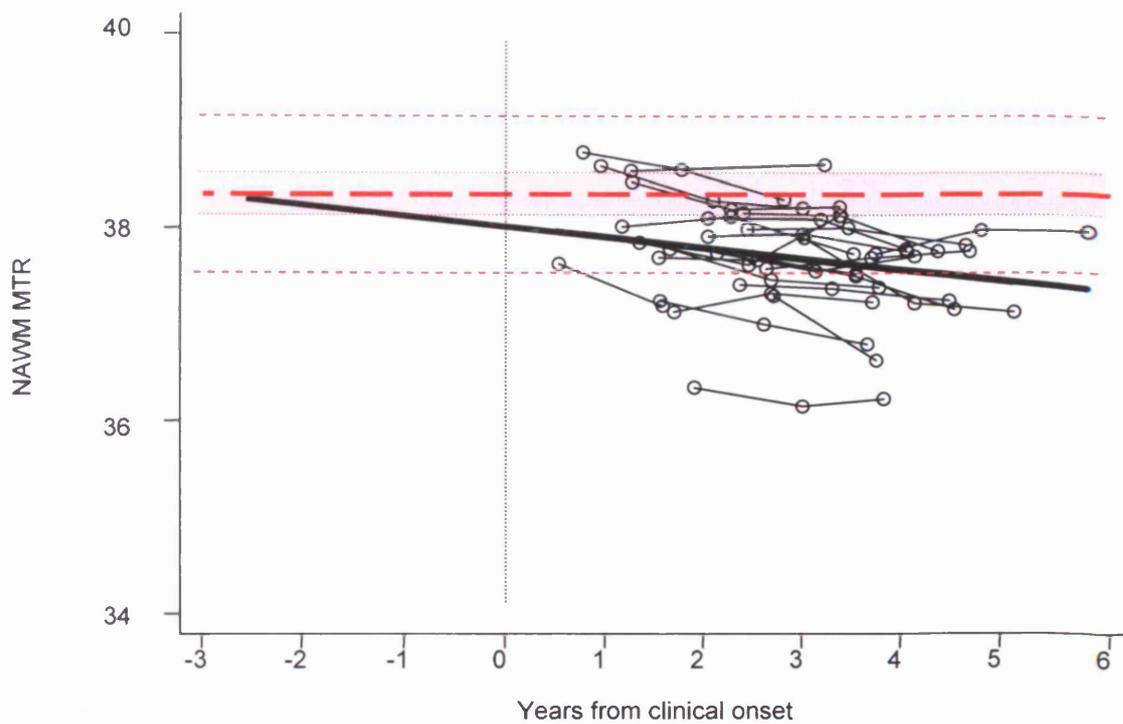
Figure 5.1. NAWM MTR in MS patients plotted against time from clinical onset. Thick red dashed line: mean control NAWM MTR value. Red shaded area: 95% confidence intervals for the control mean. Thin dashed red lines: control mean +/- two standard deviations. The line of best fit from the hierarchical regression is in solid black.
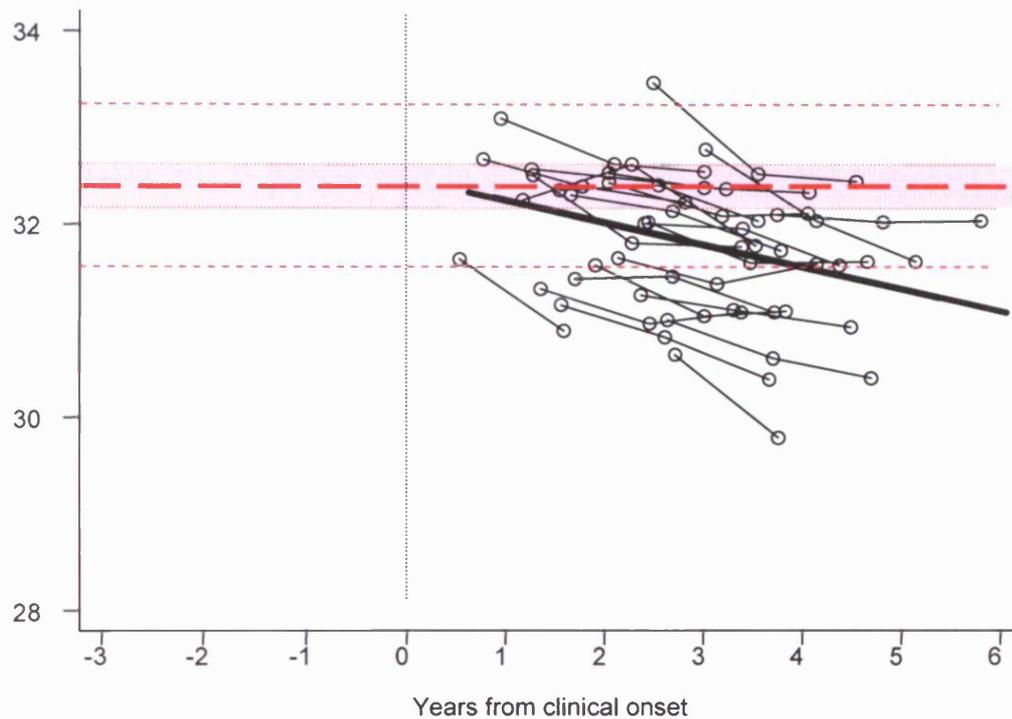
Figure 5.2. NAGM MTR in MS patients plotted against time from clinical onset. Thick red dashed line: mean control NAGM MTR value. Red shaded area: 95% confidence intervals for the control mean. Thin dashed red lines: control mean +/- two standard deviations. The line of best fit from the hierarchical regression is in solid black.

5.3 Discussion

MTR findings in NAWM and NAGM

This study extends the observation that NAWM and NAGM MTR are both abnormal in clinically early RRMS (Chapter 4), by showing that the MTR abnormalities in both regions progressively increase over two years of follow-up. In addition, backward extrapolation of the rates of change – assuming linearity – suggests that NAWM MTR abnormality is present prior to the onset of symptoms and precedes NAGM MTR abnormality.

As previously mentioned, MTR relies upon the use of an off-water-resonance radiofrequency pulse capable of selectively saturating the macromolecular magnetisation. As a result, MR visible free water is saturated via exchange with this macromolecular pool and MTR values represent the percent reduction in signal intensity observed. A fall in a tissue's macromolecular content will result in a lower MTR and, consistent with this, MTR is associated with demyelination and a reduction in axonal density (Mottershead *et al.*, 2003; van Waesberghe *et al.*, 1999). However, small changes in MTR may also be due to inflammation (Gareau *et al.*, 2000).

The subjects in this study had minimal or no disability at entry (although they did have a range of mild clinical impairments). Furthermore, as a group, they did not accumulate major disability or enter the secondary progressive phase during follow-up, (only one patient reached EDSS 4.0 by two years). Despite this, increasing MTR abnormalities were apparent in both NAWM and NAGM. An earlier study showed

that normal-appearing brain tissue MTR declines over one year following a clinically isolated syndrome suggestive of MS (Filippi *et al.*, 2000*a*) while an association between NAWM MTR and disease duration has also been observed (Laule *et al.*, 2003). Taken together with the present findings, this suggests that increasing and clinically silent pathological abnormalities are developing in normal appearing tissues early in the course of RRMS. Longer term follow-up is now needed to determine whether or not these changes are associated with later clinical worsening.

The significantly greater rate of change in NAGM compared with NAWM suggests either that the nature of the pathological changes within NAGM and NAWM differ (and hence have a different effect on MTR), or that the same pathological process is occurring more rapidly in NAGM at this stage of the disease. Based on known pathological findings (Allen and McKeown, 1979; Allen *et al.*, 2001; Evangelou *et al.*, 2000; Kidd *et al.*, 1999; Peterson *et al.*, 2001), the former explanation seems more likely. It is unlikely that atrophy affected the relative rates of NAGM and NAWM change because the analyses were performed using BPF as a covariate.

The prediction that NAWM abnormality predated symptom onset – possibly by several years – is based on an assumption that the rate of change prior to entry was the same as that observed during the study. If NAWM MTR abnormality had begun at the time of the first clinical attack, a substantially steeper decline during the two years between clinical onset and study entry would have had to occur. Although, there was no evidence of non-linearity over the study period, (giving some plausibility to the assumptions made by linear backward extrapolation), the

extrapolations relied upon data from three time points only, and should be viewed with some caution. It is possible that early changes in NAWM and NAGM are non-linear, and thus have a different dynamic to that suggested by the current data.

Pathological basis of MTR findings

What could be the pathological basis for the MTR changes seen in this study? Studies of the macroscopically normal white matter in MS have revealed evidence for astrogliosis (Allen and McKeown, 1979), microglial activation (Allen *et al.*, 2001) and axonal loss (Evangelou *et al.*, 2000). Patchy demyelination and perivascular inflammation may also occur (Allen *et al.*, 1979). Several of these processes could result in subtle MTR abnormalities. The progressive NAWM change observed is perhaps more likely to be due to the ongoing loss of myelin and axons rather than to inflammation, (which would be more likely to fluctuate than progress). In grey matter, the accumulation of cortical lesions, which are almost never seen on MRI (but are associated with axonal loss and demyelination) (Kidd *et al.*, 1999; Peterson *et al.*, 2001), might progressively decrease MTR.

Methodological issues

Progressive brain volume loss could potentially have contributed to the reduction in MTR observed, particularly as it is associated with a relative increase in the number of partial volume voxels at the CSF/brain tissue interface. Of note, a study of patients from the same cohort, using volumetric imaging, reported both grey and white matter atrophy; with a progressive decline in grey matter (but not white matter) tissue volume during the course of the study (Chard *et al.*, 2004). Rigorous efforts have

therefore been made to minimize partial volume effects using (i) a CSF minimizing threshold, and (ii) erosions of inner and outer voxels. Also, NAGM and NAWM MTR changes were analyzed after including BPF as a covariate in the regression model. Such an analysis is highly conservative as it will not only minimize MTR differences due to partial volume artifact but will also reduce true *intrinsic* MTR differences that are directly associated with atrophy. Brain volume loss *per se* is therefore unlikely to account for the progressive changes observed in MTR

The presence of white matter lesions could theoretically have altered the way in which the segmentation software classified voxels, leading to a systematic difference between patient and control segmentation. However, this has previously been investigated as laid out earlier in this thesis and the small changes caused by lesion simulation were not sufficient to account for the NAGM and NAWM MTR changes seen in patients with early RRMS (Chapter 4). However, the small effect of lesions on tissue segmentation could have contributed to the marginally larger GMF seen in the present patient cohort in comparison to controls (Chard *et al.*, 2002c), this being an otherwise unexpected finding. Of note, T_2 lesion load did not significantly change during follow-up and so segmentation bias could not account for the *changes* seen in the normal appearing tissues.

The healthy control data remained stable over the two years of follow-up with a rate of change not significantly different from zero. Although there were fewer controls than MS subjects, the patient-minus-control difference in the annual rates was significant in both tissues, suggesting that the size of the control cohort was

sufficient for comparison with patients. The number of patients was also not high, and as some were treated with IFNB, this potentially might have affected MTR. However, no difference in the rate of MTR change was observed when treated and untreated patients were compared and a previous study in secondary progressive MS reported no treatment related modification of whole brain MTR (Inglese *et al.*, 2003). Furthermore, the patient cohort appears representative of early relapsing-remitting MS in terms of their relapse rate (IFNB MS Study Group, 1993), EDSS and gender distribution.

Conclusions

This study has revealed increasing abnormalities in NAGM and NAWM MTR at an early stage of relapsing-remitting MS (mean disease duration 1.9 years). The NAWM abnormality may begin before clinical onset of the disease and may precede change in NAGM. However, the sample size was relatively small and confirmation of these findings is needed. Nevertheless, the findings are potentially important as they suggest the occurrence of a diffuse and progressive pathological process early in the course of relapsing-remitting MS. Long term follow up is now required to investigate the prognostic significance of these changes.

CHAPTER 6

Emergence of thalamic MTR abnormality in early relapsing-remitting MS

In Chapters 4 and 5, evidence was presented suggesting that NAGM MTR abnormality is clinically relevant (it correlates with the EDSS) and that increasing MTR abnormalities are developing in the NAGM and NAWM early in the course of relapsing-remitting MS. Focus will now shift to the study of the thalamus, particularly as the thalamus (as with the study of grey matter) may give useful insight into neuronal abnormality in early MS.

Axonal damage in multiple sclerosis (MS) has been investigated extensively in recent years, (Ferguson *et al.*, 1997; Trapp *et al.*, 1998; Kuhlmann *et al.*, 2002) particularly as it may be a key factor in the development of permanent disability (Bjartmar *et al.*, 2000). A number of recent studies have investigated the thalamus, (Cifelli *et al.*, 2002; Wylezinska *et al.*, 2003; Inglese *et al.*, 2004) principally because it contains a number of deep grey matter nuclei and extensive fibre tract connections including ascending and cortical-striatal pathways. However, while imaging of the thalamus in MS may provide useful insight into neuronal abnormality, it also contains a significant amount of myelin, (Ohye and Armstrong, 1990) raising the possibility that thalamic abnormality may not be entirely neuronal in origin.

One recent study, in secondary progressive MS, using both histopathological and MR techniques, (Cifelli *et al.*, 2002) reported a 17% reduction in thalamic volume, reduced thalamic N-Acetyl aspartate (NAA) concentrations, and a reduction in neuronal density, consistent with a 30% reduction in thalamic neuronal number.

Furthermore, in patients with established relapsing-remitting MS, (Wylezinska *et al.*, 2003) (mean disease duration: 7.7 years, expanded disability status scale (EDSS) range: 2.0-6.0), a significant reduction in thalamic volume and NAA concentrations were also detected.

Currently, it remains unclear how early thalamic abnormality is seen in the clinical course of MS. This study used the magnetization transfer ratio (MTR) to ask whether thalamic intrinsic abnormality occurs in our early relapsing-remitting MS cohort.

6.1 Methods

Patients with MS and Control Subjects.

Twenty three patients with early clinically-definite relapsing-remitting MS entered the study (Poser *et al.*, 1983; Lublin and Reingold, 1996), (these were the same patients studied in Chapter 5). Their demographics were as follows: (19 female, four male, mean age 37 years, range 27-55 years, median disease duration at baseline (time from first clinical event) 1.9 years, mean 1.9 years, range 0.5-3.7 years; median EDSS score: 1.0, range 0-3.0.). Nineteen healthy controls were also imaged at baseline: (10 female, 9 male, mean age 34 years, range 27-52 years) were imaged at baseline. At year one, 22 MS patients and 18 controls were followed-up; (mean follow up times were 380 days for patients and 386 days for controls). At year two, 22 patients and 14 controls completed follow-up; (mean follow up times were 752 days and 760 days respectively). (One patient missed one-year follow-up, whereas a second missed two year follow-up, but serial data was available on all 23). Prior to study entry, patients had not been on MS disease modifying medication (such as Beta interferon (IFNB) or Glatiramer Acetate) although seven began IFNB between

baseline and the one year time point. Patients had not received steroids within the month prior to any of the imaging sessions. The EDSS, (Kurtzke, 1983) and MS Functional Composite Score (MSFC), (Fischer *et al.*, 1999) were determined in patients at baseline and at the two year time point. The study was approved by the joint ethics committee for the Institute of Neurology and the National Hospital for Neurology and Neurosurgery, Queen Square, London, UK. Written informed consent was obtained from all study participants.

Magnetic Resonance Imaging

Imaging was performed on a 1.5 Tesla Signa (General Electric, Milwaukee, WI, USA). In MS patients and controls, a 2D interleaved dual-echo spin-echo magnetization transfer imaging (MTI) sequence and a 2D spin echo T_1 weighted sequence were acquired at all three time points. The MTI sequence has been described previously, (Barker *et al.*, 1996) and the acquisition parameters were given in Chapter 4. MTR maps, in percent units (pu) were calculated from the short echo images on a pixel by pixel basis according to: $\{[M_o-M_s]/[M_o]\} \times 100$ where M_s and M_o represent the signal intensities with and without the saturation pulse respectively. The acquisition parameters for the T_1 weighted sequence were: TR 540ms, TE 20ms, matrix 256x256, 28 contiguous 5mm slices covering the whole brain.

Image Analysis

Lesions were outlined on the unsaturated proton density weighted images according to previously defined criteria, (Sailer *et al.*, 1999) using a semi-automated local thresholding technique available within the Dispimage package (Plummer *et al.*, 1992). A rater (GRD), blinded to the subject identity and image time point, placed a standard cylindrical region of interest (ROI) (volume 945 mm^3) on to the MTR map such that the ROIs lay entirely within the left and right thalami. (Figure 6.1). Thalamic regions of interest were positioned, at each time point, with reference to the T$_2$ weighted unsaturated image, taking care to avoid lesions and CSF-containing partial-volume voxels. In order to assess whether patients had thalamic lesions, a rater experienced in lesion marking (GRD) examined the patient's T$_2$ weighted imaging at all time points, (inspecting all slices on which the thalamus was seen). The thalamic ROI was always carefully positioned to include only normal-appearing thalamic tissue MTR values from the left and right thalamus were averaged and the mean thalamic MTR was used in the subsequent statistical analysis. (An average was taken to limit the number of statistical comparisons).

Figure 6.1. Regions of interest placed onto the MTR map within each thalamus

(below) with reference to the T$_2$ weighted image (above).
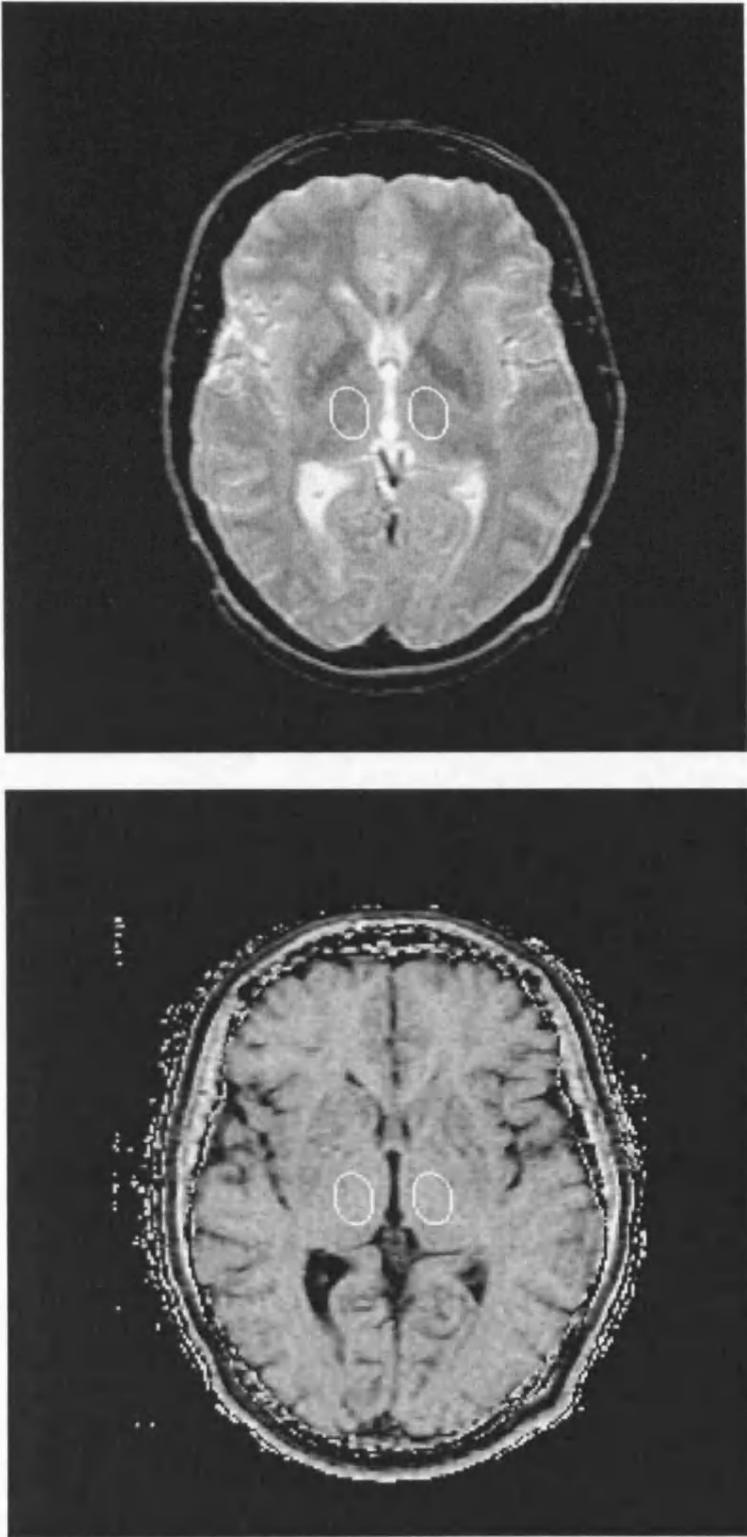
Statistical Analysis

For the comparison between patients and controls, values of MTR over the three time points were modelled using random intercepts regression, (Goldstein *et al.*, 1995) with random subject-specific intercepts and common linear slope on time from study baseline. MS indicator and MS x time interaction terms were used to estimate patient vs. control differences. Potential confounding by age and gender was examined by adding these terms as covariates, but age was omitted since it did not contribute nor materially affect parameter estimates. The longitudinal model was also used to estimate baseline, year-one and year-two cross-sectional patient vs. control differences. To investigate the effects of treatment, a similar random intercepts model was used in patients-only such that the model included a IFNB indicator term and a IFNB indicator x time interaction term to compare the effect of treatment in patients; neither age nor gender contributed to patient-only models, and both were omitted. To investigate (in patients only) the univariate associations between MTR (and MTR change) and both, lesion volume, and clinical disability, Spearman's correlation was used. To investigate whether time modified the association between MTR and baseline lesion volume, a random intercepts regression using the following terms was used: a MTR response variable on baseline lesion volume term, a time indicator term and a lesion volume x time indicator interaction term. A similar interaction model was used to investigate whether the association between MTR and clinical variables differed between baseline and year two. Changes in EDSS and in lesion loads were examined with a Wilcoxon sign rank text, and paired tests were used for changes in MSFC and for the timed walk component z score. [In order to limit the number of statistical comparisons, an *a-priori* decision was taken not to analyze the PASAT and upper-limb z-scores separately, particularly as both tests are

prone to practice effects. (Cohen *et al.*, 2001)] Statistical significance was taken as p

< 0.05. Analyzes were carried out in Stata 8.2 [StataCorp. 2003. *Stata Statistical Software: Release 8.2.* College Station, TX: Stata Corp].

6.2 Results

Clinical Status and Lesion Volume Changes

Over the two year study, the median EDSS increased from 1.0 (range 0-3.0) to 1.75 (range 0-4.0), p = 0.008; (only one patient had an EDSS score of 4.0 at two years). MSFC scores did not change during follow-up (mean MSFC scores at baseline and year two were 0.000 and -0.063 respectively, p = 0.72), though there was borderline evidence of deteriorating timed walk (z scores were 0.000 and 0.817 respectively, p = 0.064). [Mean baseline z scores and the baseline MSFC are always zero as an individual's score is expressed as the number of standard deviations from the baseline group mean. It should also be noted that the more positive the z leg score, the greater the disability, while the converse is true for the MSFC]. Mean annual relapse rate prior to study entry was 1.5, falling to 0.7 during the course of the study.

Median T_2 lesion volume at baseline (determined from the proton-density weighted MTI images) was 13.3ml [mean: 16.6ml, range: 2.1ml to 47.7ml]. In the 22 patients followed up for two years, median lesion volume at baseline was 12.7ml and 12.0ml at two years (p = 0.86). Three patients had thalamic lesions noted on T_2 weighted imaging (two with two lesions each and one with a single lesion). These patients had EDSS scores (at two-years) of 2.5, 3.0 and 2.0 respectively, with all three EDSS scores being greater than the median. Median T_1 lesion volume at baseline was 0.81ml and 0.74ml at two years (p = 0.53).

MTR Findings in the Thalamus

Mean MTR values at baseline, year one and year two are given in Table 6.1. [There was no statistical difference observed between the left and right thalami (p = 0.6, paired samples T-test for patients and controls combined)]. There was no significant cross-sectional difference between patients and controls estimated from the longitudinal model at baseline. However, during the course of the study a difference between patients and controls emerged and at two years the estimated difference (adjusted for gender) was -0.6pu, p = 0.005, 95 % confidence intervals (CI): -1.0pu, -0.17pu. Although the estimated rate of change in patients was significant (-0.33 pu/year, p < 0.001) while that in controls was not (-0.13 pu/year, p = 0.174), the difference did not reach statistical significance (-0.20 pu/year p = 0.117). When patients treated with Beta-interferon were compared with untreated patients, there was no evidence of difference in the change of thalamic MTR during the study (-0.26 pu/year versus -0.36 pu/year respectively, p = 0.515), nor of an estimated difference at two years (p = 0.509). When the changes over time in the treated and untreated groups were separately analyzed, both were significant: -0.26 pu/year, p = 0.048 and -0.36 pu/year, p < 0.001 respectively.

Table 6.1. Mean MTR values from the thalamus in MS patients and controls.

	N (patients/controls)	Mean MTR (std dev)		p value: from longitudinal model[a]
		MS Patients	Controls	
Baseline	23/19	37.2pu (0.6pu)	37.3pu (0.5pu)	0.374
One year	22/18	37.2pu (0.8pu)	37.4pu (0.6pu)	0.018
Two years	22/14	36.5pu (0.6pu)	37.0pu (0.9pu)	0.005

[a]Adjusted for gender, with no evidence of confounding by age.

Relationship between Baseline Lesion Volume and Thalamic MTR

At baseline, there was no significant correlation seen between lesion volume and thalamic MTR, (Spearman's rank correlation coefficient (r_s) = -0.06, p = 0.79). However, at year one, a significant inverse correlation between baseline lesion volume and year one thalamic MTR emerged r_s = -0.49, p = 0.02. At year two, the correlation between baseline lesion volume and thalamic MTR at that time point was of borderline significance only r_s = -0.39, p = 0.08. See Figure 6.2. The association at year one is significantly different from that at baseline (p = 0.005) but not from that at year two (p = 0.185)

For T_1 baseline lesion volume, the Spearman's correlations with MTR at baseline, year one and year two were 0.00 (p = 0.99), -0.56 (p = 0.007) and -0.15 (p = 0.500) respectively. The association at year one is significantly different from that at baseline (p = 0.003), but not from that at year two (p = 0.182).

Relationship between Disability and Thalamic MTR

Patient-specific mean EDSS, averaged over time points, was negatively correlated with patient mean MTR, r_s = -0.47, p = 0.023, and there was no evidence that the association differed between baseline and year two (p = 0.276). There was no evidence that the rate of change of MTR was associated with EDSS at year two (r_s = -0.07, p = 0.754). There was a borderline significant positive association between patient mean MSFC and mean MTR (r_s = 0.40, p = 0.068), and a stronger (and negative) association with the walk component (r_s = -0.50, p = 0.018). For neither MSFC nor the walk component was there evidence of a different association at baseline and year two, or of an association between year two values and rate of change of MTR.

Figure 6.2: No correlation is seen between baseline lesion volume and baseline MTR. However an inverse correlation emerges between baseline lesion volume and thalamus MTR at year one with borderline significance for an inverse correlation at year two.

$r_s = -0.06$
$p = 0.79$

$r_s = -0.49$
$p = 0.02$

$r_s = -0.39$
$p = 0.08$
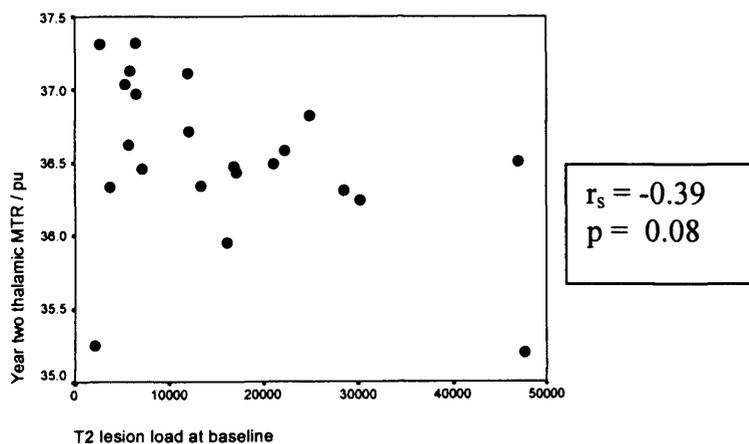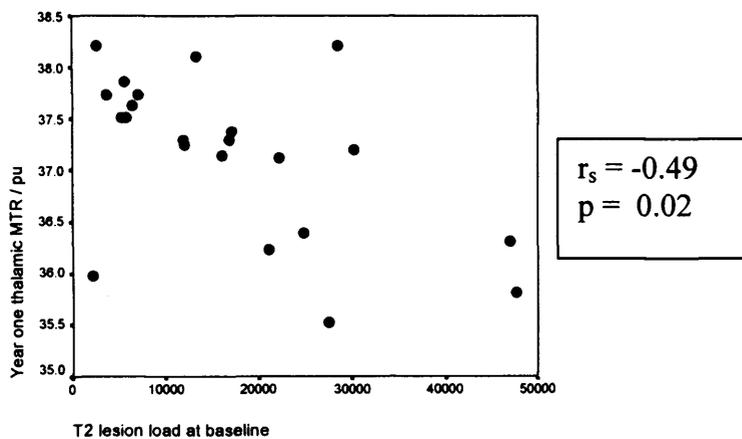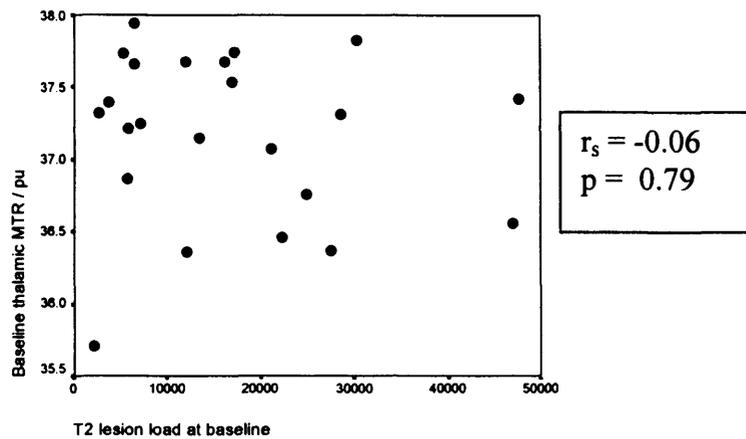
6.3 Discussion

In this study, thalamic abnormality developed within five years of the first clinical event in relapsing-remitting MS, at a stage when most patients had only mild clinical impairment. A modest relationship was also seen between lesion volume at study entry and subsequent values of thalamic MTR.

Although neuropathological findings in MS include cortical grey matter abnormality (Kidd *et al.*, 1999; Peterson *et al.*, 2001; Lumsden, 1970; Brownell and Hughes, 1962), and MRI has revealed evidence for grey matter atrophy early in the clinical course of the disease (De Stefano *et al.*, 2003; Chard *et al.*, 2002), comparatively few studies have investigated the thalamus in isolation. Recent studies have revealed thalamic atrophy and reduced thalamic NAA concentrations in patients with established secondary progressive, (Cifelli *et al.*, 2002), and relapsing remitting MS (Wylezinska *et al.*, 2003; Inglese *et al.*, 2004). While an earlier study of relapsing-remitting and secondary progressive patients did not find evidence for abnormality in the thalamus or basal ganglia when measuring mean diffusivity and MTR (Filippi *et al.*, 2001), an increase in the thalamic apparent diffusion coefficient (ADC) has been reported in a primary progressive cohort (Schmierer *et al.*, 2004*b*), and in a combined relapsing-remitting and secondary progressive study (Fabiano *et al.*, 2003). A diffusion imaging study has also reported an increase in thalamic fractional anisotropy, possibly reflecting a loss of external connectivity (thereby making the internal connectivity within the thalamus more apparent) (Ciccarelli *et al.*, 2001). Although most of these studies do provide evidence for thalamic abnormality in patients with well established MS, the present data additionally suggests that such abnormality begins during an early phase of the disease. A recently published study

(Audoin *et al.*, 2004), appears to confirm this, in that thalamic MTR abnormality was detected (using voxel-based morphometry) in patients with clinically isolated syndromes suggestive of MS.

As an MR measure, the MTR is sensitive to changes in the macro-molecular content of tissue and is reduced by a number of pathological processes, including demyelination, axonal loss, and inflammation (van Waesberghe *et al.*, 1999; Mottershead *et al.*, 2003; Gareau *et al.*, 2000; Schmierer *et al.*, 2004a; Stanisz *et al.*, 2004a). Neuro-pathological findings within the thalamus in MS include axonal loss and therefore reductions in neuronal number may be one possible explanation for the reductions in MTR seen in this study. However, the thalamus also contains a significant amount of myelin (Ohye and Armstrong, 1990), and therefore it is possible that demyelination may also result in the MTR abnormality observed. Although the changes can not be attributable to accrual of MRI visible thalamic lesions, (particularly as lesions involving the thalamus were seen in only three patients and regions of interest were positioned to lie entirely within normal-appearing tissue), small thalamic lesions (not detected on MRI) could theoretically also reduce the MTR. On MRI, cortical grey matter lesions are largely invisible (Kidd *et al.*, 1999), and this raises the possibility that thalamic lesions are also not always seen.

An association was seen between lesion volume at baseline and subsequent values of thalamic MTR but a significant correlation was not seen between baseline lesion volume and baseline MTR. The emergence of a correlation at year-one raises the possibility that early lesion pathology leads to later thalamic abnormality. Neuro-

pathological findings in MS include the transection of axons in active lesions (Ferguson *et al.*, 1997; Trapp *et al.*, 1998; Kuhlmann *et al.*, 2002), a process which could, in turn, lead to the antegrade or retrograde degeneration of axons running within the thalamus. However, alternative interpretations also need to be considered, particularly as a causal relationship between lesion volume and subsequent thalamic change has not been proven. A primary abnormality of normal appearing white matter, for instance, might lead separately to focal lesion genesis and thalamic abnormality, particularly as the thalamus also contains myelin. An additional interesting question concerns the specific location of the thalamic abnormality. However, the present technique could not adequately distinguish between thalamic nuclei and, therefore, further studies are required to address this issue.

Clinical follow-up revealed that the patients did not develop marked disability during the course of the study; none entered the secondary progressive phase and all remained ambulatory throughout the study period. It therefore appears that thalamic abnormality in MS occurs at an early stage of the disease rather than being an end-stage event associated with marked disability.

Methodological Considerations

The main limitation of the study was the relatively small sample size and although the rate of change in thalamic MTR was significant in patients and not in controls, the difference between the rates was not significant. There is therefore a need to confirm these findings in a larger cohort. In addition, the limited sample size and the use of disease modifying therapy in approximately 30% may account for the absence

of a significant increase in lesion load, something that has been shown with larger

cohorts (Sailer *et al.*, 1999). However, the patients in this study do appear to be

typical of early relapsing-remitting MS patients in terms of relapse rate (The IFNB

Multiple Sclerosis Study Group, 1993), gender distribution and EDSS. The statistical

analysis used was prospectively devised on the basis of gender imbalances seen

between patients and healthy controls and the analysis therefore corrected for any

effects of possible gender confounding. A correction for multiple comparisons was

not performed and therefore the results with borderline statistical significance should

be regarded with caution. The cohort subgroups were too small to allow an

assessment of whether MTR change was altered by disease modifying treatment.

However, a significant MTR decrease was seen in the 16 patients who were not

treated and this supports the finding obtained from the whole cohort in that thalamic

abnormality emerges early in the natural history of the disease. Finally, it is unlikely

that thalamic atrophy, during the course of the study, resulted in an artifactual

reduction of thalamic MTR (via increasing partial volume artifact) because the ROIs

were positioned to lie entirely within the thalamus and therefore partial volume

voxels were avoided.

Conclusions

In conclusion, this study found evidence for emerging thalamic MTR abnormality in

early relapsing-remitting MS, when most patients were non-disabled. As the

thalamus acts as a central relay point for a number of neuronal pathways, (and as

some of the thalamic abnormality may be neuronal in origin), these results appear to

support the view that neuronal abnormality is an early event in the course of the

disease.

PART 3

THE ESTIMATION OF UNDERLYING

MT PARAMETERS

CHAPTER 7

Estimation of the semi-solid proton fraction and semi-solid T_2 in

multiple sclerosis

As highlighted in Chapter 2, and subsequently in Chapters 4-6, the MTR can provide useful, *in-vivo,* insight into MS pathology. As mentioned, the MTR provides an indirect assessment of the semi-solid content of a tissue (van Buchem and Tofts, 2000; Dousset *et al.,* 1992; Filippi *et al.,* 1995; van Buchem *et al.,* 1996) and in the central nervous system, phospholipid bilayers may comprise much of the semi-solid proton content (van Buchem and Tofts, 2000; Morrison and Henkelman, 1995). This may explain why the MTR is sensitive to changes in both axonal and myelin density (van Waesberghe *et al.,* 1999, Schmierer *et al.,* 2004a). However, it appears that the MTR is not specific for any single pathological feature, (van Waesberghe *et al.,* 1999; Gareau *et al.,* 2000), and it is therefore possible that further insight will be obtained by estimating the parameters that *underlie* the MT effect. These parameters include the semi-solid proton fraction (*f*) and the T_2 relaxation time of the semi-solid pool (T_{2B}). (Further details are given in Chapter 2).

As mentioned, a mathematical model for the magnetization transfer effect, based on two pools of protons, has previously been proposed (Henkelman *et al.,* 1993). (However, it should be noted that Henkelman's model describes a system that uses continuous wave (CW) irradiation, and this is not directly applicable to the *in-vivo* situation). In the model, the first pool comprises protons in free water with the second representing protons within semi-solid structures (such as within macromolecules and phospholipid bilayers). The model relates the magnetisation of

the partially saturated free water to: (1) the relative size of the two pools, (2) acquisition specific parameters (including the offset frequency and amplitude of the saturating MT irradiation) and (3) a number of rate constants (including longitudinal-relaxation, cross-relaxation and absorption rate constants). An adaptation of the technique (allowing its' application to pulsed clinical sequences) has permitted f and T_{2B} to be estimated in human subjects (Ramani *et al.*, 2002; Tozer *et al.*, 2003; Tofts *et al.*, 2005). At the time that the study in this chapter was conducted, similar *in-vivo* techniques had been developed by Sled and Pike, (2001) and Yarnykh, (2002), but while these permitted parameter estimation in a single slice, the technique described here (Ramani *et al.*, 2002; Tozer *et al.*, 2003; Tofts *et al.*, 2005) allows for whole brain coverage. (Whole brain coverage may be helpful in a diffuse and multifocal disease process such as MS). Of note, Yarnykh and Yuan (2004) have recently developed a technique that also provides whole brain coverage.

The study reported in this chapter used a model for magnetization transfer (MT) to estimate the two underlying parameters: f and T_{2B} in sixty patients with clinically definite multiple sclerosis (MS). (This is a different cohort to that described in previous chapters). The aims of this study were: (1) to investigate whether abnormalities of f and T_{2B} are present in MS lesions and normal appearing tissues and, (2) to explore the relationship of the new measures with clinical status.

7.1 Theory

The binary spin bath model used for the current study has been adapted from that of Henkelman *et al.* (1993). Henkelman's model has been outlined in Chapter 2 and will not be explained in detail here. A number of adaptations have been made. Firstly, Henkelman's model describes a system that uses a continuous wave (CW) field, while on a clinical imager, off-resonance irradiation must be applied as a series of MT pulses. Ramani *et al.*, (2002) assumed that their pulse sequence, with an MT pulse repeat-time of 41ms, is sufficiently similar (in saturating effect) to a system that uses CW irradiation. Under this assumption, the root-mean-square (RMS) of the MT pulse amplitude is determined and averaged over the MT pulse repeat time, (this is known as the CW power-equivalent: ω_{CWPE}). It is assumed that an MT sequence (with a given ω_{CWPE}) has the same saturating effect as a CW field that has an amplitude equal to ω_{CWPE} (Ramani *et al.*, 2002; Tofts *et al.*, 2005).

Ramani *et al.*, (2002) reintroduced the M_0^A term (which was set to unity by Henkelman) and included a constant of proportionality (g) (reflecting the gain of the amplifier and other scanner settings). The parameter, gM_0^A (which is equivalent to the proton density of free water) is now fitted independently and the expression (see over) provides an estimate of signal intensity (S). The model therefore takes the form as laid out on the following page. The similarity to Henkelman's original model can be appreciated by comparing this formula with formula [12] in Chapter 2. M_0^B has also been replaced with $fM_0^A/(1-f)$, where f is the semi-solid proton fraction:

$$f = M_0^B \, / \, M_0^A + M_0^B.$$

$$S = g\,M_0^A \left(\frac{R_B \left[\dfrac{RM_0^A f}{R_A(1-f)} \right] + R_{RFB} + R_B + RM_0^A}{\left[\dfrac{RM_0^A f}{R_A(1-f)} \right]\!\left(R_B + R_{RFB} \right) + \left(1 + \left[\dfrac{\omega_{CWPE}}{2\pi\Delta} \right]^2 \left[\dfrac{1}{R_A T_{2A}} \right] \right)\!\left(R_{RFB} + R_B + RM_0^A \right)} \right)$$

Ramani-Tozer-Tofts adaptation of Henkelman's model.

S : Signal intensity
g : gain of the amplifier
M_0^A and M_0^B :the size of the free and semi-solid pools
R_A and R_B : free and bound longitudinal relaxation rate constants
R: rate of cross relaxation,
R_{RFA} and R_{RFB}: absorption rate constants of the free and bound pool (R_{RFB} gives T_{2B})
ω_{CWPE} effective amplitude of the saturating MT irradiation (continuous wave power equivalent)
Δ : MT pulse offset frequency
T_{2A} : free water T_2

f: semi-solid (macromolecular) proton fraction : $M_0^B / [M_0^A + M_0^B]$

A final consideration is the absorption line shape for the semi-solid pool (R_{RFB}). (This is the rate that the semi-solid pool absorbs magnetisation for any given off-set frequency). R_{RFB} depends on the T_2 of the semi-solid pool (T_{2B}) and by fitting R_{RFB}, (via T_{2B}), a value for T_{2B} can be obtained. Generally the shorter the T_2 the broader the line shape.

Although Henkelman initially used a Gaussian line shape to model MT in agar, the Gaussian proved to be inaccurate for biological tissue. The super-Lorentzian line shape (which is expected to arise from partially ordered materials, for example,

polymers, liquid crystals or biological membranes) allowed for better fits in biological material (Morrison and Henkelman, 1995). The super-Lorentzian line shape was therefore adopted for the present work (Tofts *et al.*, 2005; Tozer *et al.*, 2002). The integral describing the super-Lorentzian line shape can be seen in: Morrison and Henkelman, (1995).

In the present study, 10 data points are acquired (using differing MT pulse amplitudes (each with a corresponding ω_{CWPE}) and differing off set frequencies – see Table 7.1) and the model is fitted to the resulting signal intensities. In the least square fitting, five fitted parameters are estimated: gM_0^A, RM_0^A, $f/(1-f)R_A$, $1/R_AT_{2A}$, and T_{2B} (via R_{RFB}) since it is not possible to independently fit all eight parameters. R_B is fixed at $1s^{-1}$ as the change in sum of squares with respect to R_B was zero. This means that R_B may take any value without changing the quality of fit and if R_B is unconstrained the model will not meaningfully converge. This is in accordance with Henkelman *et al.*, (1993) who concluded that R_B could not be determined in such experiments. A value of $1s^{-1}$ was selected since this was the value previously assumed, (Morrison and Henkelman, 1995; Sled and Pike, 2001) allowing data from this study to be compared more easily with data from previous work.

Table 7.1: The continuous-wave-power-equivalents (ω_{CWPE}) and off set frequencies

(Δ) of the 10 acquired data points.

ω_{CWPE} (rad s^{-1})	Δ (Hz)
185	1000
185	2500
185	7500
378	1000
378	3500
378	15000
435	1000
435	2500
435	5000
435	7500

f can then be calculated from $f/(1-f)R_A$ by firstly obtaining an independent estimate

of the observed T_1: (T_{1Aobs} i.e.: $1/R_{Aobs}$) – (this is estimated using a previously

described method (Parker *et al.*, 2001) – see Chapter 3 for details) – and R_A can then

be estimated according to the following relationship (for a derivation of this see

Henkelman *et al.*, 1993):

$$R_A = \frac{R_{Aobs}}{1 + \frac{RM_0{}^A f}{R_A(1-f)}\frac{(R_B - R_{Aobs})}{R_B - R_{Aobs} + RM_0{}^A}}$$

7.2 Methods.

Patients and Controls

Sixty subjects with clinically definite MS, (Poser *et al.*, 1983) [38 female and 22 male; mean age 47 years, range 27 to 73 years; 27 with relapsing remitting (RRMS), eight with benign (BMS), 12 with primary progressive (PPMS) and 13 with secondary progressive MS (SPMS), (Lublin and Reingold, 1996)] and 27 healthy control subjects (13 female and 14 male; mean age 35 years, range 23 to 52 years) were studied. (Table 7.2). As there was a large age difference between controls and the MS group, comparisons between MS patients and controls were made using only those patients aged less than 50. The demographics of this subset were as follows: 18 female, 15 male; mean age 39, range 27 to 50 years; 22 with RRMS, one with BMS, six with SPMS and four with PPMS. In subjects affected by MS, the expanded disability status scale (EDSS) score, (Kurtzke, 1983) and the MS functional composite scores (MSFC), (Fischer *et al.*, 1999) were determined.

The study was approved by the joint ethics committee of the Institute of Neurology and the National Hospital for Neurology and Neurosurgery. All subjects gave informed written consent prior to the study.

Table 7.2: EDSS and disease duration in the full patient cohort and in the four clinical subgroups.

	N	Median EDSS (range)	Mean disease duration/ years (range)
Full MS cohort	60	3.0 (1.0-7.5)	15 (0.5-38)
Relapsing-remitting MS	27	2.0 (1.0-5.0)	9 (0.5-27)
Benign MS	8	2.5 (2.0-2.5)	23 (19-32)
Secondary progressive MS	12	6.0 (3.5-7.5)	24 (5-38)
Primary progressive MS	13	6.0 (2.0-7.0)	12 (9-21)

MRI acquisition

Imaging was performed on a 1.5 Tesla Signa scanner (General Electric, Milwaukee, USA).Three sequences were acquired in all subjects. 1) A dual echo fast spin echo (FSE) sequence (repetition time (TR) 2000ms, echo times (TE) 19/95ms, 28 contiguous 5mm axial slices covering the whole brain). 2) A MT sequence consisting of a Gaussian MT pulse (duration 14.6ms) applied before each slice of a 2D spoiled gradient echo sequence (TR 1180ms, TE 12ms, excitation flip angle 25°, field of view (FOV) 24x18cm^2, slice thickness 5mm; (a line of k-space is acquired from each of the 28 slices in one TR). To minimize acquisition time a partial k-space acquisition was used, collecting 48 phase encode steps to one side of k = 0 and 8 to the other; this was reconstructed to a 256x256 matrix over a 24x24cm^2 FOV). The interval between the start of successive MT pulses (TR') was 41ms. Ten independent

measurements each consisting of 28 contiguous oblique axial slices covering the whole brain were made at differing MT pulse offsets and powers, (See Table 7.1) (Ramani *et al.*, 2002; Tofts *et al.*, 2005) 3) PD and T_1 weighted gradient echo data sets (TR/TE/flip-angle/no.-of-averages: 1500ms/11ms/45°/8 and 50ms/11ms/45°/2 respectively) permitting the calculation of T_1 relaxation time (Parker *et al.*, 2001). (As mentioned, an independent measurement of the observed T_1 relaxation time is required in order for *f* to be estimated). Total scan time was 1 hour.

Image processing

The first MT data set was used as a template to which the FSE images were registered (using the AIR package) (Woods *et al.*, 1993). The calculated T_1 relaxation map and other 9 MT data sets were also registered to this template using mutual information registration (Studholme *et al.*, 1999). Lesions were then contoured on the FSE data set using DispImage (Plummer, Dept of Medical Physics and Bioengineering, UCL, UK) according to previously defined rules (Sailer *et al.*, 1999). Fourteen normal appearing white matter (NAWM) regions and six normal appearing grey matter (NAGM) regions of interest (ROI) were also outlined on the first MT data set, with care taken to avoid lesion ROIs. ROIs in normal appearing regions were cylindrical and had a volume of 130 mm^3 in the corpus callosum and internal capsule and 230 mm^3 elsewhere. The following regions were outlined bilaterally in NAWM: frontal and occipital lobes, anterior and posterior limbs of the internal capsule, centrum semiovale and middle cerebellar peduncles. Single mid-line regions were outlined in the genu and splenium of the corpus callosum (Figure 7.1 illustrates some of the white matter ROIs). In grey matter, bilateral regions were

placed in the thalamus, the caudate and the lentiform nucleus. Cortical grey matter regions were not used as partial volume artefact could not confidently be excluded.

Figure 7.1: Regions of interest in a normal control placed (from top) in: frontal white matter, genu of the corpus callosum, anterior and posterior limbs of the internal capsule, splenium of the corpus callosum and occipital white matter.

The ROIs defined were then transferred to the 10 (co-registered) MT data sets and the T_1 map, and the model was fitted to values thus determined. Five fitted parameters were estimated: gM_0^A, RM_0^A, $f/(1-f)R_A$, $1/R_AT_{2A}$, and T_{2B} (via R_{RFB}). Fitting was achieved with a least squares technique based on a Numerical Algorithms Group routine, (Ford *et al.*, 1979) and *f* was calculated from $f/(1-f)R_A$ using the observed T_1, (which is related to R_A) (Henkelman *et al.*, 1993). R_B (the longitudinal relaxation rate constant of the bound pool) was fixed at $1s^{-1}$.

A super-Lorentzian line shape was assumed for the absorption line shape of the bound pool (Morrison and Henkelman, 1995). The average of the root mean square residuals for parameter fitting in NAWM (patients and controls combined) was 1.2% (range 0.8% to 2.1%).

The same analysis was performed on a pixel by pixel basis in a single subject and the resulting parameters maps can be seen in Figure 7.2.

Statistical Analysis

Group comparisons, were made using the Mann Whitney U test (SPSS11.0). Control and MS patient comparisons were made using a subset of patients below the age of 50 which allowed for better age and gender matching. The relationships between parameters (all 60 MS patients) were assessed using Spearman's rank correlation coefficient (r_s). The coefficient of variation was used as a measure of repeatability. p values of ≤ 0.05 were regarded as significant.

7.3 Results.

Reproducibility

Five controls were imaged twice (mean time from scan to rescan was 42 weeks; range 21-70 weeks) and coefficients of variation for f and T_{2B} from NAWM were 5.4% and 4.7% respectively.

Age and Gender effects

There was no gender difference (patients and controls combined) for mean NAWM f (p = 0.5), deep grey matter f (p = 0.6), mean NAWM T_{2B}, (p = 0.8) or deep grey matter T_{2B} (p = 0.6). Age was inversely correlated with mean NAWM f (r_s = -0.42, p < 0.001) and with deep grey matter f (r_s = -0.28, p = 0.01) but not with mean NAWM T_{2B} (r_s = 0.16, p = 0.13) or deep grey matter T_{2B} (r_s = 0.04, p = 0.7).

Comparisons between patients and controls and correlations between parameters:
Findings in lesions

In lesions, mean f was 4.6 percent units (pu) versus 9.0 pu in control white matter, p < 0.001. Mean lesion T_{2B} was 11.5 µs versus 10.6 µs in control white matter, p < 0.001 (See Table 7.3).

Table 7.3: Lesion characteristics of the MS subgroups

	Mean lesion f (range) / pu	Mean lesion T_{2B} (range) / μs	Mean lesion T_1 (range) / ms
Full MS cohort	4.7 (3.0-6.9)	11.5 (8.7-13.8)	980 (770-1210)
Relapsing-remitting MS	4.9 (3.4-6.9)	11.2 (8.7-13.4)	950 (820-1130)
Benign MS	4.4 (3.4-5.2)	12.1 (11.3-13.8)	1000 (940-1140)
Secondary progressive MS	4.4 (3.0-5.8)	11.6 (9.1-13.5)	1000 (840-1210)
Primary progressive MS	4.8 (3.6-6.5)	11.4 (9.7-13.4)	990 (770-1110)

Findings in NAWM, Deep grey matter and posterior fossa white matter

In total NAWM, mean f was 8.0 pu in MS patients versus 9.0 pu in control white matter, $p < 0.001$. f values from separate white matter regions, deep grey matter regions and the cerebellar peduncles are shown in Table 7.4. f was abnormal in a number of the supra-tentorial white matter regions, but not in the middle cerebellar peduncles or deep grey matter.

T_{2B} was not significantly increased in total NAWM. T_{2B} values from separate regions are also given (Table 7.4) and the only significant increase was seen in occipital white matter.

In total NAWM, (MS patients and controls combined), f and T_{2B} were inversely correlated; $r_s = -0.58$, $p < 0.001$.

Cross relaxation rate in white and grey matter

The cross relaxation term (RM_0^A), which provides an indication of the rate of cross exchange between the bound and free pools, was found to be uniformly high in all regions in MS patients and controls ($>10^5$ s^{-1}).

Relationship between T_1 relaxation time and MT parameters

An estimate of the spin lattice relaxation time (T_1) was required in order for f to be estimated. Data on T_1 was derived from NAWM and lesions so that this data could be compared with f and T_{2B}. In comparison to controls, T_1 was increased in lesions and in NAWM (Table 7.4). An inverse correlation was seen between T_1 and f in total NAWM (patients and controls combined); $r_s = -0.80$, $p < 0.001$ and a positive correlation was seen between T_{2B} and T_1; $r_s = 0.32$, $p = 0.003$.

Table 7.4: f, T_{2B} and T_1 values compared between 33 MS patients and 27 healthy controls.

Region	f / pu			T_{2B} / µs			T_1 / ms		
	MS	Cont	p	MS	Cont	p	MS	Cont	p
Lesions[a]	**4.6**	**9.0**	**<0.001**	**11.5**	**10.6**	**<0.001**	**970**	**650**	**<0.001**
Total WM[b]	**8.0**	**9.0**	**<0.001**	10.8	10.6	0.39	**710**	**650**	**<0.001**
Frontal WM	**8.6**	**9.8**	**0.001**	10.5	10.5	0.95	**680**	**610**	**<0.001**
Genu of CC	**8.1**	**9.5**	**0.002**	10.8	10.6	0.77	**700**	**620**	**<0.001**
Anterior IC	**7.0**	**7.7**	**0.013**	11.4	10.9	0.24	740	710	0.06
Posterior IC	8.0	8.2	0.54	11.3	11.6	0.46	**730**	**680**	**0.002**
Splenium of CC	**8.4**	**9.5**	**0.002**	10.0	9.4	0.10	**730**	**660**	**<0.001**
Occipital WM	**7.7**	**9.1**	**<0.001**	**11.0**	**10.6**	**0.03**	**700**	**630**	**<0.001**
CSO	**8.2**	**9.2**	**<0.001**	10.6	10.5	0.95	**690**	**630**	**<0.001**
Cerebellar Ped.	7.4	7.4	0.99	10.4	10.2	0.52			
Total deep GM	4.6	4.7	0.45	10.7	10.6	0.61			
Caudate	3.6	3.6	0.16	10.8	11.1	0.61			
Lentiform	4.7	4.8	0.67	10.5	10.0	0.30			
Thalamus	5.6	5.6	0.80	10.9	10.6	0.67			

Bold type: significant at $p < 0.05$ level; using Mann-Whitney U test. Cont = values from 27 healthy controls, MS = values from 33 MS patients. WM = white matter, GM = grey matter, CC = corpus callosum, CSO = centrum semi ovale, IC = internal capsule. Cerebellar Ped. = middle cerebellar peduncle. [a]lesions compared to total control white matter. [b] supra-tentorial WM pooled.

T_2 lesion load measures

Mean T_2 lesion load was 19.3 ml (median 16.3 ml, range 0.5 to 79.3 ml). T_2 lesion load correlated with NAWM T_{2B} ($r_s = 0.37$, $p = 0.004$) and was inversely correlated with NAWM f ($r_s = -0.52$, $p < 0.001$)

Clinical Status and correlations with MT parameters and T_1 relaxation time

Median EDSS and mean disease durations for all 60 subjects with MS and for the four clinical subgroups are given in Table 7.2. Table 7.5 shows all significant correlations between clinical function and MT measures. A modest correlation was seen between total NAWM f and the MSFC. f also correlated with the MSFC in several white matter tracts (the genu and splenium of the corpus callosum, the anterior limb of the internal capsule and the cerebellar peduncles). A modest correlation was seen in frontal NAWM. The only significant correlation between f and the EDSS was seen in the genu of the corpus callosum. T_{2B} showed a modest correlation with the MSFC (and EDSS) in the splenium of the corpus callosum (Table 7.5). T_1 correlated weakly with the MSFC in total NAWM. It also correlated with the MSFC and the EDSS in the corpus callosum (Table 7.5).

Table 7.5. Spearman's r values for clinical- MR correlations

Region	f/ pu		T_{2B}/ µs		T_1 / ms	
	EDSS	MSFC	EDSS	MSFC	EDSS	MSFC
Lesions	ns	ns	ns	ns	ns	ns
Total WM[a]	-0.24	**0.43***	ns	ns	ns	**-0.28**
Frontal WM	ns	**0.30**	ns	ns	ns	ns
Genu of CC	**-0.34***	**0.40***	ns	ns	**0.32**	**-0.34**
Anterior IC	ns	**0.33**	ns	ns	ns	ns
Posterior IC	ns	0.26	ns	ns	ns	ns
Splenium of CC	ns	**0.38***	**0.28**	**-0.34**	0.24	**-0.36***
Occipital WM	ns	0.25	ns	ns	ns	ns
CSO	-0.24	0.26	ns	ns	ns	ns
Cerebellar Ped.	ns	**0.28**	ns	ns		
Total deep GM	ns	ns	ns	ns		
Caudate	ns	ns	ns	ns		
Lentiform	ns	ns	ns	ns		
Thalamus	ns	ns	ns	ns		

Non Bold type: borderline only: $p < 0.08$. Bold: significant at $p < 0.05$ level.

Bold* $p < 0.01$, ns: $p > 0.08$. WM = white matter, GM = grey matter, CC = corpus callosum, CSO = centrum semi ovale, IC = internal capsule. Cerebellar Ped. = middle cerebellar peduncle. [a] supra-tentorial WM pooled.

Figure 7.2: Parameter maps in a patient with MS. Top row from left to right: PD map, T_{2B} map, $f/(1-f)R_A$ map. Bottom row, left to right: T_{1A}/T_{2A} map, T_{1Aobs} map, f map.
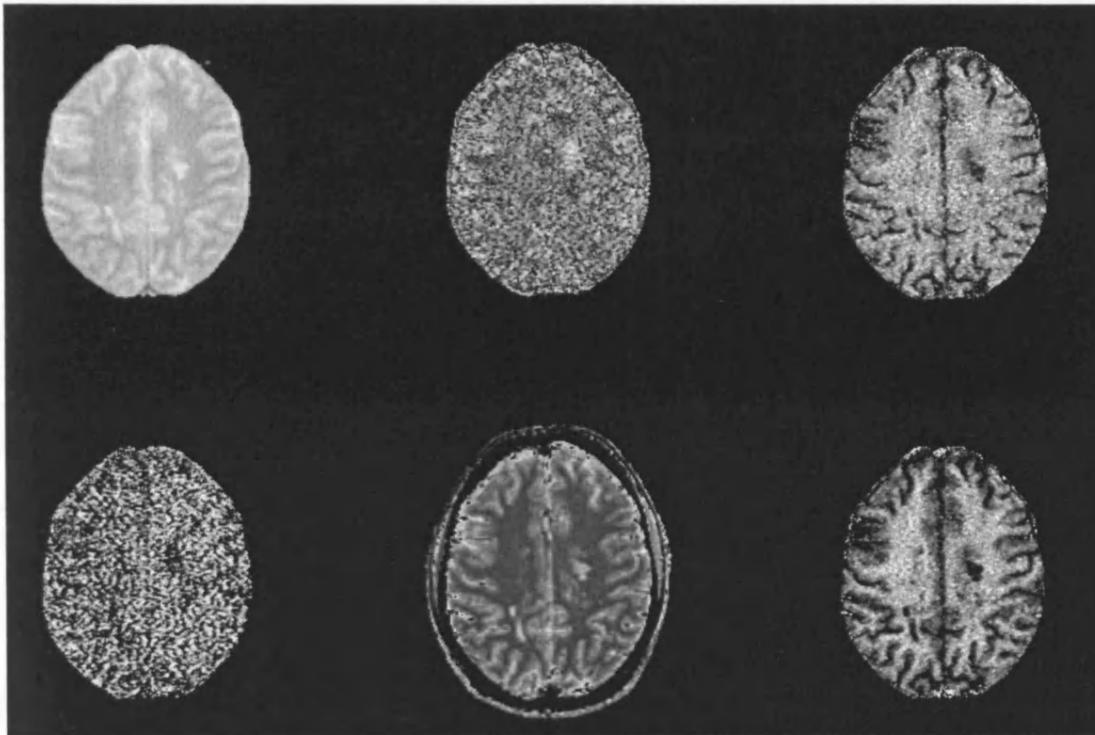
7.4 Discussion.

In the study of MS, one limitation of conventional MRI is that it lacks the pathological specificity seen with histopathological techniques (van Waesberghe *et al.*, 1999; Gareau *et al.*, 2000). Consequently, a MR technique that offers greater pathological specificity might improve upon the description or the monitoring of in-vivo changes. A potential way of achieving this would be to use the magnetisation transfer effect to derive a set of underlying parameters which, in turn, provide a more detailed description of tissue structure. Such an approach has been attempted here. This quantitative analysis of the MT effect yielded two parameters that provide complementary information. T_{2B}, a measure of the motional restriction of semi-solid protons, is increased in lesions whereas f, a measure of the semi-solid proton to total proton ratio, shows more diffuse but clinically relevant abnormality.

Although the nature of the semi-solid proton fraction is uncertain, the improvement seen in fitting when the model is altered to more accurately account for the nature of phospholipid bilayers, (Morrison and Henkelman, 1995) would suggest that phospholipid bilayers are an important component of the semi-solid content in this instance. Principle changes within lesions include T-cell mediated inflammation, demyelination, (Lassman *et al.*, 1998), axonal loss, (Trapp *et al.*, 1998) and gliosis, (Adams, 1977). In NAWM, axonal loss and gliosis (and, to a lesser extent, perivascular inflammation and demyelination) have also been demonstrated (Allen and Mckeown, 1979; Evangelou *et al.*, 2000). Although f could be reduced by a decrease in the semi-solid content either via demyelination or axonal loss, it should also be noted that f is a ratio of semi-solid protons to total protons and an increase in

the free water component (as in oedema) could also result in a reduction in f.

Histopathological studies correlating f with pathological findings are now required to investigate these relationships.

Correlations were seen between f and disability, particularly when f was estimated from long white matter tracts (the corpus callosum, the internal capsule and the cerebellar peduncles), indicating that the changes detected by this parameter do have clinical relevance. These correlations might suggest that long white matter tract pathology has a role in the accrual of disability.

T_{2B} was sensitive to pathology within lesions but was much less sensitive to abnormality within normal appearing brain tissue. The parameter is an estimate of the T_2 relaxation time of semi-solid protons and therefore is likely to detect changes to the structure of the semisolid content (rather than changes to the semi-solid/free water ratio). The increase in T_{2B} in lesions suggests that there has been a change in the nature of the remaining semi-solids, conceivably due to a disruption of myelin and axonal phospholipid bilayers.

The results need to be interpreted in the context of a number of methodological considerations. Firstly, although the fitting of the model to experimental data is reasonable, (giving some confidence in its validity), the model contains a number of assumptions which are only partially met in practice. The assumption of two pools, made by both Henkelman and ourselves is, in itself an approximation, and a fuller description might include longer and shorter T_2 components in both the 'bound' and 'free' pools, along with interactions between them. The original model (proposed by

164

Henkelman *et al*, 1993) also describes a system with a continuous saturating power and we have therefore made the assumption that our pulse sequence sufficiently approximates a continuous power. This might lead to some error in parameter accuracy and although f and T_{2B} were similar when estimated with other models, (Sled and Pike, 2001; Yarnykh, 2002) it may explain the discrepancy in the rate of cross relaxation; (which was uniformly high in our case). A better estimate of the rate of cross-relaxation might allow for a more accurate estimate of f, and, with this in mind we are continuing to refine the model and pulse sequence.

Secondly, the statistical analyses used did not correct for multiple comparisons and so it is possible that some of statistically significant results occurred by chance. For this reason the data has been presented in tabulated form so that the number of comparisons (and the proportion that are significant) can be appreciated. The pattern of abnormality seen in NAWM and the correlations with disability were similar between parameters, adding support to the view that these were biological effects.

The parameter f appears to be sensitive to abnormality within lesions and normal appearing brain tissue and its correlation with disability indicates that it has some clinical relevance. However, histopathological post mortem data is now required to assess the pathological specificity of f and T_{2B}. Imaging techniques that quantify demyelination would be of use in following MS pathology (for instance in symptomatic demyelinating lesions of the optic nerve or spinal cord) and especially in monitoring therapies to promote remyelination. Quantitative MT techniques are therefore likely to be the subject of further work, with the aim of refining the technique to improve upon specificity for the detection of myelin. Of note, Stanisz *et*

al., (2004*a*, *b*) have recently found that the relative size of the bound pool (M_0^B), (estimated in rat sciatic nerve), altered in the presence of experimentally induced inflammation and demyelination. It will now be relevant to directly correlate *f* and T_{2B} with *post mortem* histopathological data and to obtain global in vivo measures via histogram analysis.

PART 4

CONCLUSIONS

CHAPTER 8

Conclusions

This thesis describes a number of studies that have investigated the changes within the normal-appearing brain tissue in patients with early relapsing-remitting MS. One objective was to describe the early evolution of abnormality within the normal-appearing white matter and grey matter, prior to the onset of major disability. At the time that the studies in this thesis were conducted, it was unclear whether abnormalities within the normal-appearing white matter (NAWM), the cerebral grey matter, and the thalamus progressively accumulated in early disease and at what stage such abnormalities began.

In the context of clinical trials, measures that detect abnormality within grey matter and NAWM, have the *potential* to improve the effectiveness of MRI surrogate endpoints. As discussed in Chapter 2, a key requirement of any surrogate is that it should be strongly predictive of long term disability (McFarland *et al.*, 2002), and that it should be sensitive to change over time prior to the onset of disability. Brain T_2 lesion load is a widely used measure, used to follow the course of the disease; and – in clinical trials – to evaluate treatment efficacy; however, although it *can* detect change over time in early MS (Sailer *et al.*, 1999), it is only modestly predictive of long term disability (Brex *et al.*, 2002). Possible reasons for this modest correlation include: (1) that lesions are pathologically heterogeneous, (2) that lesions vary in their anatomical distribution (and hence clinical relevance), and (3) that lesion accrual in early disease may have a greater effect on disability accumulation than lesion accrual in late MS. However, a further potential reason for the modest

correlation is that changes within grey matter and NAWM are also contributing to later disability. By quantifying these changes (and by combining them with lesion load measures), it may be possible to develop surrogate endpoints which are more strongly predictive of future clinical impairment. *Hypothetically*, such measures could provide useful insight into which therapies have *potential* to prevent long term disability (and so provide guidance into which therapies should be further investigated using clinical endpoints). However, prior to concluding that a measure of early abnormality in grey matter and NAWM could usefully contribute as a surrogate endpoint, it is necessary to show that such measures are strongly predictive of future clinical impairment. At present, the long term data necessary to show this is not available and further follow-up of the cohort is required. This thesis has therefore focussed on another key question: namely whether these measures are sufficiently sensitive and reproducible to detect a change over time in minimally-disabled patients with early relapsing-remitting MS.

In a clinical trial, a treatment effect is likely to manifest as a difference in the rate at which abnormalities accumulate, when the placebo and treatment groups are compared. Therefore, if measures of normal-appearing tissue abnormality are to be useful, they must be able to detect increasing abnormality over the 2-3 year time frame typical of many trials. Although many measures, (including clinical ones), can detect increasing abnormality in *progressive* MS, measures which can *also* detect increasing abnormality prior to the onset of progressive disability may be particularly useful. As discussed in Chapter 1, once clinical progression has commenced, a self-propagating pathological deterioration may occur, and at this stage, disease-

modifying treatments are likely to be less effective (or not at all effective). Furthermore, once permanent disability has occurred, it may be very difficult to reverse. Measures therefore that can detect increasing and clinically relevant grey matter and NAWM abnormality, early in the disease course, could be useful. In all, the ideal surrogate would provide a complete assessment of accumulating pathological abnormality in early MS (encompassing measures of grey matter and NAWM abnormality); it should be sensitive and specific for the pathological changes that lead to later disability, and it should be strongly predictive of later clinical impairment. Finally the measure should be sufficiently sensitive and reproducible to detect increasing change over a 2-3 year time frame in patients with early MS and minimal disability.

Prior to the studies included in this thesis, two measures showed particular promise for investigating normal-appearing brain tissue abnormality. These were: the MTR and, the related measure, the T_1 relaxation time. T_1 measurement is able to detect grey matter and NAWM abnormality in early relapsing-remitting MS (Griffin *et al.*, 2002*b*) and T_1 measured globally, throughout the brain, shows an association with the mild clinical impairments already present (Griffin *et al.*, 2002*a*). Furthermore, a study of patients with more advanced disease (including some with secondary progressive MS) reported that T_1 histograms were sufficiently sensitive to detect increasing abnormality over a 20 month period (Parry *et al.*, 2003). Therefore, in Chapter 3, the objective was to assess whether grey matter and NAWM T_1 histograms were sufficiently sensitive and reproducible to detect a change over time in patients with early relapsing-remitting MS. As discussed in Chapter 3, there was

no strong evidence that T_1 measures (acquired using a two-point non-interleaved technique), were able to detect such a change. Although there *was* borderline evidence for a decline in patient NAWM peak-height, there was no serial change in either mean T_1 or peak-location. Although these findings may have arisen because the peak-height may be more sensitive than either the mean or the peak location, it should also be noted that peak-height had limited reproducibility in comparison to other parameters, making it potentially less useful. Reasons for the poor reproducibility include the possibility that peak-height might fluctuate with inflammatory activity; (it should be recalled that, in Chapter 3, patient peak-height COV was more than double that of control peak-height COV; in addition, previous studies have shown that T_1 is sensitive to changes in cerebral oedema). In all, there was no conclusive evidence that grey matter and NAWM T_1 histograms were able to detect a change over time in early relapsing-remitting MS. There appears to be two possible reasons for this finding. Firstly, a measure derived from a two-point non-interleaved technique may be insufficiently reproducible to allow a subtle serial change to be detected. Secondly, the T_1 relaxation time appears to be a non-specific measure; and although it may detect pathologies that might gradually worsen (such as axonal loss), it may also detect reversible pathology (such as inflammatory activity) which may fluctuate rather than progressively deteriorate.

In Chapters 4 and 5, attention was turned to the use of MTR in early relapsing-remitting MS. The extensive literature on MTR reveals that the parameter may be semi-specific for changes in myelin and axonal density (with smaller changes seen with inflammation). As a result, MTR might be more effective than T_1 at detecting

increasing structural abnormality (that reflects the loss of axons and/or myelin) in early MS. Furthermore, the MTR sequence used in this work was interleaved, potentially making it less prone to the short term changes in scanner gain (Jackson *et al.*, 2004) which may have contributed to the limited reproducibility of T_1. However, prior to conducting the studies of MTR, there was uncertainty whether the technique was able to detect grey matter abnormality in early MS. One earlier study had shown that grey matter MTR was abnormal in patients with CIS suggestive of MS (Traboulsee *et al.*, 2002); but a further study, investigating the present cohort using a region of interest approach, did not find evidence for grey matter MTR abnormality (Griffin *et al.*, 2002*b*). In Chapter 4, the objective was therefore to obtain a more complete assessment of grey matter MTR in early relapsing-remitting MS, using MTR histograms. This study revealed that both grey matter and NAWM MTR were abnormal in the cohort, and that MTR abnormality within grey matter (as opposed to abnormality within white matter) was associated with the mild clinical impairments already apparent.

Chapter 5 extended the observations reported in Chapter 4 by presenting serial data on a subset of patients who had been followed up for ~2 years. This study revealed that grey matter and NAWM MTR abnormality continued to increase during the two years of the study. The rates of change were not related to relapse frequency, nor to changes in T_2 lesion load. Furthermore, the rate of change in grey matter was significantly greater than the rate of change in white matter. (In this analysis, brain-parenchymal-fraction was included as a covariate and so differences in rate would be unlikely to be secondary to the effects of atrophy). Furthermore, backward

extrapolation of the data – under the assumption that the rate of change was linear - suggested that (i) NAWM MTR abnormality began prior to symptom onset and (ii) grey matter abnormality began around the time of the first episode (which was significantly later than the onset of white matter abnormality). However, it should be noted that early changes in grey matter and NAWM may be non-linear and thus have a different dynamic to that suggested by the extrapolations. Although it appears reasonable to conclude (from inspection of the raw data plots) that increasing abnormalities are genuinely occurring in both tissues, caution should nonetheless be used when interpreting the result. The cohort was relatively small, and although it appeared to be representative (in terms of relapse rate, EDSS and disease duration), confirmation of these results in a larger cohort is now needed.

The results from Chapters 4 and 5 revealed that MTR was a useful technique in the study of early relapsing-remitting MS. Attention was therefore turned to the study of the thalamus using MTR, particularly as investigation of thalamic abnormality may provide useful insight into neuronal/axonal abnormality in early MS. Furthermore, a number of recent studies have reported thalamic abnormality in patients with established secondary progressive and relapsing-remitting MS. At the time that the study was conducted, it was unclear whether thalamic abnormality developed in early MS, or whether it was a feature that developed following the onset of major disability. In Chapter 6, details on a study investigating thalamic MTR in early relapsing-remitting MS patients were presented. The results indicated that thalamic MTR became abnormal during the first five years of clinical disease. There was also an association between baseline lesion volume and the degree of thalamic MTR abnormality subsequently observed; however, there was no significant cross-

sectional correlation between *baseline* lesion volume and *baseline* thalamic MTR. In interpreting the results, it is possible that some of the thalamic MTR abnormality observed resulted from the Wallerian degeneration of axons transected in lesions, thus accounting for the temporal dissociation between baseline lesion volume and thalamic MTR. However, before concluding that thalamic MTR abnormality relates, in part, to the Wallerian degeneration of axons, confirmation of these findings in a larger cohort is required.

Implications for understanding the pathogenic mechanisms in early RRMS

In summary, Chapters 3-6 have provided evidence for accumulating abnormality within NAWM and grey matter in early relapsing-remitting MS. While a number of previous studies have reported NABT abnormality early in the course of the disease, some additional features have been highlighted by the present work: Firstly, evidence has been presented for grey matter MTR abnormality in early relapsing-remitting MS - supporting the prior observation of grey matter MTR abnormality in CIS patients (Traboulsee *et al.*, 2002). Secondly, an extrapolation of the serial data suggests that NAWM MTR abnormality predates symptom onset, (and that this change begins before the changes in grey matter). Thirdly, NAWM and grey matter MTR abnormalities increase over time in early MS, and this suggests that clinically-silent and progressive abnormalities are occurring in both tissues at an early stage of the disease. As there is a limited relationship between lesion load and long term disability, it appears reasonable to speculate that these early, progressive changes have a role to play in MS pathogenesis, and that they might have an effect upon long term prognosis.

Questions remain regarding the pathological basis for the observed MTR abnormalities. As mentioned, in Chapter 2, demyelination and axonal loss may result in a reduced MTR, with smaller reductions seen with inflammation. The pathological abnormalities observed in MS NAWM - at post-mortem - include axonal loss (Evangelou et al., 2000a), some of which could result from the Wallerian degeneration of axons transected in acute inflammatory lesions (Trapp et al., 1998). Of note, axonal transection has been shown to occur at an early stage of the disease (Kuhlmann et al., 2002), and a reduction in NAWM N-acetyl-aspartate (a neuronal marker) has previously been reported in early relapsing-remitting MS (Chard et al., 2002b). Axonal degeneration could therefore be one explanation for the accumulating NAWM MTR abnormalities observed. However, it should be noted that a number of other pathological abnormalities (including gliosis, microglial activation, patchy demyelination and peri-vascular inflammation) have been reported (Allen and McKeown, 1979; Allen et al., 2001); and previous studies have observed an increase in myo-inositol concentrations, (suggestive of glial proliferation), in early relapsing-remitting MS and CIS suggestive of MS (Chard et al., 2002b; Fernando et al., 2004). Some of these additional processes could therefore also be contributing to the MTR abnormalities observed.

Lesions within grey matter, [which are typically less inflammatory than white matter lesions (Peterson et al., 2001) and often less MR visible (Kidd et al., 1999)], are associated with demyelination and axonal loss (Peterson et al., 2001). Both of these changes could account for the grey matter MTR changes observed. Furthermore, it is conceivable that an accumulation of grey matter lesions and the degeneration of transected axons could account for the progressive decline in grey matter MTR seen in the cohort.

Estimation of the underlying MT parameters

Although MTR has been used widely in the study of MS, additional information could be obtained by estimating parameters that underlie the MT effect. These include the semisolid proton fraction (f) and the T_2 of the semisolid pool (T_{2B}). In Chapter 7, these parameters were estimated using a model for the MT effect, in sixty patients with clinically-definite MS. The parameter f was abnormal in lesions and NAWM, while T_{2B} was only abnormal in lesions. NAWM f was also associated with disability. It remains uncertain whether these parameters are able to provide pathologically specific information and a correlation of f and T_{2B} with histopathological data now needs to be performed. However, the technique is likely to be the subject of future work and with further refinement of the model and sequence it may be possible to improve upon specificity for the detection of myelin.

Conclusion

In conclusion, the MTR has provided useful insight into the pathological processes that occur in the NAWM and grey matter in patients with early relapsing-remitting MS. The MTR is able to detect increasing abnormality in both tissues over a two year follow-up period, and it is possible that these early and progressive pathological changes have a role to play in the pathogenesis of MS. There is therefore an argument for performing further serial MTR investigation in patients participating in natural history studies or in treatment trials. If the evolving changes are shown to correlate with later disability, the MTR might – in the future – be adopted as a reliable surrogate measure of disease progression.

Appendix

The technique used to segment tissue into NAWM and grey matter was adapted from

previous work (Chard *et al.*, 2002*c*; Traboulsee *et al.*, 2002) in collaboration with Dr

Andreas Hadjiprocopis. In brief, Statistical Parametric Mapping 1999 (SPM99)

(Ashburner and Friston, 1997, 2000) was used to segment raw images (namely: T_2

weighted images for the MTR analysis and T_1 weighted images for T_1 measurement)

into grey matter and white matter. The segmentation tool in SPM99 uses prior

anatomical information and a clustering algorithm to estimate probability maps for

white matter, grey matter and CSF (Ashburner and Friston, 1997, 2000). Whole brain

masks were then generated in SPM99, using the grey matter and white matter

probability maps, and these masks were used to remove non-brain parenchyma from

the T_1 and MTR maps (See Figure A.1 on next page).

Next, the whole brain maps were segmented onto grey matter, white matter and CSF

using the three SPM99 probability outputs. (Voxels were classified as belonging to a

particular tissue depending upon which probability map showed the greatest

probability at that location – See Figure A.2 on page 159).
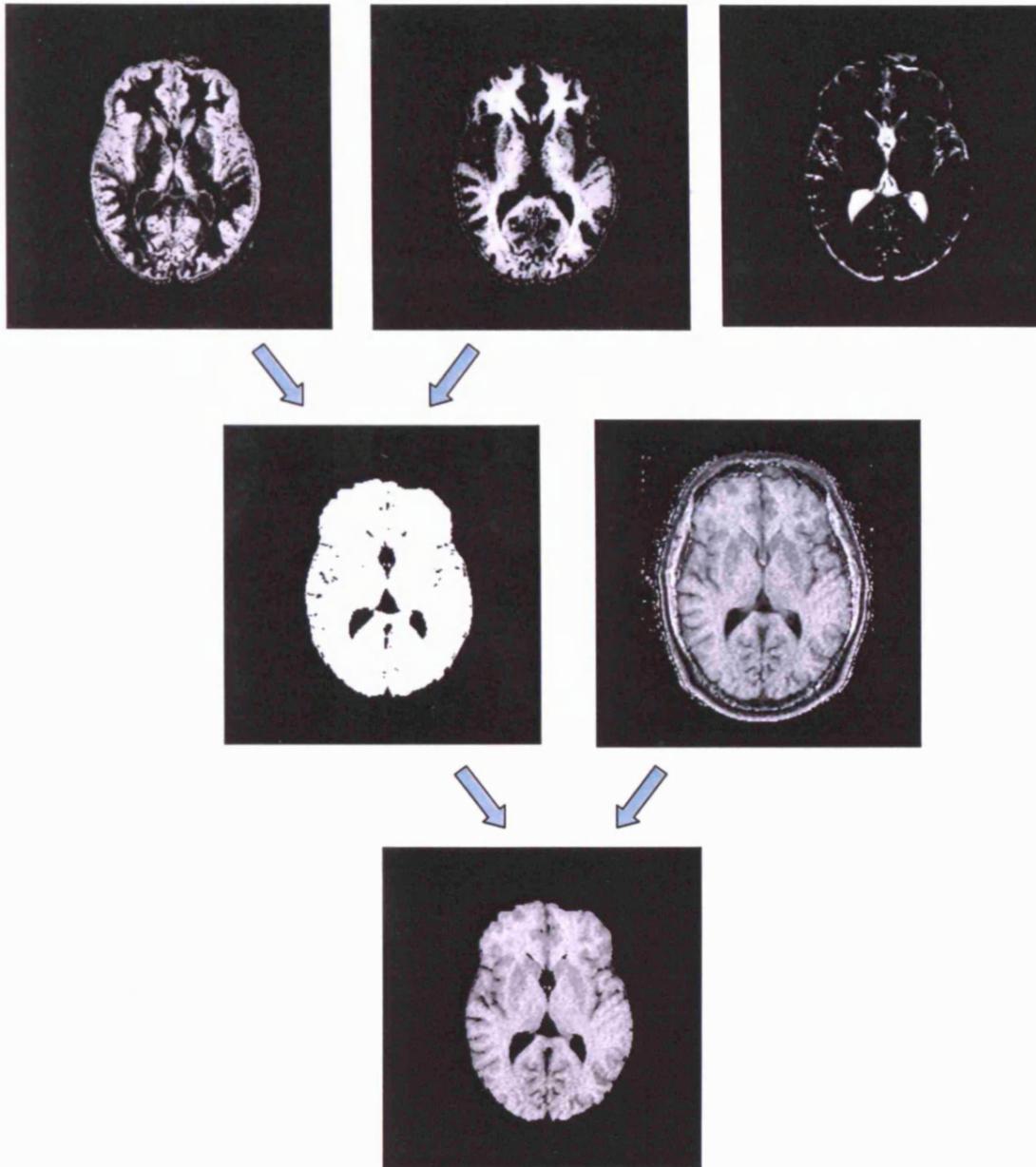
Figure A.1. Grey matter, white matter and CSF probability maps from a control subject (above). The grey matter and white matter probability maps are combined to create a whole brain mask (middle left) and this is applied to the MTR map (middle right) to remove non-brain parenchyma (below).
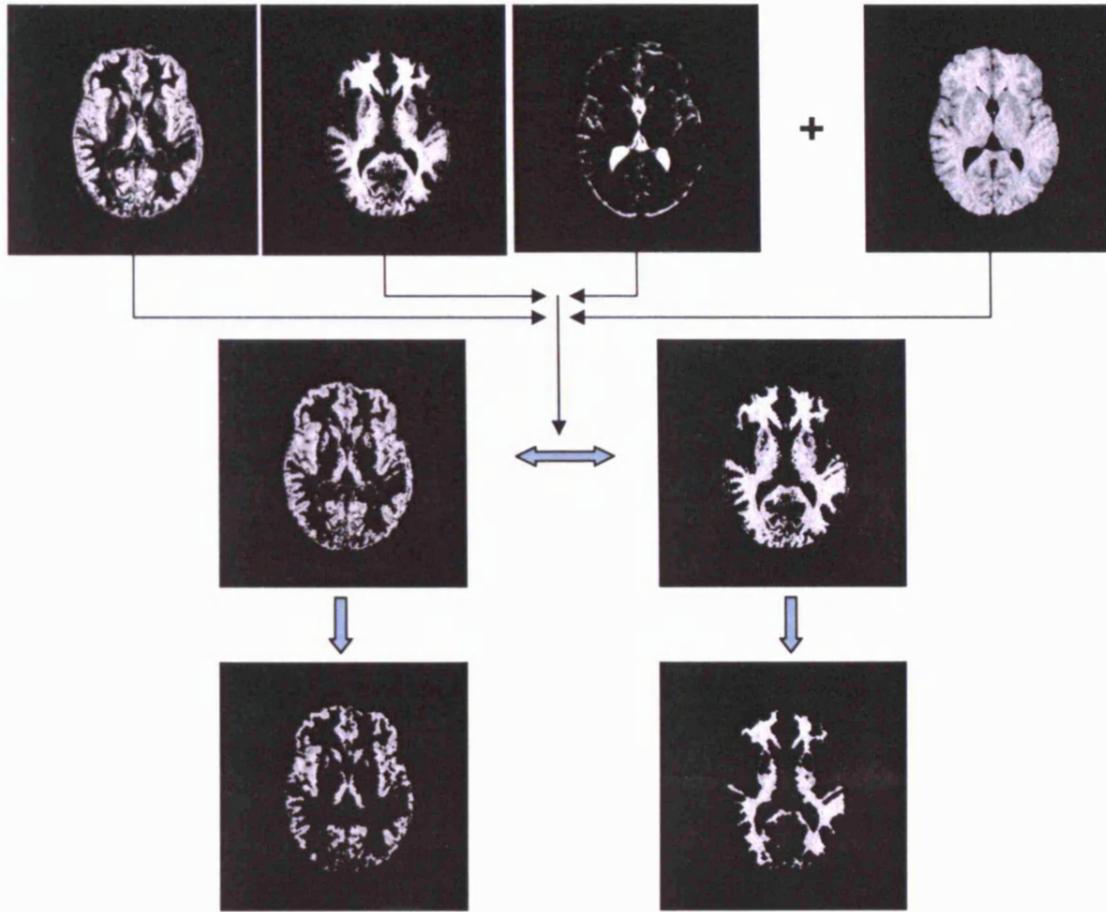
Figure A.2. The SPM probability outputs are used to segment the whole brain MTR map into grey matter and white matter. Following the application of a 10pu threshold, two voxel erosions are performed in white matter and single erosion is performed in grey matter (see text below).

Following tissue segmentation, the pixel value of lesions was set to zero to leave only NAWM and NAGM. Thresholds were then applied to both the T_1 and MTR maps to further minimize the number of misclassified voxels. Following a pilot study of five MS patients and six healthy control subjects, (in which the T_1 values of white matter and grey matter were ascertained), a 1000ms threshold was applied to white matter (which minimized both grey matter and CSF containing voxels), and a 1700ms threshold was applied to grey matter (to minimize CSF). With the MTR analysis, a threshold of 10pu was applied to both grey matter and the white matter; (the same threshold was used for both tissues as there was only a 6pu difference (range 3pu-9pu) between the mean grey matter and mean white matter MTR). To further reduce the number of partial volume voxels, inner and outer voxel erosions were performed; two erosions were performed in white matter and a single erosion was performed in grey matter; (visual inspection of the grey matter maps revealed that, with two or more erosions, only limited numbers of grey matter voxels remained). The effect of sequential erosions on white matter and grey matter T_1 values in five MS patients and six controls is shown below.
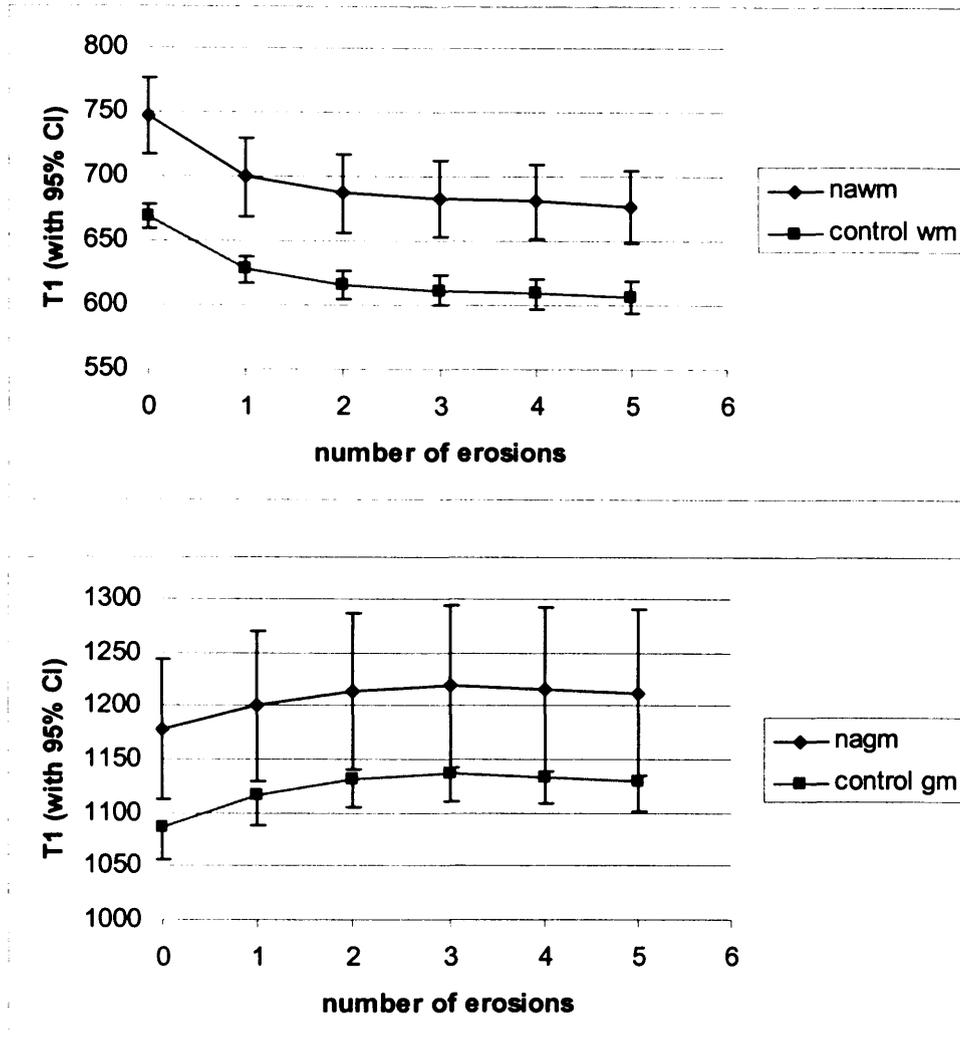
Figure A.3. The effect of sequential erosions on white matter and grey matter in five MS patients and six healthy controls. The white matter T_1 falls, possibly because of the elimination of grey matter and CSF containing voxels. The grey matter T_1 initially rises, possibly because of elimination of white matter containing voxels. It should be noted that the erosions do not appear to effect patient-control differences.

Validation of Segmentation Algorithm in MS

In order to ascertain the effect that MS lesions might have upon tissue segmentation, simulated lesions were placed within the brain images of healthy controlled subjects (Figure A.4).
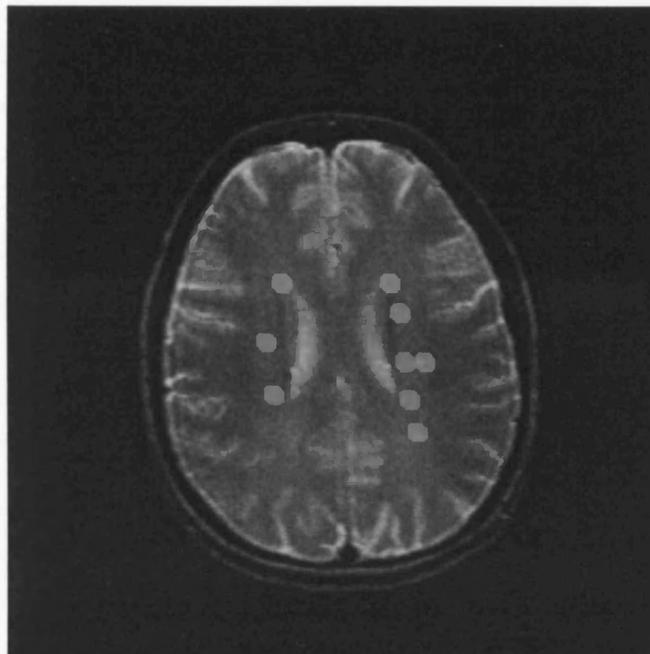
Figure A.4. Simulated lesions placed with the white matter of a healthy control. The signal intensity is set at a value mid-way between grey matter and CSF signal intensity, (which approximates the average signal intensity of MS lesions - see text below).

Initially, (in a single healthy control), 15ml of simulated lesions were positioned within the T_2 image subsequently used for tissue segmentation. Simulated lesions were arranged in a periventicular distribution within the cerebral white matter. In a series of separate experiments, the signal intensity of the simulated lesions was varied (relative to the WM, GM and CSF signal intensity) and the effect on white matter and grey matter MTR ascertained. Results are illustrated in the graphs (Figure A.5a) below.
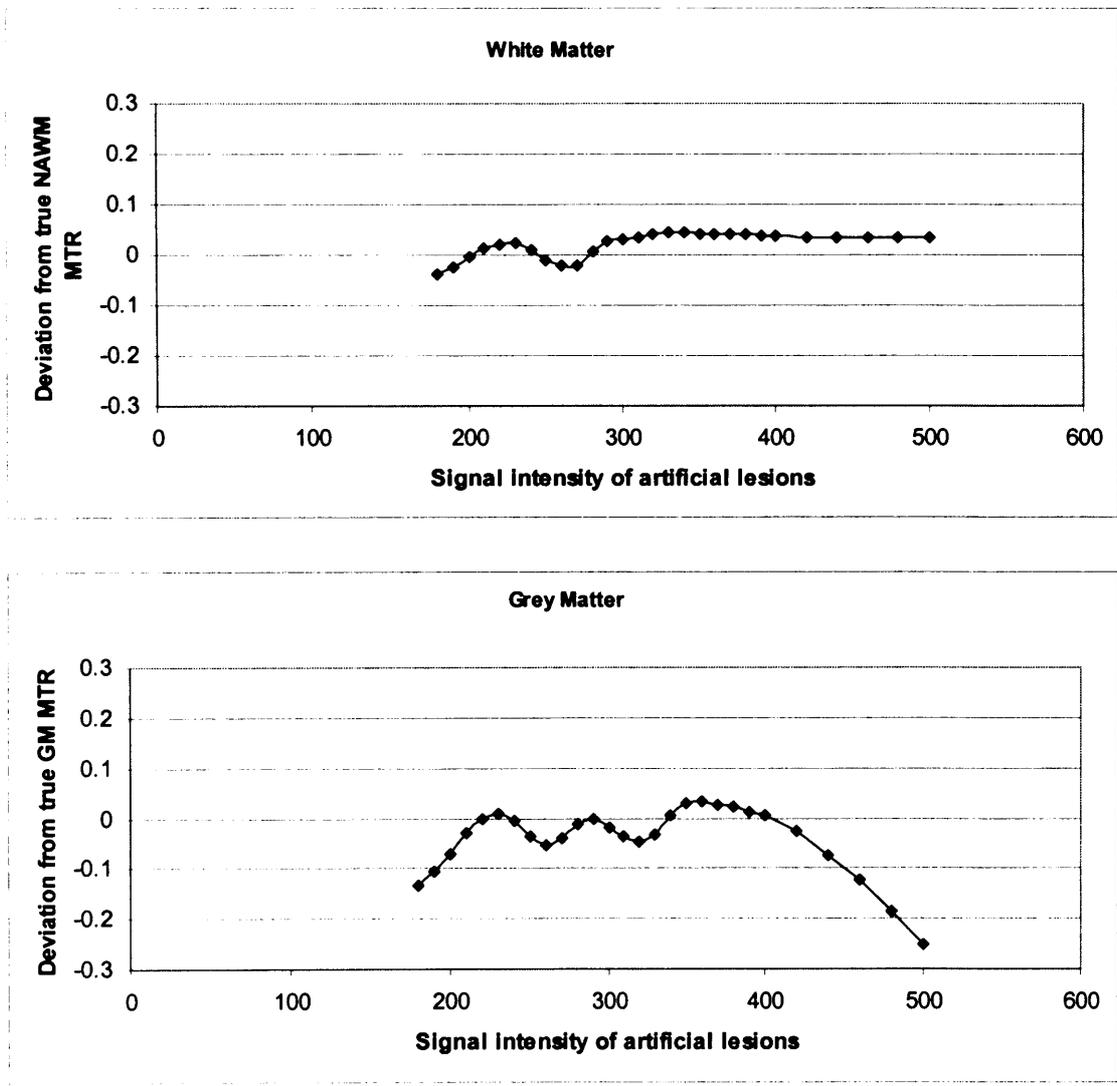
Results revealed that the observed MTR values deviated from the true tissue values in a manner dependent on the simulated lesion signal intensity. The observed peaks (seen mostly clearly with grey matter) correspond to the average signal intensity of

white matter, grey matter and CSF. In the 38 patients (described in Chapter 4), the average signal intensity of lesions was then evaluated. This was found to approximate the mid-point between grey matter and CSF signal intensity and therefore this was the value selected for the second experiment (in which the simulated lesion load was sequentially increased in a single healthy control subject). The results of this are illustrated in the following graphs (Figure A.5b):

Effect of artificial lesions on WM MTR

artificial lesion load / ml

Effect of artificial lesions on GM MTR

artificial lesion load / ml
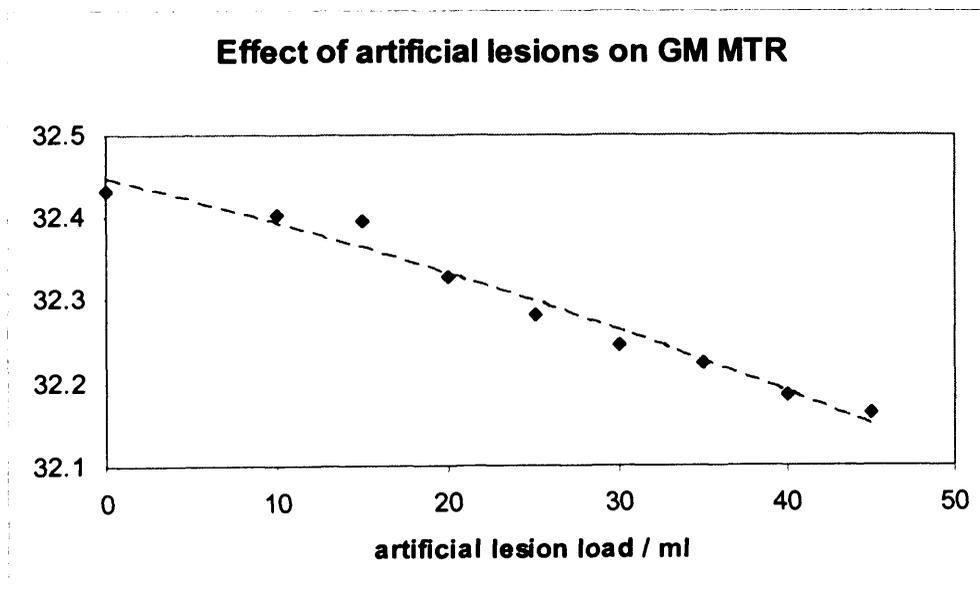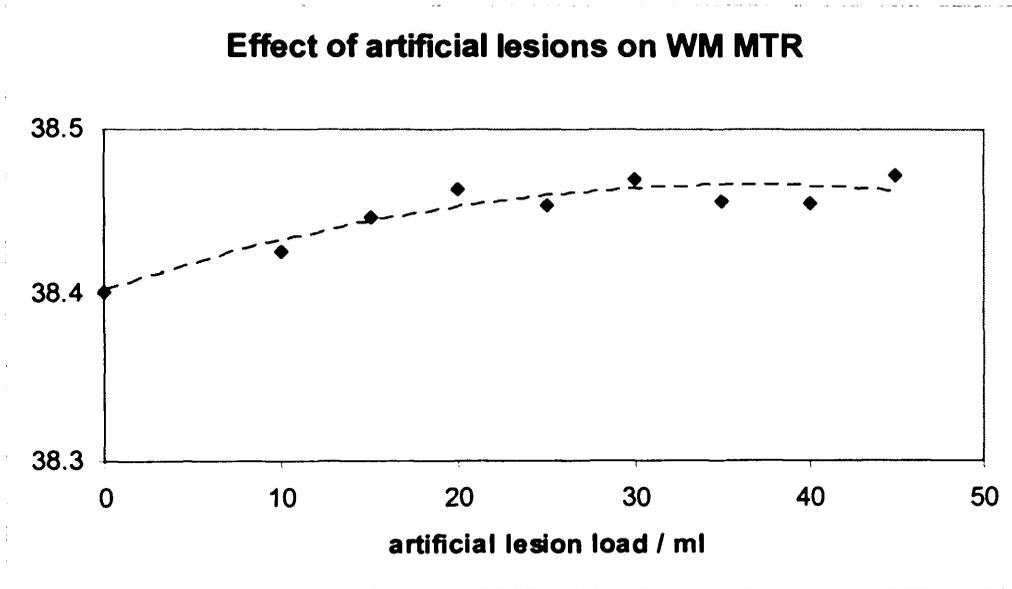
In the last experiment, 15 ml of simulated lesions were added, in a periventricular distribution, to the 35 healthy control subjects detailed in Chapter 4, (the mean lesion volume of the 38 patients was 14.9ml). Grey matter and white matter signal intensity were assessed (via a region of interest approach) and the signal intensity of the simulated lesions set at the mid-point between grey matter and CSF signal intensity.

The effect was to increase the control WM MTR value by, on average, 0.03pu and decrease the GM MTR value, by 0.09pu. A cross-sectional comparison between patients and controls, (using the control values obtained following insertion of simulated lesions), was undertaken. As in Chapter 4, the comparison was made using a linear model which included gender as a fixed factor and age as a continuous covariate. The grey matter MTR difference between patients and controls remained significant at $p = 0.004$; (the difference in white matter was also significant at $p < 0.001$).

REFERENCES

Adams CWM. Pathology of multiple sclerosis: progression of the lesion. Br Med Bull 1977;33:15-22.

Allen IV, McKeown SR. A histological, histochemical and biochemical study of the macroscopically normal white matter in multiple sclerosis. J Neurol Sci 1979;41:81-91.

Allen IV, McQuaid S, Mirakhur M, Nevin G. Pathological abnormalities in the normal-appearing white matter in multiple sclerosis. Neurol Sci 2001;22:141-144.

Andersen O, Lygner PE, Bergstrom T, Andersson M, Vahlne A. Viral infections trigger multiple sclerosis relapses: a prospective seroepidemiological study. J Neurol. 1993;240:417-422.

Ashburner J, Friston K. Multimodal image coregistration and partitioning--a unified framework. Neuroimage 1997;6:209-217.

Ashburner J, Friston KJ. Voxel-based morphometry--the methods. Neuroimage 2000;11:805-821.

Audoin B, Ranjeva JP, Duong MV, Ibarrola D, Malikova I, Confort-Gouny S, Soulier E, Viout P, Ali-Cherif A, Pelletier J, Cozzone PJ. Voxel-based analysis of

MTR images: a method to locate gray matter abnormalities in patients at the earliest stage of multiple sclerosis. J Magn Reson Imaging 2004;20:765-771.

Bagnato F, Jeffries N, Richert ND, Stone RD, Ohayon JM, McFarland HF, Frank JA. Evolution of T1 black holes in patients with multiple sclerosis imaged monthly for 4 years. Brain 2003;126:1782-1789.

Bailes DR, Young IR, Thomas DJ, Straughan K, Bydder GM, Steiner RE. NMR imaging of the brain using spin-echo sequences. Clin.Radiol. 1982;33:395-414.

Barbosa S, Blumhardt LD, Roberts N, Lock T, Edwards RH. Magnetic resonance relaxation time mapping in multiple sclerosis: normal appearing white matter and the "invisible" lesion load. Magn Reson Imaging 1994;12:33-42.

Barker GJ, Tofts PS, Gass A. An interleaved sequence for accurate and reproducible clinical measurement of magnetization transfer ratio. Magn Reson Imaging 1996;14:403-411.

Barkhof F, Filippi M, Miller DH, Scheltens P, Campi A, Polman CH, Comi G, Ader HJ, Losseff N, Valk J. Comparison of MRI criteria at first presentation to predict conversion to clinically definite multiple sclerosis. Brain 1997;120:2059-2069.

Barnett MH, Prineas JW. Relapsing and remitting multiple sclerosis: pathology of the newly forming lesion. Ann Neurol. 2004;55:458-468.

Barnes D, Hughes RA, Morris RW, Wade-Jones O, Brown P, Britton T, Francis DA, Perkin GD, Rudge P, Swash M, Katifi H, Farmer S, Frankel J. Randomised trial of oral and intravenous methylprednisolone in acute relapses of multiple sclerosis. Lancet 1997;349:902-906.

Barnes D, McDonald WI, Landon DN, Johnson G. The characterization of experimental gliosis by quantitative nuclear magnetic resonance imaging. Brain 1988;111:83-94.

Barnes D, Munro PM, Youl BD, Prineas JW, McDonald WI. The longstanding MS lesion. A quantitative MRI and electron microscopic study. Brain 1991;114:1271-1280.

Beall SS, Hockertz M, Thomson G, Hoar DL, Paty DW. Susceptibility for multiple sclerosis is positively associated with recessive inheritance with a gene linked to the DR2-Dgβ1b haplotype in HLA class II locus. Neurology 1995;45:A163.

Beck RW, Cleary PA. Optic neuritis treatment trial. One-year follow-up results. Arch.Ophthalmol. 1993; 111:773-775.

Berry I, Barker GJ, Barkhof F, Campi A, Dousset V, Franconi JM, Gass A, Schreiber

W, Miller DH, Tofts PS. A multicenter measurement of magnetization transfer ratio

in normal white matter. J.Magn Reson.Imaging 1999;9:441-446.

Bjartmar C, Kidd G, Mork S, Rudick R, Trapp BD. Neurological disability correlates

with spinal cord axonal loss and reduced N-acetyl aspartate in chronic multiple

sclerosis patients. Ann Neurol 2000;48:893-901.

Bjartmar C, Wujek JR, Trapp BD. Axonal loss in the pathology of MS:

consequences for understanding the progressive phase of the disease. J Neurol Sci.

2003;206:165-171.

Bloch F. Nuclear Induction. Physical Review 1946;70:460-474.

Bo L, Vedeler CA, Nyland H, Trapp BD, Mork SJ. Intracortical multiple sclerosis

lesions are not associated with increased lymphocyte infiltration. Mult Scler.

2003;9:323-31.

Bo L, Vedeler CA, Nyland HI, Trapp BD, Mork SJ. Subpial demyelination in the

cerebral cortex of multiple sclerosis patients. J Neuropathol Exp Neurol.

2003;62:723-32.

Bozzali M, Rocca MA, Iannucci G, Pereira C, Comi G, Filippi M. Magnetization-transfer histogram analysis of the cervical cord in patients with multiple sclerosis. AJNR Am J Neuroradiol 1999;20:1803-1808.

Brex PA, Parker GJ, Leary SM, Molyneux PD, Barker GJ, Davie CA, Thompson AJ, Miller DH. Lesion heterogeneity in multiple sclerosis: a study of the relations between appearances on T1 weighted images, T1 relaxation times, and metabolite concentrations. J Neurol Neurosurg Psychiatry 2000;68:627-632.

Brex PA, Ciccarelli O, O'Riordan JI, Sailer M, Thompson AJ, Miller DH. A longitudinal study of abnormalities on MRI and disability from multiple sclerosis. N.Engl.J.Med. 2002;346:158-164.

Brownell B, Hughes JT. The distribution of plaques in the cerebrum in multiple sclerosis. J Neurol Neurosurg Psychiatry 1962;25:315-320.

Bronnum-Hansen H, Koch-Henriksen N, Stenager E. Trends in survival and cause of death in Danish patients with multiple sclerosis. Brain 2004;127:844-850.

Bruck W, Bitsch A, Kolenda H, Bruck Y, Stiefel M, Lassmann H. Inflammatory central nervous system demyelination: correlation of magnetic resonance imaging findings with lesion pathology. Ann Neurol. 1997;42:783-93.

Buljevac D, Hop WC, Reedeker W, Janssens AC, van der Meche FG, van Doom PA, Hintzen RQ. Self reported stressful life events and exacerbations in multiple sclerosis: prospective study. BMJ 2003;327:646.

Bulman D, Ebers GC. The geography of multiple sclerosis reflects genetic susceptibility. Journal of Tropical and Geographical Neurology 1992;2:66-72.

Canadian MS Research Group. A randomized controlled trial of amantadine in fatigue associated with multiple sclerosis. Can J Neurol Sci 1987;14:273-278.

Carpenter JR, Bithall JF. Bootstrap confidence intervals: when, which, what? A practical guide for medical statisticians. Statistics in Medicine 2000;19:1141-1164

Cercignani M, Iannucci G, Rocca MA, Comi G, Horsfield MA, Filippi M. Pathologic damage in MS assessed by diffusion-weighted and magnetization transfer MRI. Neurology 2000;54:1139-1144.

Cercignani M, Bozzali M, Iannucci G, Comi G, Filippi M. Magnetisation transfer ratio and mean diffusivity of normal appearing white and grey matter from patients with multiple sclerosis. J Neurol Neurosurg Psychiatry 2001;70:311-317.

Chard DT, Griffin CM, Parker GJ, Kapoor R, Thompson AJ, Miller DH. Brain atrophy in clinically early relapsing-remitting multiple sclerosis. Brain 2002*a*;125: 327-337.

Chard DT, Griffin CM, McLean MA, Kapeller P, Kapoor R, Thompson AJ, Miller DH. Brain metabolite changes in cortical grey and normal-appearing white matter in clinically early relapsing-remitting multiple sclerosis. Brain 2002*b*;125:2342-2352.

Chard DT, Parker GJ, Griffin CM, Thompson AJ, Miller DH. The reproducibility and sensitivity of brain tissue volume measurements derived from an SPM-based segmentation methodology. J Magn Reson Imaging 2002*c*;15:259-267

Chard DT, Brex PA, Ciccarelli O, Griffin CM, Parker GJ, Dalton C, Altmann DR, Thompson AJ, Miller DH. The longitudinal relation between brain lesion load and atrophy in multiple sclerosis: a 14 year follow up study.
J.Neurol.Neurosurg.Psychiatry 2003;74:1551-1554.

Chard DT, Griffin CM, Rashid W, Davies GR, Altmann DR, Kapoor R, Barker GJ, Thompson AJ, Miller DH. Progressive grey matter atrophy in clinically early relapsing-remitting multiple sclerosis. Mult Scler 2004;10:387-391.

Ciccarelli O, Werring DJ, Wheeler-Kingshott CA, Barker GJ, Parker GJ, Thompson AJ, Miller DH. Investigation of MS normal-appearing brain using diffusion tensor MRI with clinical correlations. Neurology 2001;56:926-933.

Cifelli A, Arridge M, Jezzard P, Esiri MM, Palace J, Matthews PM. Thalamic

neurodegeneration in multiple sclerosis. Ann Neurol 2002;52:650-653.

Charcot JM. Lectures on the diseases of the nervous system. Tranl. by G. Sigerson.

London: New Sydenham Society, 1877.

Cohen JA, Cutter GR, Fischer JS, Goodman AD, Heidenreich FR, Jak AJ, Kniker JE,

Kooijmans MF, Lull JM, Sandrock AW, Simon JH, Simonian NA, Whitaker JN. Use

of the multiple sclerosis functional composite as an outcome measure in a phase 3

clinical trial. Arch Neurol 2001;58:961-967.

Cohen JA, Cutter GR, Fischer JS, Goodman AD, Heidenreich FR, Kooijmans MF,

Sandrock AW, Rudick RA, Simon JH, Simonian NA, Tsao EC, Whitaker JN. Benefit

of interferon beta-1a on MSFC progression in secondary progressive MS. Neurology

2002;59:679-687.

Coles AJ, Wing MG, Molyneux P, Paolillo A, Davie CM, Hale G, Miller D,

Waldmann H, Compston A. Monoclonal antibody treatment exposes three

mechanisms underlying the clinical course of multiple sclerosis. Ann Neurol

1999;46:296-304.

Comi G, Rovaris M, Falautano M, Santuccio G, Martinelli V, Rocca MA, Possa F, Leocani L, Paulesu E, Filippi M. A multiparametric MRI study of frontal lobe dementia in multiple sclerosis. J Neurol Sci 1999;171:135-144.

Comi G, Filippi M, Wolinsky JS. European/Canadian multicenter, double-blind, randomized, placebo-controlled study of the effects of glatiramer acetate on magnetic resonance imaging--measured disease activity and burden in patients with relapsing multiple sclerosis. European/Canadian Glatiramer Acetate Study Group. Ann Neurol. 2001;49:290-297.

Compston A. Distribution of multiple sclerosis. In: Compston A, Ebers E, Lassmann H, McDonald I, Matthews B, Wekerle H, eds. McAlpine's multiple sclerosis (third edition). London, Edinburgh, New York, Philadelphia, Sydney, Toronto: Churchill Livingstone, 1998*a*:63-100.

Compston A. Genetic susceptibility to multiple sclerosis. In: Compston A, Ebers E, Lassmann H, McDonald I, Matthews B, Wekerle H, eds. McAlpine's multiple sclerosis (third edition). London, Edinburgh, New York, Philadelphia, Sydney, Toronto: Churchill Livingstone, 1998*b*:101-142.

Compston A. The story of multiple sclerosis. In: Compston A, Ebers E, Lassmann H, McDonald I, Matthews B, Wekerle H, eds. McAlpine's multiple sclerosis (third edition). London, Edinburgh, New York, Philadelphia, Sydney, Toronto: Churchill Livingstone, 1998*c*:3-42.

Compston A. Treatment and management of multiple sclerosis. In: Compston A, Ebers E, Lassmann H, McDonald I, Matthews B, Wekerle H, eds. McAlpine's multiple sclerosis (third edition). London, Edinburgh, New York, Philadelphia, Sydney, Toronto: Churchill Livingstone, 1998*d*:437-498.

Compston A, Coles A. Multiple sclerosis. Lancet 2002;359:1221-1231.

Confavreux C, Hutchinson M, Hours MM, Cortinovis-Tourniaire P, Moreau T. Rate of pregnancy-related relapse in multiple sclerosis. Pregnancy in Multiple Sclerosis Group. N Engl J Med. 1998;339:285-291.

Confavreux C, Vukusic S, Adeleine P. Early clinical predictors and progression of irreversible disability in multiple sclerosis: an amnesic process. Brain 2003;126:770-782.

Dalton CM, Brex PA, Miszkiel KA, Hickman SJ, MacManus DG, Plant GT, Thompson AJ, Miller DH. Application of the new McDonald criteria to patients with clinically isolated syndromes suggestive of multiple sclerosis. Ann Neurol 2002;52:47-53.

Dalton CM, Chard DT, Davies GR, Miszkiel KA, Altmann DR, Fernando K, Plant GT, Thompson AJ, Miller DH. Early development of multiple sclerosis is associated with progressive grey matter atrophy in patients presenting with clinically isolated syndromes. Brain 2004;127:1101-1107.

Davie CA, Barker GJ, Thompson AJ, Tofts PS, McDonald WI, Miller DH. 1H magnetic resonance spectroscopy of chronic cerebral white matter lesions and normal appearing white matter in multiple sclerosis. J Neurol Neurosurg Psychiatry 1997;63:736-742.

Davies GR, Ramani A, Dalton CM, Tozer DJ, Wheeler-Kingshott CA, Barker GJ, Thompson AJ, Miller DH, Tofts PS. Preliminary magnetic resonance study of the macromolecular proton fraction in white matter: a potential marker of myelin? Mult Scler 2003;9:246-249.

De Stefano N, Narayanan S, Francis SJ, Smith S, Mortilla M, Tartaglia MC, Bartolozzi ML, Guidi L, Federico A, Arnold DL. Diffuse axonal and tissue injury in patients with multiple sclerosis with low cerebral lesion load and no disability. Arch.Neurol. 2002;59:1565-1571.

De Stefano N, Matthews PM, Filippi M, Agosta F, De Luca M, Bartolozzi ML, Guidi L, Ghezzi A, Montanari E, Cifelli A, Federico A, Smith SM. Evidence of early cortical atrophy in MS: relevance to white matter changes and disability. Neurology 2003;60:1157-1162.

Dean G, Kurtzke JF. On the risk of multiple sclerosis according to age at immigration to South Africa. Br Med J 1971;3:725-729.

Dehmeshki J, Silver NC, Leary SM, Tofts PS, Thompson AJ, Miller DH.
Magnetisation transfer ratio histogram analysis of primary progressive and other
multiple sclerosis subgroups. J Neurol Sci 2001;185:11-17.

Dousset V, Grossman RI, Ramer KN, Schnall MD, Young LH, Gonzalez-Scarano F,
Lavi E, Cohen JA. Experimental allergic encephalomyelitis and multiple sclerosis:
lesion characterization with magnetization transfer imaging. Radiology
1992;182:483-491.

Dousset V, Brochet B, Vital A, Gross C, Benazzouz A, Boullerne A, Bidabe AM,
Gin AM, Caille JM. Lysolecithin-induced demyelination in primates: preliminary in
vivo study with MR and magnetization transfer. AJNR Am J Neuroradiol
1995;16:225-231.

Dousset V, Armand JP, Lacoste D, Mieze S, Letenneur L, Dartigues JF, Caill JM.
Magnetization transfer study of HIV encephalitis and progressive multifocal
leukoencephalopathy. Groupe d'Epidemiologie Clinique du SIDA en Aquitaine.
AJNR Am J Neuroradiol. 1997;18:895-901.

Dousset V, Gayou A, Brochet B, Caille JM. Early structural changes in acute MS
lesions assessed by serial magnetization transfer studies. Neurology 1998;51:1150-
1155.

197

Ebers GC, Bulman DE, Sadovnick AD, Paty DW, Warren S, Hader W, Murray TJ, Seland TP, Duquette P, Grey T, . A population-based study of multiple sclerosis in twins. N.Engl.J.Med. 1986;315:1638-1642.

Ebers GC, Sadovnick AD, Risch NJ. A genetic basis for familial aggregation in multiple sclerosis. Canadian Collaborative Study Group. Nature 1995;377:150-151.

European Study Group on interferon beta-1b in secondary progressive MS. Placebo-controlled multicentre randomised trial of interferon beta-1b in treatment of secondary progressive multiple sclerosis. Lancet 1998;352:1491-1497.

Evangelou N, Esiri MM, Smith S, Palace J, Matthews PM. Quantitative pathological evidence for axonal loss in normal appearing white matter in multiple sclerosis. Ann Neurol. 2000a;47:391-395.

Evangelou N, Konz D, Esiri MM, Smith S, Palace J, Matthews PM. Regional axonal loss in the corpus callosum correlates with cerebral white matter lesion volume and distribution in multiple sclerosis. Brain 2000b;123:1845-1849.

Evangelou N, Konz D, Esiri MM, Smith S, Palace J, Matthews PM. Size-selective neuronal changes in the anterior optic pathways suggest a differential susceptibility to injury in multiple sclerosis. Brain 2001;124:1813-1820.

Fabiano AJ, Sharma J, Weinstock-Guttman B, Munschauer FE, III, Benedict RH, Zivadinov R, Bakshi R. Thalamic involvement in multiple sclerosis: a diffusion-weighted magnetic resonance imaging study. J Neuroimaging 2003;13:307-314.

Fazekas F, Offenbacher H, Fuchs S, Schmidt R, Niederkorn K, Horner S, Lechner H. Criteria for an increased specificity of MRI interpretation in elderly subjects with suspected multiple sclerosis. Neurology 1988;38:1822-1825.

Ferguson B, Matyszak MK, Esiri MM, Perry VH. Axonal damage in acute multiple sclerosis lesions. Brain 1997;120:393-399.

Fernando KT, McLean MA, Chard DT, MacManus DG, Dalton CM, Miszkiel KA, Gordon RM, Plant GT, Thompson AJ, Miller DH. Elevated white matter myo-inositol in clinically isolated syndromes suggestive of multiple sclerosis. Brain 2004;127:1361-369.

Filippi M, Campi A, Dousset V, Baratti C, Martinelli V, Canal N, Scotti G, Comi G. A magnetization transfer imaging study of normal-appearing white matter in multiple sclerosis. Neurology 1995;45:478-82.

Filippi M, Rocca MA, Martino G, Horsfield MA, Comi G. Magnetization transfer changes in the normal appearing white matter precede the appearance of enhancing lesions in multiple sclerosis. Ann Neurol 1998;43:809-814.

Filippi M, Iannucci G, Tortorella C, Minicucci L, Horsfield MA, Colombo B, Sormani MP, Comi G. Comparison of MS clinical phenotypes using conventional and magnetization transfer MRI. Neurology 1999;52:588-594.

Filippi M, Inglese M, Rovaris M, Sormani MP, Horsfield P, Iannucci PG, Colombo B, Comi G. Magnetization transfer imaging to monitor the evolution of MS: a 1-year follow-up study. Neurology 2000a;55:940-946.

Filippi M, Bozzali M, Horsfield MA, Rocca MA, Sormani MP, Iannucci G, Colombo B, Comi G. A conventional and magnetization transfer MRI study of the cervical cord in patients with MS. Neurology 2000b;54:207-213.

Filippi M, Bozzali M, Comi G. Magnetization transfer and diffusion tensor MR imaging of basal ganglia from patients with multiple sclerosis. J Neurol Sci 2001;183:69-72.

Filippi M, Dousset V, McFarland HF, Miller DH, Grossman RI. Role of magnetic resonance imaging in the diagnosis and monitoring of multiple sclerosis: consensus report of the White Matter Study Group. J Magn Reson Imaging 2002a;15:499-504.

Filippi M, Grossman RI. MRI techniques to monitor MS evolution: the present and the future. Neurology 2002b;58:1147-1153.

Filippi M, Rovaris M, Inglese M, Barkhof F, De Stefano N, Smith S, Comi G. Interferon beta-1a for brain tissue loss in patients at presentation with syndromes

suggestive of multiple sclerosis: a randomised, double-blind, placebo-controlled trial. Lancet 2004;364:1489-1496.

Fischer HW, Rinck PA, Van Haverbeke Y, Muller RN. Nuclear relaxation of human brain gray and white matter: analysis of field dependence and implications for MRI. Magn Reson Med 1990;16:317-334.

Fischer HW, Van Haverbeke Y, Schmitz-Feuerhake I, Muller RN. The uncommon longitudinal relaxation dispersion of human brain white matter. Magn Reson Med 1989;9:441-446.

Fischer JS, Jak AJ, Kniker JE, Rudick RA, Cutter G. Administration and scoring manual for the multiple sclerosis functional composite measure (MSFC). National Multiple Sclerosis Society. Demos Medical Publishing, New York, 1999.

Fischer JS, Rudick RA, Cutter GR, Reingold SC. The Multiple Sclerosis Functional Composite Measure (MSFC): an integrated approach to MS clinical outcome assessment. National MS Society Clinical Outcomes Assessment Task Force. Mult Scler 1999;5:244-250.

Ford B, Bentley J, Du Croz JJ, Hague SJ. The NAG library 'machine'. Softw Pract Exper 1979;9:65-72.

Fox NC, Jenkins R, Leary SM, Stevenson VL, Losseff NA, Crum WR, Harvey RJ, Rossor MN, Miller DH, Thompson AJ. Progressive cerebral atrophy in MS: a serial study using registered, volumetric MRI. Neurology 2000;54:807-812.

Fu L, Matthews PM, De Stefano N, Worsley KJ, Narayanan S, Francis GS, Antel JP, Wolfson C, Arnold DL. Imaging axonal damage of normal-appearing white matter in multiple sclerosis. Brain 1998;121:103-113.

Freeman JA, Langdon DW, Hobart JC, Thompson AJ. The impact of inpatient rehabilitation on progressive multiple sclerosis. Ann Neurol. 1997;42:236-244.

Gareau PJ, Rutt BK, SJ Karlik, Mitchell JR. Magnetization transfer and multicomponent T2 relaxation measurements with histopathologic correlation in an experimental model of MS. J Magn Reson Imaging 2000;11:586-595.

Gass A, Barker GJ, Kidd D, Thorpe JW, MacManus D, Brennan A, Tofts PS, Thompson AJ, McDonald WI, Miller DH. Correlation of magnetization transfer ratio with clinical disability in multiple sclerosis. Ann Neurol 1994;36:62-67.

Ge Y, Grossman RI, Udupa JK, Wei L, Mannon LJ, Polansky M, Kolson DL. Brain atrophy in relapsing-remitting multiple sclerosis and secondary progressive multiple sclerosis: longitudinal quantitative analysis. Radiology 2000;214:665-670.

Ge Y, Grossman RI, Udupa JK, Babb JS, Kolson DL, McGowan JC. Magnetization transfer ratio histogram analysis of gray matter in relapsing-remitting multiple sclerosis. AJNR Am J Neuroradiol 2001;22:470-475.

Ge Y, Grossman RI, Udupa JK, Babb JS, Mannon LJ, McGowan JC. Magnetization transfer ratio histogram analysis of normal-appearing gray matter and normal-appearing white matter in multiple sclerosis. J Comput Assist Tomogr 2002;26:62-68.

Goodkin DE, Rooney WD, Sloan R, Bacchetti P, Gee L, Vermathen M, Waubant E, Abundo M, Majumdar S, Nelson S, Weiner MW. A serial study of new MS lesions and the white matter from which they arise. Neurology 1998;51:1689-1697.

Goldstein H. Multilevel statistical models. London: Arnold, 1995.

Griffin CM, Dehmeshki J, Chard DT, Parker GJ, Barker GJ, Thompson AJ, Miller DH. T1 histograms of normal-appearing brain tissue are abnormal in early relapsing-remitting multiple sclerosis. Mult.Scler. 2002*a*;8:211-6.

Griffin CM, Chard DT, Parker GJ, Barker GJ, Thompson AJ, Miller DH. The relationship between lesion and normal appearing brain tissue abnormalities in early relapsing remitting multiple sclerosis. J.Neurol. 2002*b*;249:193-9.

Grossman RI, Gonzalez-Scarano F, Atlas SW, Galetta S, Silberberg DH. Multiple sclerosis: gadolinium enhancement in MR imaging. Radiology 1986;161:721-725.

Halliday AM, McDonald WI, Mushin J. Delayed visual evoked response in optiv neuritis. Lancet 1972;1:982-985.

Hammond SR, English DR, McLeod JG. The age-range of risk of developing multiple sclerosis: evidence from a migrant population in Australia. Brain 2000;123 (Pt 5):968-974.

Hartung HP, Gonsette R, Konig N, Kwiecinski H, Guseo A, Morrissey SP, Krapf H, Zwingers T. Mitoxantrone in progressive multiple sclerosis: a placebo-controlled, double-blind, randomised, multicentre trial. Lancet 2002;360:2018-2025.

Hashemi RH, Bradley WG. MRI the basics. Baltimore, Philadelphia, London, Paris, Bangkok, Buenos Aires, Hong Kong, Munich, Sydney, Tokyo, Wroclaw: Williams and Wilkins, 1997.

Haughton VM, Yetkin FZ, Rao SM, Rimm AA, Fischer ME, Papke RA, Breger RK, Khatri BO. Quantitative MR in the diagnosis of multiple sclerosis. Magn Reson.Med. 1992;26:71-8.

Henkelman RM, Huang X, Xiang QS, Stanisz GJ, Swanson SD, M. J. Bronskill MJ. Quantitative interpretation of magnetization transfer. Magn Reson Med 1993; 29: 759-766.

Hickman SJ, Miller DH. Imaging of the spine in multiple sclerosis. Neuroimaging Clin.N.Am. 2000;10:689-704.

Hickman SJ, Brierley CM, Silver NC, Moseley IF, Scolding NJ, Compston DA, Miller DH. Infratentorial hypointense lesion volume on T1-weighted magnetic resonance imaging correlates with disability in patients with chronic cerebellar ataxia due to multiple sclerosis. J Neurol Sci. 2001;187:35-39.

Hickman SJ, Toosy AT, Jones SJ, Altmann DR, Miszkiel KA, MacManus DG, Barker GJ, Plant GT, Thompson AJ, Miller DH. Serial magnetization transfer imaging in acute optic neuritis. Brain 2004;127:692-700.

The IFNB Multiple Sclerosis Study Group. Interferon beta-1b is effective in relapsing-remitting multiple sclerosis. I. Clinical results of a multicenter, randomized, double-blind, placebo-controlled trial. Neurology 1993;43:655-666.

The IFNB Multiple Sclerosis Study Group and The University of British Columbia MS/MRI Analysis Group.Interferon beta-1b in the treatment of multiple sclerosis: final outcome of the randomized controlled trial. Neurology 1995;45:1277-1285.

Inglese M, Ghezzi A, Bianchi S, Gerevini S, Sormani MP, Martinelli V, Comi G, Filippi M. Irreversible disability and tissue loss in multiple sclerosis: a conventional and magnetization transfer magnetic resonance imaging study of the optic nerves. Arch Neurol 2002;59:250-255.

Inglese M, van Waesberghe JH, Rovaris M, Beckmann K, Barkhof F, Hahn D, Kappos L, Miller DH, Polman C, Pozzilli C, Thompson AJ, Yousry TA, Wagner K, Comi G, Filippi M. The effect of interferon beta-1b on quantities derived from MT MRI in secondary progressive MS. Neurology 2003;60:853-860.

Inglese M, Liu S, Babb JS, Mannon LJ, Grossman RI, Gonen O. Three-dimensional proton spectroscopy of deep gray matter nuclei in relapsing-remitting MS. Neurology 2004;63:170-172.

Iannucci G, Minicucci L, Rodegher M, Sormani MP, Comi G, Filippi M. Correlations between clinical and MRI involvement in multiple sclerosis: assessment using T(1), T(2) and MT histograms. J Neurol Sci 1999;171:121-129.

Iannucci G, Tortorella C, Rovaris M, Sormani MP, Comi G, Filippi M. Prognostic value of MR and magnetization transfer imaging findings in patients with clinically isolated syndromes suggestive of multiple sclerosis at presentation. AJNR Am J Neuroradiol 2000;21:1034-1038.

Jackson JS, Tozer DJ, Tofts PS. Measurement of subtle scanner changes using a constant temperature phantom. ESMRMB 21st Annual meeting, 2004;431.

Jacobs LD, Cookfair DL, Rudick RA, Herndon RM, Richert JR, Salazar AM, Fischer JS, Goodkin DE, Granger CV, Simon JH, Alam JJ, Bartoszak DM, Bourdette DN, Braiman J, Brownscheidle CM, Coats ME, Cohan SL, Dougherty DS, Kinkel RP,

Mass MK, Munschauer FE, III, Priore RL, Pullicino PM, Scherokman BJ, Whitham RH. Intramuscular interferon beta-1a for disease progression in relapsing multiple sclerosis. The Multiple Sclerosis Collaborative Research Group (MSCRG). Ann Neurol. 1996;39:285-294.

Johnson KP, Brooks BR, Cohen JA, Ford CC, Goldstein J, Lisak RP, Myers LW, Panitch HS, Rose JW, Schiffer RB. Copolymer 1 reduces relapse rate and improves disability in relapsing-remitting multiple sclerosis: results of a phase III multicenter, double-blind placebo-controlled trial. The Copolymer 1 Multiple Sclerosis Study Group. Neurology 1995;45:1268-76.

Kantarci OH, Hebrink DD, Achenbach SJ, Pittock SJ, Altintas A, Schaefer-Klein JL, Atkinson EJ, De Andrade M, McMurray CT, Rodriguez M, Weinshenker BG. Association of APOE polymorphisms with disease severity in MS is limited to women. Neurology 2004;62:811-814.

Kalkers NF, Bergers E, Castelijns JA, van Walderveen MA, Bot JC, Ader HJ, Polman CH, Barkhof F. Optimizing the association between disability and biological markers in MS. Neurology 2001;57:1253-1258.

Kalkers NF, Vrenken H, Uitdehaag BM, Polman CH, Barkhof F. Brain atrophy in multiple sclerosis: impact of lesions and damage of whole brain tissue. Mult Scler 2002;8:410-414.

Kappos L, Moeri D, Radue EW, Schoetzau A, Schweikert K, Barkhof F, Miller D, Guttmann CR, Weiner HL, Gasperini C, Filippi M. Predictive value of gadolinium-enhanced magnetic resonance imaging for relapse rate and changes in disability or impairment in multiple sclerosis: a meta-analysis. Gadolinium MRI Meta-analysis Group. Lancet 1999;353:964-969.

Katz D, Taubenberger JK, Cannella B, McFarlin DE, Raine CS, McFarland HF. Correlation between magnetic resonance imaging findings and lesion development in chronic, active multiple sclerosis. Ann Neurol. 1993;34:661-669.

Kesselring J, Miller DH, MacManus DG, Johnson G, Milligan NM, Scolding N, Compston DA, McDonald WI. Quantitative magnetic resonance imaging in multiple sclerosis: the effect of high dose intravenous methylprednisolone. J.Neurol.Neurosurg.Psychiatry 1989;52:14-7.

Kidd D, Thorpe JW, Thompson AJ, Kendall BE, Moseley IF, MacManus DG, McDonald WI, Miller DH. Spinal cord MRI using multi-array coils and fast spin echo. II. Findings in multiple sclerosis. Neurology 1993;43:2632-2637.

Kidd D, Thompson AJ. Prospective study of neurorehabilitation in multiple sclerosis. J.Neurol.Neurosurg.Psychiatry 1997;62:423-424.

Kidd D, Barkhof F, McConnell R, Algra PR, Allen IV, Revesz T. Cortical lesions in multiple sclerosis. Brain 1999;122:17-26.

Kornek B, Lassmann H. Neuropathology of multiple sclerosis-new concepts. Brain Res.Bull. 2003;61:321-6.

Kremenchutzky M, Cottrell D, Rice G, Hader W, Baskerville J, Koopman W, Ebers GC. The natural history of multiple sclerosis: a geographically based study. 7. Progressive-relapsing and relapsing-progressive multiple sclerosis: a re-evaluation. Brain 1999;122:1941-1950.

Kuhlmann T, Lingfeld G, Bitsch A, Schuchardt J, Bruck W. Acute axonal damage in multiple sclerosis is most extensive in early disease stages and decreases over time. Brain 2002;125:2202-2212.

Kurtzke JF. Rating neurologic impairment in multiple sclerosis: an expanded disability status scale (EDSS). Neurology 1983;33:1444-1452.

Kurtzke JF, Kurland LT, Goldberg ID. Mortality and migration in multiple sclerosis. Neurology 1971;21:1186-1197.

Lai M, Hodgson T, Gawne-Cain M, Webb S, MacManus D, McDonald WI, Thompson AJ, Miller DH. A preliminary study into the sensitivity of disease activity detection by serial weekly magnetic resonance imaging in multiple sclerosis. J.Neurol.Neurosurg.Psychiatry 1996; 60:339-41.

Lai HM, Davie CA, Gass A, Barker GJ, Webb S, Tofts PS, Thompson AJ, McDonald WI, Miller DH. Serial magnetisation transfer ratios in gadolinium-enhancing lesions in multiple sclerosis. J Neurol 1997;244:308-311.

Larsson HB, Barker GJ, MacKay A. Nuclear magnetic resonance relaxation in multiple sclerosis. J.Neurol.Neurosurg.Psychiatry 1998;64 Suppl 1:S70-S76.

Lassmann H. Pathology of multiple sclerosis. In: Compston A, Ebers E, Lassmann H, McDonald I, Matthews B, Wekerle H, eds. McAlpine's multiple sclerosis (third edition). London, Edinburgh, New York, Philadelphia, Sydney, Toronto: Churchill Livingstone, 1998a:323-358.

Lassmann H. Neuropathology in multiple sclerosis: new concepts. Mult Scler 1998b;4: 93-98.

Laule C, Vavasour IM, Whittall KP, Oger J, Paty DW, Li DK, MacKay AL, Arnold DL. Evolution of focal and diffuse magnetisation transfer abnormalities in multiple sclerosis. J Neurol 2003;250:924-931.

Lauterbur PC. Imaging of biological structures by nuclear magnetic-resonance zeugmatography. Bulletin of the America physical society1974;19:374-374.

Lexa FJ, Grossman RI, Rosenquist AC. Dyke Award paper. MR of wallerian degeneration in the feline visual system: characterization by magnetization transfer rate with histopathologic correlation. AJNR Am J Neuroradiol. 1994;15:201-212.

Loevner LA, Grossman RI, Cohen JA, Lexa FJ, Kessler D, Kolson DL. Microscopic disease in normal-appearing white matter on conventional MR images in patients with multiple sclerosis: assessment with magnetization-transfer measurements. Radiology 1995;196:511-515.

Losseff NA, Wang L, Lai HM, Yoo DS, Gawne-Cain ML, McDonald WI, Miller DH, Thompson AJ. Progressive cerebral atrophy in multiple sclerosis. A serial MRI study. Brain 1996*a*;119:2009-2019.

Losseff NA, Webb SL, O'Riordan JI, Page R, Wang L, Barker GJ, Tofts PS, McDonald WI, Miller DH, Thompson AJ. Spinal cord atrophy and disability in multiple sclerosis. A new reproducible and sensitive MRI method with potential to monitor disease progression. Brain 1996*b*;119:701-708.

Lublin FD, Reingold SC. Defining the clinical course of multiple sclerosis: results of an international survey. National Multiple Sclerosis Society (USA) Advisory Committee on Clinical Trials of New Agents in Multiple Sclerosis. Neurology 1996;46:907-911.

Lucchinetti C, Bruck W, Parisi J, Scheithauer B, Rodriguez M, Lassmann H. Heterogeneity of multiple sclerosis lesions: implications for the pathogenesis of demyelination. Ann Neurol. 2000;47:707-717.

Lumsden CE. The neuropathology of multiple sclerosis. In: Vinken PJ, Bruyn GW, eds. Handbook of clinical neurology. Amsterdam: North-Holland, 1970:217-309.

Katz D, Taubenberger JK, Cannella B, McFarlin DE, Raine CS, McFarland HF. Correlation between magnetic resonance imaging findings and lesion development in chronic, active multiple sclerosis. Ann Neurol 1993;34:661-669.

Kimura H, Meaney DF, McGowan JC, Grossman RI, Lenkinski RE, Ross DT, McIntosh TK, Gennarelli TA, Smith DH. Magnetization transfer imaging of diffuse axonal injury following experimental brain injury in the pig: characterization by magnetization transfer ratio with histopathologic correlation. J Comput Assist Tomogr 1996;20:540-546.

Kita M, Goodkin DE, Bacchetti P, Waubant E, Nelson SJ, Majumdar S. Magnetization transfer ratio in new MS lesions before and during therapy with IFNbeta-1a. Neurology 2000;54:1741-1745.

MacDonald BK, Cockerell OC, Sander JW, Shorvon SD. The incidence and lifetime prevalence of neurological disorders in a prospective community-based study in the UK. Brain 2000;123:665-676.

Marburg O. Die Sogennante "akute multiple sklerose". Jahrbucher fur Psychiatre und Neurologie 1906;27:211-312.

Mansfield P. Proton spin imaging by nuclear magnetic-resonance. Contemporary Physics. 1976;17:553-576.

Matthews B. Symptoms and signs of multiple sclerosis. In: Compston A, Ebers E, Lassmann H, McDonald I, Matthews B, Wekerle H, eds. McAlpine's multiple sclerosis (third edition). London, Edinburgh, New York, Philadelphia, Sydney, Toronto: Churchill Livingstone, 1998:145-190.

McDonald WI, Compston A, Edan G, Goodkin D, Hartung HP, Lublin FD, McFarland HF, Paty DW, Polman CH, Reingold SC, Sandberg-Wollheim M, Sibley W, Thompson A, van den NS, Weinshenker BY, Wolinsky JS. Recommended diagnostic criteria for multiple sclerosis: guidelines from the International Panel on the diagnosis of multiple sclerosis. Ann Neurol. 2001;50:121-127.

McDonnell GV, Hawkins SA. An epidemiologic study of multiple sclerosis in Northern Ireland. Neurology 1998;50:423-428.

McFarland HF, Barkhof F, Antel J, Miller DH. The role of MRI as a surrogate outcome measure in multiple sclerosis. Multiple Sclerosis 2002;8:40-51.

Mehta RC, Pike GB, Enzmann DR. Magnetization transfer MR of the normal adult brain. AJNR Am J Neuroradiol. 1995;16:2085-2091.

Miller DH, Rudge P, Johnson G, Kendall BE, MacManus DG, Moseley IF, Barnes D, McDonald WI. Serial gadolinium enhanced magnetic resonance imaging in multiple sclerosis. Brain 1988;111:927-939.

Miller DH, Molyneux PD, Barker GJ, MacManus DG, Moseley IF, Wagner K. Effect of interferon-beta1b on magnetic resonance imaging outcomes in secondary progressive multiple sclerosis: results of a European multicenter, randomized, double-blind, placebo-controlled trial. European Study Group on Interferon-beta1b in secondary progressive multiple sclerosis. Ann Neurol 1999;46:850-859.

Miller DH. MRI monitoring of MS in clinical trials. Clin.Neurol.Neurosurg. 2002;104:236-243.

Miller DH, Barkhof F, Frank JA, Parker GJ, Thompson AJ. Measurement of atrophy in multiple sclerosis: pathological basis, methodological aspects and clinical relevance. Brain 2002;125:1676-1695.

Miller DH, Khan OA, Sheremata WA, Blumhardt LD, Rice GP, Libonati MA, Willmer-Hulme AJ, Dalton CM, Miszkiel KA, O'Connor PW. A controlled trial of natalizumab for relapsing multiple sclerosis. N Engl J Med 2003;348:15-23.

Milligan NM, Newcombe R, Compston DA. A double-blind controlled trial of high dose methylprednisolone in patients with multiple sclerosis: 1. Clinical effects. J Neurol Neurosurg Psychiatry 1987;50:511-516.

Molyneux PD, Kappos L, Polman C, Pozzilli C, Barkhof F, Filippi M, Yousry T, Hahn D, Wagner K, Ghazi M, Beckmann K, Dahlke F, Losseff N, Barker GJ, Thompson AJ, Miller DH. The effect of interferon beta-1b treatment on MRI measures of cerebral atrophy in secondary progressive multiple sclerosis. European Study Group on Interferon beta-1b in secondary progressive multiple sclerosis. Brain 2000;123:2256-2263.

Molyneux PD, Barker GJ, Barkhof F, Beckmann K, Dahlke F, Filippi M, Ghazi M, Hahn D, MacManus D, Polman C, Pozzilli C, Kappos L, Thompson AJ, Wagner K, Yousry T, Miller DH. Clinical-MRI correlations in a European trial of interferon beta-1b in secondary progressive MS. Neurology 2001;57:2191-2197.

Morrison C, Henkelman RM. A model for magnetization transfer in tissues. Magn Reson Med 1995;33:475-482.

Mottershead JP, Schmierer K, Clemence M, Thornton JS, Scaravilli F, Barker GJ, Tofts PS, Newcombe J, Cuzner ML, Ordidge RJ, McDonald WI, Miller DH. High field MRI correlates of myelin content and axonal density in multiple sclerosis: a post mortem study of spinal cord. J Neurol 2003;250:1293-1301.

Mumford CJ, Wood NW, Kellar-Wood H, Thorpe JW, Miller DH, Compston DA. The British Isles survey of multiple sclerosis in twins. Neurology 1994;44:11-15.

Naruse S, Horikawa Y, Tanaka C, Hirakawa K, Nishikawa H, Yoshizaki K. Proton nuclear magnetic resonance studies on brain edema. J Neurosurg 1982;56:747-752.

Nijeholt GJ, Barkhof F, Scheltens P, Castelijns JA, Ader H, van Waesberghe JH, Polman C, Jongen SJ, Valk J. MR of the spinal cord in multiple sclerosis: relation to clinical subtype and disability. AJNR Am.J.Neuroradiol 1997;18:1041-1048.

Nijeholt GJ, Castelijns JA, Lazeron RH, van Waesberghe JH, Polman CH, Uitdehaag BM, Barkhof F. Magnetization transfer ratio of the spinal cord in multiple sclerosis: relationship to atrophy and neurologic disability. J Neuroimaging 2000;10:67-72.

Ohye C, Armstrong E. The Thalamus and The Limbic Thalamus. In: Paxinos G, ed. The Human Nervous System. San Diego, New York, Boston, London, Sydney, Tokyo, Toronto: Academic Press, Inc, 1990:439-482.

Ormerod IE, Miller DH, McDonald WI, du Boulay EP, Rudge P, Kendall BE, Moseley IF, Johnson G, Tofts PS, Halliday AM, . The role of NMR imaging in the assessment of multiple sclerosis and isolated neurological lesions. A quantitative study. Brain 1987;110:1579-616.

O'Riordan JI, Thompson AJ, Kingsley DP, MacManus DG, Kendall BE, Rudge P, McDonald WI, Miller DH. The prognostic value of brain MRI in clinically isolated syndromes of the CNS. A 10-year follow-up. Brain 1998;121:495-503.

Panitch HS. Influence of infection on exacerbations of multiple sclerosis. Ann Neurol. 1994;36 Suppl:S25-S28.

Paolillo A, Pozzilli C, Giugni E, Tomassini V, Gasperini C, Fiorelli M, Mainero C, Horsfield M, Galgani S, Bastianello S, Buttinelli C. A 6-year clinical and MRI follow-up study of patients with relapsing-remitting multiple sclerosis treated with Interferon-beta. Eur J Neurol 2002;9:645-655.

Parker GJ, Barker GJ, Tofts PS. Accurate multislice gradient echo T(1) measurement in the presence of non-ideal RF pulse shape and RF field nonuniformity. Magn Reson.Med. 2001;45:838-845.

Patel UJ, Grossman RI, Phillips MD, Udupa JK, McGowan JC, Miki Y, Wei L, Polansky M, van Buchem MA, Kolson D. Serial analysis of magnetization-transfer histograms and Expanded Disability Status Scale scores in patients with relapsing-remitting multiple sclerosis. AJNR Am J Neuroradiol 1999;20:1946-1950.

Paty DW, Oger JJ, Kastrukoff LF, Hashimoto SA, Hooge JP, Eisen AA, Eisen KA, Purves SJ, Low MD, Brandejs V, . MRI in the diagnosis of MS: a prospective study with comparison of clinical evaluation, evoked potentials, oligoclonal banding, and CT. Neurology 1988;38:180-185.

Paty D, Li DK, the UBC MS/MRI Study Group, the IFNB Multiple Sclerosis Study Group. Interferon beta-lb is effective in relapsing-remitting multiple sclerosis. II.

MRI analysis results of a multicenter, randomized, double-blind, placebo-controlled trial. Neurology 1993;43:662-667.

Parry A, Clare S, Jenkinson M, Smith S, Palace J, Matthews PM. White matter and lesion T1 relaxation times increase in parallel and correlate with disability in multiple sclerosis. J Neurol 2002;249:1279-1286.

Parry A, Clare S, Jenkinson M, Smith S, Palace J, Matthews PM. MRI brain T1 relaxation time changes in MS patients increase over time in both the white matter and the cortex. J Neuroimaging 2003;13:234-239.

Petajan JH, Gappmaier E, White AT, Spencer MK, Mino L, Hicks RW. Impact of aerobic training on fitness and quality of life in multiple sclerosis. Ann Neurol 1996;39:432-441.

Peterson JW, Bo L, Mork Chang SA, Trapp BD. Transected neurites, apoptotic neurons, and reduced inflammation in cortical multiple sclerosis lesions. Ann Neurol. 2001;50:389-400.

Pike GB, De Stefano N, Narayanan S, Worsley KJ, Pelletier D, Francis GS, Antel JP, Arnold DL. Multiple sclerosis: magnetization transfer MR imaging of white matter before lesion appearance on T2-weighted images. Radiology 2000;215:824-30.

Pittock SJ, McClelland RL, Mayr WT, Jorgensen NW, Weinshenker BG, Noseworthy J, Rodriguez M. Clinical implications of benign multiple sclerosis: a 20-year population-based follow-up study. Ann Neurol. 2004;56:303-306.

Plummer DL. DispImage: a display and analysis tool for medical images. Revista Di Neuroradiologica 1992;5:489-495.

Poser CM, Paty DW, Scheinberg L, McDonald WI, Davis FA, Ebers GC, Johnson KP, Sibley WA, Silberberg DH, Tourtellotte WW. New diagnostic criteria for multiple sclerosis: guidelines for research protocols. Ann Neurol 1983;13:227-231.

Prineas JW, Barnard RO, Revesz T, Kwon EE, Sharer L, Cho ES. Multiple sclerosis. Pathology of recurrent lesions. Brain 1993;116:681-693.

PRISMS (Prevention of Relapses and Disability by Interferon beta-1a Subcutaneously in Multiple Sclerosis) Study Group. Randomised double-blind placebo-controlled study of interferon beta-1a in relapsing/remitting multiple sclerosis. Lancet 1998;352:1498-1504.

Ramani A, Dalton C, Miller DH, Tofts PS, Barker GJ. Precise estimate of fundamental in-vivo MT parameters in human brain in clinically feasible times. Magn Reson Imaging 2002;20:721-731.

Rammohan KW, Rosenberg JH, Lynn DJ, Blumenfeld AM, Pollak CP, Nagaraja HN. Efficacy and safety of modafinil (Provigil) for the treatment of fatigue in multiple sclerosis: a two centre phase 2 study. J Neurol Neurosurg Psychiatry 2002;72:179-183.

Rashid W, Hadjiprocopis A, Griffin CM, Chard DT, Davies GR, Barker GJ, Tofts PS, Thompson AJ, Miller DH. Diffusion tensor imaging of early relapsing-remitting multiple sclerosis with histogram analysis using automated segmentation and brain volume correction. Mult.Scler. 2004;10:9-15.

Reynolds R, Dawson M, Papadopoulos D, Polito A, Di Bello IC, Pham-Dinh D, Levine J. The response of NG2-expressing oligodendrocyte progenitors to demyelination in MOG-EAE and MS. J Neurocytol. 2002;31:523-536.

Richert ND, Ostuni JL, Bash CN, Duyn JH, McFarland HF, Frank JA. Serial whole-brain magnetization transfer imaging in patients with relapsing-remitting multiple sclerosis at baseline and during treatment with interferon beta-1b. AJNR Am J Neuroradiol 1998;19:1705-1713.

Richert ND, Ostuni JL, Bash CN, Leist TP, McFarland HF, Frank JA. Interferon beta-1b and intravenous methylprednisolone promote lesion recovery in multiple sclerosis. Mult Scler 2001;7:49-58.

Robertson NP, O'Riordan JI, Chataway J, Kingsley DP, Miller DH, Clayton D, Compston DA. Offspring recurrence rates and clinical characteristics of conjugal multiple sclerosis. Lancet 1997;349:1587-1590.

Rocca MA, Mastronardo G, Rodegher M, Comi G, Filippi M. Long-term changes of magnetization transfer-derived measures from patients with relapsing-remitting and secondary progressive multiple sclerosis. AJNR Am J Neuroradiol 1999;20:821-827.

Rodriguez M, Siva A, Cross SA, O'Brien PC, Kurland LT. Optic neuritis: a population-based study in Olmsted County, Minnesota. Neurology 1995;45:244-250.

Rovaris M, Filippi M, Falautano M, Minicucci L, Rocca MA, Martinelli V, Comi G. Relation between MR abnormalities and patterns of cognitive impairment in multiple sclerosis. Neurology 1998;50:1601-1608.

Rovaris M, Filippi M, Minicucci L, Iannucci G, Santuccio G, Possa F, Comi G. Cortical/subcortical disease burden and cognitive impairment in patients with multiple sclerosis. AJNR Am.J.Neuroradiol. 2000;21:402-408.

Rovaris M, Agosta F, Sormani MP, Inglese M, Martinelli V, Comi G, Filippi M. Conventional and magnetisation transfer MRI predictors of clinical multiple sclerosis evolution: a medium-term follow-up study. Brain 2003;126:2323-3332.

Rudick RA, Fisher E, Lee JC, Simon J, Jacobs L. Use of the brain parenchymal fraction to measure whole brain atrophy in relapsing-remitting MS. Multiple Sclerosis Collaborative Research Group. Neurology 1999;53:1698-704.

Runmarker B, Andersen O. Prognostic factors in a multiple sclerosis incidence cohort with twenty-five years of follow-up. Brain 1993;116:117-134.

Sailer M, O'Riordan JI, Thompson AJ, Kingsley DP, MacManus DG, McDonald WI, Miller DH. Quantitative MRI in patients with clinically isolated syndromes suggestive of demyelination. Neurology 1999;52:599-606.

Santos AC, Narayanan S, De Stefano N, Tartaglia MC, Francis SJ, Arnaoutelis R, Caramanos Z, Antel JP, Pike GB, Arnold DL. Magnetization transfer can predict clinical evolution in patients with multiple sclerosis. J Neurol 2002;249:662-8.

Schumacher GA, Beebe G, Kibler RF, et al. Problems of experimental trials of therapy in multiple sclerosis; report by the panel on the evaluation of experimental trials of therapy in multiple sclerosis. Annals of the New York Academy of Sciences 1965;122:552-568.

Schmierer K, Scaravilli F, Altmann DR, Barker GJ, Miller DH. Magnetization transfer ratio and myelin in postmortem multiple sclerosis brain. Ann.Neurol. 2004a;56:407-15.

Schmierer K, Altmann DR, Kassim N, Kitzler H, Kerskens CM, Doege CA, Aktas O, Lunemann JD, Miller DH, Zipp F, Villringer A. Progressive change in primary progressive multiple sclerosis normal-appearing white matter: a serial diffusion magnetic resonance imaging study. Mult Scler 2004*b*;10:182-187.

Sellebjerg F, Frederiksen JL, Nielsen PM, Olesen J. Double-blind, randomized, placebo-controlled study of oral, high-dose methylprednisolone in attacks of MS. Neurology 1998;51:529-534.

Sicotte NL, Liva SM, Klutch R, Pfeiffer P, Bouvier S, Odesa S, Wu TC, Voskuhl RR. Treatment of multiple sclerosis with the pregnancy hormone estriol. Ann Neurol 2002;52:421-428.

Silver NC, Barker GJ, MacManus DG, Miller DH, Thorpe JW, Howard RS. Decreased magnetisation transfer ratio due to demyelination: a case of central pontine myelinolysis. J Neurol Neurosurg Psychiatry 1996;61:208-209.

Silver NC, Barker GJ, MacManus DG, Tofts PS, Miller DH. Magnetisation transfer ratio of normal brain white matter: a normative database spanning four decades of life. J Neurol Neurosurg Psychiatry1997*a*;62:223-228.

Silver NC, Barker GJ, Losseff NA, Gawne-Cain ML, MacManus DG, Thompson AJ, Miller DH. Magnetisation transfer ratio measurement in the cervical spinal cord: a preliminary study in multiple sclerosis. Neuroradiology 1997*b*;39:441-445.

Silver NC, Lai M, Symms MR, Barker GJ, McDonald WI, Miller DH. Serial magnetization transfer imaging to characterize the early evolution of new MS lesions. Neurology 1998;51:758-764.

Simon JH, Jacobs LD, Campion M, Wende K, Simonian N, Cookfair DL, Rudick RA, Herndon RM, Richert JR, Salazar AM, Alam JJ, Fischer JS, Goodkin DE, Granger CV, Lajaunie M, Martens-Davidson AL, Meyer M, Sheeder J, Choi K, Scherzinger AL, Bartoszak DM, Bourdette DN, Braiman J, Brownscheidle CM, Whitham RH, . Magnetic resonance studies of intramuscular interferon beta-1a for relapsing multiple sclerosis. The Multiple Sclerosis Collaborative Research Group. Ann Neurol 1998;43:79-87.

Simon JH, Jacobs LD, Campion MK, Rudick RA, Cookfair DL, Herndon RM, Richert JR, Salazar AM, Fischer JS, Goodkin DE, Simonian N, Lajaunie M, Miller DE, Wende K, Martens-Davidson A, Kinkel RP, Munschauer FE, III, Brownscheidle CM. A longitudinal study of brain atrophy in relapsing multiple sclerosis. The Multiple Sclerosis Collaborative Research Group (MSCRG). Neurology 1999;53:139-148.

Simon JH, Kinkel RP, Jacobs L, Bub L, Simonian N. A Wallerian degeneration pattern in patients at risk for MS. Neurology 2000;54:1155-1160.

Sled JG, Pike GB. Quantitative interpretation of magnetization transfer in spoiled gradient echo MRI sequences. J.Magn Reson. 2000;145:24-36.

Sled JG, Pike GB. Quantitative imaging of magnetization transfer exchange and relaxation properties in vivo using MRI. Magn Reson Med 2001;46:923-931.

(SPECTRIMS) Secondary Progressive Efficacy Clinical Trial of Recombinant Interferon-beta-1a in MS Study Group. Randomized controlled trial of interferon-beta-1a in secondary progressive MS: Clinical results. Neurology 2001;56:1496-1504.

Stanisz GJ, Webb S, Munro CA, Pun T, Midha R. MR properties of excised neural tissue following experimentally induced inflammation. Magn Reson.Med 2004a;51:473-479.

Stanisz GJ, Odrobina E, Munro CA, Pun T, Toby L, Xu QG, Midha R. MR properties of neural tissue following experimentally induced demyelination. International society for magnetic resonance in medicine: Twelfth scientific meeting 2004b:469.

Stewart WA, Hall LD, Berry K, Paty DW. Correlation between NMR scan and brain slice data in multiple sclerosis. Lancet 1984;2:412.

Stevenson VL, Leary SM, Losseff NA, Parker GJ, Barker GJ, Husmani Y, Miller DH, Thompson AJ. Spinal cord atrophy and disability in MS: a longitudinal study. Neurology 1998;51:234-238.

Studholme C, Hill DLG, Hawkes DJ. An overlap invariant entropy measure of 3D

medical image alignment. Pattern Recognit 1999;32:71-86.

Sundstrom P, Juto P, Wadell G, Hallmans G, Svenningsson A, Nystrom L, Dillner J,

Forsgren L. An altered immune response to Epstein-Barr virus in multiple sclerosis:

a prospective study. Neurology 2004;62:2277-2282.

Swingler RJ, Compston DA. The prevalence of multiple sclerosis in south east

Wales. J Neurol Neurosurg Psychiatry 1988;51:1520-1524.

Thompson AJ, Polman CH, Miller DH, McDonald WI, Brochet B, Filippi M,

Montalban, X, De Sa J. Primary progressive multiple sclerosis. Brain

1997;120:1085-1096.

Thorpe JW, Barker GJ, Jones SJ, Moseley I, Losseff N, MacManus DG, Webb S,

Mortimer C, Plummer DL, Tofts PS, . Magnetisation transfer ratios and transverse

magnetisation decay curves in optic neuritis: correlation with clinical findings and

electrophysiology. J Neurol Neurosurg Psychiatry 1995;59:487-492.

Thorpe JW, Kidd D, Moseley IF, Thompson AJ, MacManus DG, Compston DA,

McDonald WI, Miller DH. Spinal MRI in patients with suspected multiple sclerosis

and negative brain MRI. Brain 1996a;119:709-714.

Thorpe JW, Kidd D, Moseley IF, Kenndall BE, Thompson AJ, MacManus DG,

McDonald WI, Miller DH. Serial gadolinium-enhanced MRI of the brain and spinal

cord in early relapsing-remitting multiple sclerosis. Neurology 1996*b*;46:373-378.

Tiberio M, Chard DT, Altmann DR, Davies G, Griffin CM, Rashid W, Sastre-

Garriga J, Thompson AJ, Miller DH. Gray and white matter volume changes in early

RRMS: a two year longitudinal study. Neurology 2005; *in press*.

Tofts PS, Cercignani M, Tozer DJ, Symms MR, Davies GR, Ramani A, Barker GJ.

"Tozer *et al.*, Quantitative magnetization transfer mapping of bound protons in

multiple sclerosis Magn Reson Med 2003;50:83-91." – *erratum*. Magn Reson Med

2005;53:492-493.

Tortorella C, Viti B, Bozzali M, Sormani MP, Rizzo G, Gilardi MF, Comi G, Filippi

M. A magnetization transfer histogram study of normal-appearing brain tissue in MS.

Neurology 2000;54:186-193.

Tozer D, Ramani A, Barker GJ, Davies GR, Miller DH, Tofts PS. Quantitative

magnetization transfer mapping of bound protons in multiple sclerosis. Magn Reson

Med 2003;50:83-91.

Traboulsee A, Dehmeshki J, Brex PA, Dalton CM, Chard D, Barker GJ, Plant GT,

Miller DH. Normal-appearing brain tissue MTR histograms in clinically isolated

syndromes suggestive of MS. Neurology 2002;59:126-128.

Traboulsee A, Dehmeshki J, Peters KR, Griffin CM, Brex PA, Silver N, Ciccarelli O, Chard DT, Barker GJ, Thompson AJ, Miller DH. Disability in multiple sclerosis is related to normal appearing brain tissue MTR histogram abnormalities. Mult Scler 2003;9:566-573.

Trapp BD, Peterson J, Ransohoff RM, Rudick R, Mork S, Bo L. Axonal transection in the lesions of multiple sclerosis. N Engl J Med 1998;338:278-285.

Truyen L, van Waesberghe JH, van Walderveen MA, van Oosten BW, Polman CH, Hommes OR, Ader HJ, Barkhof F. Accumulation of hypointense lesions ("black holes") on T1 spin-echo MRI correlates with disease progression in multiple sclerosis. Neurology 1996;47:1469-76.

Tubridy N, Behan PO, Capildeo R, Chaudhuri A, Forbes R, Hawkins CP, Hughes RA, Palace J, Sharrack B, Swingler R, Young C, Moseley IF, MacManus DG, Donoghue S, Miller DH. The effect of anti-alpha4 integrin antibody on brain lesion activity in MS. The UK Antegren Study Group. Neurology 1999;53:466-472.

Weinshenker BG, Bass B, Rice GP, Noseworthy J, Carriere W, Baskerville J, Ebers GC. The natural history of multiple sclerosis: a geographically based study. I. Clinical course and disability. Brain 1989;112:133-146.

Vaithianathar L, Tench CR, Morgan PS, Lin X, Blumhardt LD. White matter T(1) relaxation time histograms and cerebral atrophy in multiple sclerosis. J Neurol Sci 2002;197:45-50.

van Buchem MA, McGowan JC, Kolson DL, Polansky M, Grossman RI. Quantitative volumetric magnetization transfer analysis in multiple sclerosis: estimation of macroscopic and microscopic disease burden. Magn Reson Med 1996;36:632-636.

van Buchem MA, Grossman RI, Armstrong C, Polansky M, Miki Y, Heyning FH, Boncoeur-Martel MP, Wei L, Udupa JK, Grossman M, Kolson DL, McGowan JC. Correlation of volumetric magnetization transfer imaging with clinical data in MS. Neurology 1998;50:1609-1617.

van Buchem MA, Tofts PS. Magnetization transfer imaging. Neuroimaging Clin N Am 2000;10:771-788.

van Waesberghe JH, van Buchem MA, Filippi M, Castelijns JA, Rocca MA, van der BR, Polman CH, Barkhof F. MR outcome parameters in multiple sclerosis: comparison of surface-based thresholding segmentation and magnetization transfer ratio histographic analysis in relation to disability (a preliminary note). AJNR Am.J.Neuroradiol. 1998a;19:1857-62.

van Waesberghe JH, van Walderveen MA, Castelijns JA, Scheltens P, Nijeholt GJ, Polman CH, Barkhof F. Patterns of lesion development in multiple sclerosis: longitudinal observations with T1-weighted spin-echo and magnetization transfer MR. AJNR Am.J.Neuroradiol. 1998b;19:675-83.

van Waesberghe JH, Kamphorst W, De Groot CJ, van Walderveen MA, Castelijns JA, Ravid R, Nijeholt GJ, van der Valk P, Polman CH, Thompson AJ, Barkhof F. Axonal loss in multiple sclerosis lesions: magnetic resonance imaging insights into substrates of disability. Ann Neurol 1999;46:747-754.

van Walderveen MA, Barkhof F, Hommes OR, Polman CH, Tobi H, Frequin ST, Valk J. Correlating MRI and clinical disease activity in multiple sclerosis: relevance of hypointense lesions on short-TR/short-TE (T1-weighted) spin-echo images. Neurology 1995;45:1684-1690.

van Walderveen MA, Barkhof F, Pouwels PJ, van Schijndel RA, Polman CH, Castelijns JA. Neuronal damage in T1-hypointense multiple sclerosis lesions demonstrated in vivo using proton magnetic resonance spectroscopy. Ann Neurol. 1999;46:79-87.

Werring DJ, Clark CA, Barker GJ, Thompson AJ, Miller DH. Diffusion tensor imaging of lesions and normal-appearing white matter in multiple sclerosis. Neurology 1999;52:1626-1632.

Wolff SD, Balaban RS. Magnetization transfer contrast (MTC) and tissue water proton relaxation in vivo. Magn Reson Med. 1989;10:135-144.

Wolinsky JS. The PROMiSe trial: baseline data review and progress report. Mult Scler 2004;10 Suppl 1:S65-S71.

Woods RP, Mazziotta JC, Cherry SR. MRI-PET registration with automated

algorithm. J Comput Assist Tomogr 1993;17:536-546.

Wylezinska M, Cifelli A, Jezzard P, Palace J, Alecci M, Matthews PM. Thalamic

neurodegeneration in relapsing-remitting multiple sclerosis. Neurology

2003;60:1949-1954.

Yarnykh VL. Pulsed Z-spectroscopic imaging of cross-relaxation parameters in

tissues for human MRI: theory and clinical applications. Magn Reson Med

2002;47:929-939.

Yarnykh VL, Yuan C. Cross-relaxation imaging reveals detailed anatomy of white

matter fiber tracts in the human brain. Neuroimage. 2004;23:409-424.

Young IR, Hall AS, Pallis CA, Legg NJ, Bydder GM, Steiner RE. Nuclear magnetic

resonance imaging of the brain in multiple sclerosis. Lancet 1981;2:1063-1066.

Zajicek J, Fox P, Sanders H, Wright D, Vickery J, Nunn A, Thompson A.

Cannabinoids for treatment of spasticity and other symptoms related to multiple

sclerosis (CAMS study): multicentre randomised placebo-controlled trial. Lancet

2003;362:1517-1526.

Zivadinov R, De Masi R, Nasuelli D, Bragadin LM, Ukmar M, Pozzi-Mucelli RS, Grop A, Cazzato G, Zorzon M. MRI techniques and cognitive impairment in the early phase of relapsing-remitting multiple sclerosis. Neuroradiology 2001;43:272-278.